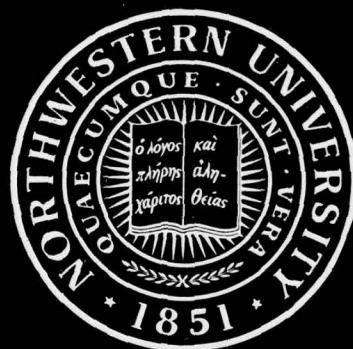


AD A 053181

AD NO.

DDC FILE COPY

**NORTHWESTERN UNIVERSITY**  
**MATERIALS RESEARCH CENTER**



EVANSTON, ILLINOIS

**ANNUAL TECHNICAL REPORT**

**1976-77**



**DISTRIBUTION STATEMENT A**

Approved for public release  
Distribution Unlimited

6  
EIGHTEENTH ANNUAL REPORT  
ON

MATERIALS RESEARCH (18th),

1 July 1976 to 30 June 1977

The research described herein was sponsored primarily  
by the following Agencies  
of the United States Government:

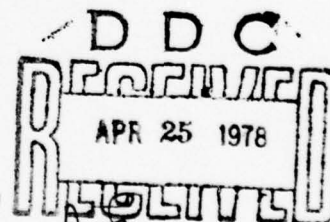
Advanced Research Projects Agency ✓  
Air Force Office of Scientific Research ✓  
Energy Research and Development Administration  
National Science Foundation  
North American Treaty Organization  
Office of Naval Research ✓  
U. S. Army Research Office-Durham ✓

submitted to the  
NATIONAL SCIENCE FOUNDATION

15 ✓ NSF-Grant DMR76-01057

REVISION for	
White Section	<input checked="" type="checkbox"/>
Buff Section	<input type="checkbox"/>
UNANNOUNCED	<input type="checkbox"/>
JUSTIFICATION	
BY	
DISTRIBUTION/AVAILABILITY CODES	
Dist.	AVAIL. and/or SPECIAL
A	

by the  
Materials Research Center  
Northwestern University  
Evanston, Illinois



12 114p.

11 Aug 1977

DISTRIBUTION STATEMENT A  
Approved for public release  
Distribution Unlimited

220 570

LB



## INTRODUCTION

The Eighteenth Annual Technical Report of the Materials Research Center of Northwestern University includes the abstracts of publications and theses which describe the results of materials research conducted during the period 1 July 1976 to 30 June 1977. The research is described in two sections: (1) Thrust Area Research and (2) General Materials Research. The Thrust Area Research has four components: Charge Transport and Electronic Structure; Fatigue of Metals and Alloys; Metals, Alloys and Intermetallic Compounds; and Polymer Processing and Properties. Within each Thrust Area the research supported under the MRL program is presented along with the allied thrust research supported by the agencies indicated. In a number of instances Center members are active in several areas of endeavor, and their contributions appear in different sections. The General Materials Research section includes (1) the MRL supported collaborative research of several faculty as well as the individual research projects supported under the MRL program and (2) the non-MRL individually funded research projects. A summary highlighting the principle accomplishments for the Thrust Area Research groups and General Materials Research precedes the listing of the individual items in this report. Some support was extended in all cases from the Materials Research Laboratory program of the National Science Foundation through funding, use of the Central Facilities or space of the Materials Research Center, or through participation in the MRC bimonthly seminars. Titles, authors, abstracts, principal investigators and thesis advisors are shown for each faculty member's research as well as the source of the financial support for each project.

Each faculty member's research is listed in the appropriate section and indexed. For reprints or preprints, please communicate directly with the investigator. Since this report is a private communication of the Materials Research Center, it must not be reproduced in whole or in part without permission. No public reference should be made to any of the items in the report, rather make reference to the appropriate journal after the publication appears in print.

The Central Facilities of the Materials Research Center contribute significantly to this interdisciplinary research program. These Central Facilities, along with those maintained by the academic departments, as well equipped with

modern equipment and provide the analytical tools and services necessary to maintain the high level of research expected of Center members. Each Facility is operated by an individual member of the faculty; the Central Facilities and their Directors are appended at the end of the report.

The operation of the Center is administered by a Director, who is aided by an Assistant Director. Three separate committees advise the Director concerning the operation of the Center. The Scientific Advisory Committee advises the Director on matters concerning the evaluation of research efforts, distribution of research funds, acquisition of capital equipment and long range planning of research projects. This committee is composed of faculty participants from the Thrust Groups and Departments. The Administrative Committee, which consists of the Vice President for Research, the Deans of the College of Arts and Science and of the Technological Institute and the Department Chairmen of the disciplines participating in the Center, is the second group that advises the Director concerning the broad-range policies of the Center. The Materials Research Center's Advisory Committee consists of twelve prominent members of the Academic and Industrial Community that annually reviews the overall program of the Center and advises the Vice President for Research, to whom the Center's Director reports, on the status of the research and administration of the Center.

J. O. Brittain, Director  
Materials Research Center

## TABLE OF CONTENTS

	Page
CHARGE TRANSPORT AND ELECTRONIC STRUCTURE - Thrust Group	1
FATIGUE OF METALS AND ALLOYS - Thrust Group	32
METALS, ALLOYS AND INTERMETALLIC COMPOUNDS - Thrust Group	55
POLYMER PROCESSING AND PROPERTIES - Thrust Group	69
GENERAL MATERIALS RESEARCH:	
Part I	80
Part II	86
FACILITIES	108
INDEX	109

Thrust Area Research

Support:  
NSF-MRL Program

CHARGE TRANSPORT AND ELECTRONIC STRUCTURE

Faculty:

D. F. Shriver, Professor, Chemistry, Group Leader  
D. E. Ellis, Professor, Physics and Astronomy and Chemistry  
M. E. Fine, Professor, Materials Science and Engineering  
A. J. Freeman, Professor, Physics and Astronomy  
B. M. Hoffman, Professor, Chemistry  
J. A. Ibers, Professor, Chemistry  
C. R. Kannewurf, Professor, Electrical Engineering  
T. J. Marks, Associate Professor, Chemistry  
M. A. Ratner, Associate Professor, Chemistry  
D. H. Whitmore, Professor, Materials Science and Engineering

Research Staff:

T. Asada, Physics and Astronomy  
L. D. Brown, Postdoctoral Fellow, Chemistry  
D. Greig, Postdoctoral Associate, Chemistry  
M. Gupta, Research Associate, Physics and Astronomy  
R. P. Gupta, Research Associate, Physics and Astronomy  
B. L. Kundalkar, NSF Fellow, Chemistry  
T. Phillips, Chemistry, Postdoctoral Fellow  
J. Revelli, Postdoctoral Fellow, Electrical Engineering  
S. Topiol, NSF Fellowship, Chemistry  
A. Zunger, Physics and Astronomy

Graduate Students:

R. L. Ammlung, Chemistry  
G. A. Benesh, Physics and Astronomy  
C. A. Gaw, Electrical Engineering  
D. Greig, Chemistry  
D. Jacy, Electrical Engineering  
D. W. Kalina, Chemistry  
D. King, Materials Science and Engineering  
T. J. Langill, Materials Science and Engineering  
L.-S. Lin, Chemistry  
J. W. Lyding, Electrical Engineering  
M. McClure, Electrical Engineering  
J. McOmber, Chemistry  
M. Ondrechen, Chemistry  
M. T. Ratajack, Electrical Engineering  
C. Schramm, Chemistry  
D. R. Stojakovic, Chemistry  
R. C. Teitelbaum, Chemistry  
J. Thompson, Chemistry  
C. Umrigar, Physics and Astronomy



Personnel Who Have Left:

L. D. Brown, EXXON Research Corp., Baytown, Texas  
D. Greig, Assistant Professor, Lake Forest College, Lake Forest, Ill.  
M. T. Ratajack, Assistant Professor, Chicago Circle University,  
Chicago, Ill.  
S. Topiol, Carnegie-Mellon University, Pittsburgh, Penn.

Degrees Granted:

D. Greig, Ph.D.  
M. T. Ratajack, Ph.D.

Other Sponsorship:

NSF-MRL, National Science Foundation, Materials Research Laboratory  
AFOSR, Air Force Office of Scientific Research  
ARPA, Advanced Research Projects Agency (through the Materials Research  
Center)  
Dreyfus, Camille and Henry Dreyfus Foundation  
ERDA, Energy Research and Development Administration  
NASA, National Aeronautics and Space Administration  
NSF, National Science Foundation  
ONR, Office of Naval Research  
PRI, Paint Research Institute  
Sloan, Alfred P. Sloan Foundation

Introduction

The Charge Transport Thrust Group is active in the study of both electronic and ionic conductors. Our approach is to synthesize and study new materials, and to parallel these experimental studies with a vigorous theoretical program. Some of the main lines of research, which are described in the present report, are linear-chain conductors, metal dichalcogenides, metal carbides, and heavy metal ionic conductors. Even though the research projects are fundamental in character the phenomena being studied have many practical implications.

As outlined here in several reports, work on iodine-oxidized mixed valence metal phthalocyanines by Marks', Hoffman's and Ibers' groups has introduced a unique new class of quasi-metallic linear-chain conductors. This work has been closely coupled with resonance Raman and iodine Mössbauer spectroscopic techniques for measuring the degree of partial oxidation. These materials permit wide variations in stoichiometry to be studied for the first time in linear chain systems. The present charge transport studies by McClure (Prof. Kannewurf's group) on linear-chain metal complexes are an outgrowth of previous syntheses and characterization by Marks' and Ibers' students. Current



elaboration of this concept for a rational synthesis of mixed valence materials involves the partial oxidation of metal porphyrin and other tetraazaannulene metal complexes. This work is complemented by two reports on the electronic structure of metal porphyrins (Hoffman and Ratner).

Theoretical descriptions of charge transport in chains were considered by Professor Mark Ratner and his student Mary Ondrechen, who report on studies of the site-to-site electron transport in some simple model systems. Several reports by Ratner in collaboration with Zunger and Moskowitz describe the development and testing of pseudopotential representations for inner-shell electrons. These pseudopotentials greatly simplify current calculations on complex solids, such as AgI based ionic conductors, and various linear-chain electronic conductors.

The abstract by Ammlung, Shriver, Kamimoto and Whitmore, represent the first published account of fast ion transport in  $\text{In}^+$  and  $\text{Tl}^+$  halide systems. As reported, Raman spectroscopy is an excellent tool for the characterization of these materials and for the identification of the best prospects for high ionic conductivity. Detailed temperature and pressure dependent Raman studies by Greig and Shriver on  $\text{Ag}_2\text{HgI}_4$  reveal a high degree of anharmonicity in certain Ag-I modes, and suggest that this property may be an important contributor to ion transport.

The development of accurate methods for band structure calculations on complex systems has been one of the major achievements of Professors Freeman and Ellis and their co-workers. As shown in the present report, the electronic properties of  $\text{TiS}_2$  and  $\text{TiSe}_2$ , calculated by Zunger and Freeman, agree well with experiment, and the results provide insight into the occurrence of charge density waves and into the semimetal properties of  $\text{TiS}_2$ . Similar theoretical approaches are being taken in the study of  $\text{ZrSe}_2$ , which has been the topic of considerable research in this thrust group. Some of the experimental work in this area is reported here by Ratajack on the transport and optical properties of iron intercalated  $\text{ZrSe}_2$ . This work on iron intercalated  $\text{ZrSe}_2$  is part of a broad program involving syntheses, structures and transport properties of metal intercalated dichalcogenides.

Freeman, Ellis and their co-workers also have had a strong interest in refractory electronic materials, such as the metal carbides and borides. Some of the most recent work in this area is reported by M. Gupta and Freeman on the phonon anomalies of  $\text{NbC}$  and  $\text{TaC}$ . These results link the phonon mode softening to an anomalous response function of the conducting electrons.

Ellis and co-workers report here on calculated band structure and Fermi surfaces of  $\text{LaB}_6$  and  $\text{YB}_6$ , which show that the high superconductivity transition of these systems cannot be explained by simple density of states arguments. Other studies on refractory materials include the use of the local density formalism to the calculation of cohesive properties of diamond cubic boron nitride and lithium fluoride. The paper by M. Gupta, Freeman and Ellis on  $\text{VO}_2$ , which is abstracted below, provides band structure information, which compare well with experiment. These results will be important in the magnetic studies of clustering in  $\text{VO}_2$ , which are being undertaken by a new member of the Charge Transport Thrust Group, Professor Fine.

Professor Ellis has had a continuing interest in relativistic effects, which are expected to be important in many of the heavy-metal materials being studied by members of the Thrust Group. In the present report he describes a simple moment-polarization scheme for handling relativistic effects.

This year marked the beginning of Professor Whitmore's association with the group. His current research work is in the area of ionic and mixed ionic-electronic conductors, particularly heavy-metal ionic conductors and alkali metal intercalated layered dichalcogenides which are mixed conductors.

A NEW CLASS OF HIGHLY CONDUCTIVE MOLECULAR SOLIDS:  
THE PARTIALLY OXIDIZED PHTHALOCYANINES

J. L. Petersen, C. S. Schramm, D. R. Stojakovic,  
B. M. Hoffman and T. J. Marks  
[J. Amer. Chem. Soc. 99, 1977]

The solid state oxidation of purified Fe, Co and Ni, Cu, Zn, Pt and metal-free phthalocyanines by iodine vapor or solutions, results in darkly-colored solid materials with a range of stoichiometries. Resonance Raman, Iodine-129 Mössbauer and X-ray powder diffraction studies indicate the oxidized material contains  $\text{I}_3^-$  and phthalocyanine units with non-integral formal oxidation states. Conductivity and magnetic susceptibility results for the Fe, Ni and Co phthalocyanines are presented. These results, along with the structural data cited above lead us to conclude that the partial iodine oxidation reported here produces molecular solids with highly anisotropic (quasi-one dimensional) metallic properties. We note in particular that these compounds are the first such materials to include 3d transition metals.

Support: NSF-MRL, PRI, Sloan and Dreyfus

ORGANIC ELECTRICAL CONDUCTORS

Tobin J. Marks

[McGraw-Hill Yearbook of Science and Technology]

A feature of one-dimensional organic and metal-organic solids which is believed to be essential for metallic properties is the presence of stacked molecular entities which have fractional formal oxidation states, i.e., which have fractionally occupied electronic valence shells. One attractive scheme for synthesizing new types of materials with this characteristic would be to array stacks of flat (to insure stacking) highly polarizable (small electron site correlation energies) donor molecules (D) which interact strongly and which each transfer a non-integral amount (per D molecule) of electronic charge to some acceptor, A, in the lattice. The A moiety must also be polarizable and must be sufficiently compact to be easily incorporated into the lattice of D stacks. Most importantly, to guarantee "partial oxidation" of the D units, the A must form stable polynuclear anions,  $A_n^{-1}$ . Thus each A would increase the formal oxidation state of each D by the fraction  $+1/n$ . This strategy is highly successful when the donor units are a variety of readily accessible and chemically flexible organic and metal-organic macrocycles, e.g., certain planar organics and heterocycles, phthalocyanines, bisdioximates, and when the acceptor is iodine. Because of the high stability of polyiodides such as  $I_3^{-1}$  and  $I_5^{-1}$  in nonpolar environments and because the shape of these molecules allows them to occupy relatively narrow channels in one-dimensional lattices, these acceptors are ideally suited for introducing mixed valency. In a solid of stoichiometry DI, if iodine is present at  $I_3^{-1}$ , then D has given up 0.33 units of electronic charge and is thus in a fractional oxidation state. Furthermore, the powerful combination of resonance Raman and iodine -129 Mössbauer spectroscopy readily identifies the form of the iodine present in the lattice, i.e.,  $I_2$ ,  $I^{-1}$ ,  $I_3^{-1}$ ,  $I_5^{-1}$  or a combination thereof, and thus allows a direct measurement of the extent of electronic charge transfer from D to A. This information is of considerable importance in refining present theories of electron transport.

Support: NSF-MRL, PRI, Sloan and Dreyfus



ASSESSING THE DEGREE OF PARTIAL OXIDATION IN  
ONE-DIMENSIONAL CONDUCTING IODIDES

T. J. Marks, D. F. Webster, S. L. Ruby and S. Schultz  
[J. Chem. Soc., Chemical Communications 444, 1976]

The solid-state electron transport properties of stacked planar inorganic and organic molecular systems are frequently enhanced by chemical oxidation. In the case of square planar transition metal complexes, halogen oxidation can produce highly (and anisotropically) conducting mixed valence materials such as  $\text{K}_2\text{Pt}(\text{CN})_4\text{Br}_{0.30} \cdot 3\text{H}_2\text{O}$ . Any rational synthetic program to expand the diversity and to control the properties of such compounds must be guided by a means of assaying the degree of oxidation. This is also true for any theoretical attempts to understand the physical properties. In many cases the actual degree to which the stacked square planar moieties have been oxidized, i.e., the extent of electron transfer from donor to acceptor, remains a mystery. This is especially true of a number of iodine-containing materials where frequently x-ray diffraction structures are nonexistent or disordered, and where iodine could be present as  $\text{I}_3^-$ ,  $\text{I}^-$ ,  $\text{I}_5^-$  or  $\text{I}_2$ . We demonstrate here that the combination of resonance Raman and iodine -129 Mössbauer spectroscopy represents a powerful and convenient tool for structure and oxidation state elucidation in such iodine-containing compounds. Studies of the stacked unidimensional materials  $(1,2\text{-benzoquinone-dioximato})_2\text{NiI}_x$ ,  $x = 0.5 - 0.7$  reveal that iodine is present predominantly as  $\text{I}_3^-$ , hence that the square planar nickel moieties are in the formal fractional oxidation state  $x/3$ . Though we illustrate with an inorganic example, the approach should be applicable to numerous organic donor systems as well.

Support: NSF-MRL, NSF, ERDA, Sloan and Dreyfus

NEW RESULTS AND DIRECTIONS IN PHTHALOCYANINE CHEMISTRY

Tobin J. Marks  
[J. Coatings Technology 48, 1976]

New reactions and possible technical applications of phthalocyanine and phthalocyanine-like materials are reported. The synthesis and properties of a uranium "superphthalocyanine" complex which contains five rather than four isoindoline subunits in the macrocyclic ring are discussed. Also, it has been found that partial oxidation of a number of metal and metal-free phthalocyanines with iodine yields mixed valence solids with high electrical conductivity. These materials have been characterized by a variety of spectroscopic

and structural techniques. The new partially oxidized phthalocyanine materials are unique for two important reasons. First, they possess a great chemical flexibility in terms of metal and ligand which offers the opportunity to "fine tune" solid state properties. Second, unlike the starting materials for other highly conductive molecular solids, phthalocyanines are today produced on a millions of pounds per year scale by the pigment industry and are thus extremely cheap.

Support: NSF-MRL, NSF, PRI, Sloan and Dreyfus

RATIONAL SYNTHESIS OF NEW UNIDIMENSIONAL SOLIDS:  
CHEMICAL AND PHYSICAL STUDIES OF MIXED VALENCE POLYIODIDES

Tobin J. Marks

[Annals of the New York Academy of Sciences, in press]

There has recently been intense interest on the part of chemists and physicists in the solid state properties of materials which contain strong unidimensional structural and electronic interactions. The reason for this interest is that such one-dimensional and quasi one-dimensional systems sometimes exhibit rather spectacular and highly anisotropic electrical, magnetic, and optical properties. Many of these materials which contain molecular stacks have in common the property of mixed valency, i.e., the entities in the stack have formal fractional oxidation states. A crucial test of solid state theory and a challenge to chemical methodology would be to devise a rational synthesis of such mixed valence lattices. One approach that we have pursued is the use of iodine oxidants and the high stability of the polyiodide products to convert various flat, stackable donor systems (D) into unidimensional mixed valence lattices. Thus, in a solid of stoichiometry DI, if iodine is present as  $I_3^{-1}$ , then D has increased its formal oxidation state by +0.33. Furthermore, iodine-containing acceptors are readily amenable to spectroscopic characterization. The powerful combination of resonance Raman and iodine -129 Mössbauer spectroscopy readily identifies the form of the iodine present in the lattice, i.e.  $I_2$ ,  $I^{-1}$ ,  $I_3^{-1}$ ,  $I_5^{-1}$  or a combination thereof, and thus allows a direct and accurate estimation of the extent of electronic charge transfer from D. This technique is easily applied to even non-crystalline and severely disordered materials. Such charge distribution information is of great importance in refining present theories of electron transport and has never before been acquired with such ease or for such a wide range (vide infra) of materials.



This article surveys recent research on the rational synthesis of uni-dimensional mixed valence materials by the strategy outlined above, and on the physicochemical properties of the resulting products. The physical basis of the resonance Raman/iodine -129 Mössbauer technique of charge distribution measurement is first discussed, then results are presented in the areas of partially-oxidized metal bisdioximates and phthalocyanines.

Support: NSF-MRL, NSF, ONR, PRI and Dreyfus

METAL-METAL BOND CLEAVAGE REACTIONS. THE CRYSTALLIZATION  
AND SOLID STATE STRUCTURAL CHARACTERIZATION  
OF CADMIUMTETRACARBONYLIRON

Richard D. Ernst, Tobin J. Marks and James A. Ibers  
[J. Am. Chem. Soc. 99, 1977]

Reversible bond cleavage reactions represent an attractive synthetic approach to the synthesis and purification of polymeric materials containing chains of metal atoms. Thus we have found that the classical compound  $\text{CdFe}(\text{CO})_4$ , long believed to be a polymer, can be cleaved by certain Lewis bases to produce soluble species of the formulation  $\text{B}_n\text{CdFe}(\text{CO})_4$ ,  $n = 2$  or  $3$ . Reversal of the cleavage allows, for the first time, crystallization of  $\text{CdFe}(\text{CO})_4$  and determination of its molecular structure by single crystal x-ray diffraction. The compound crystallizes from acetone-water in the monoclinic space group  $\text{C}_{2h}^5\text{-P2}_1/n$ , with two tetrameric  $[\text{CdFe}(\text{CO})_4]_4$  units and four molecules of acetone in a unit cell of dimensions  $a = 6.292(4) \text{ \AA}$ ,  $b = 10.566(6) \text{ \AA}$ ,  $c = 26.024(11) \text{ \AA}$ ,  $\beta = 97.80(3)^\circ$ . Full-matrix least-squares refinement gave a final value of the conventional R index (on F) of 0.032 for 1602 reflections having  $F_o^2 > 3\sigma(F_o^2)$ . The molecular structure consists of a nearly planar, centrosymmetric eight-membered ring of alternating Cd and cis- $\text{Fe}(\text{CO})_4$  units. The geometry deviates from square  $\text{D}_{4h}$  symmetry principally in that two opposite Fe-Cd-Fe angles are  $170.25(5)^\circ$  and two are  $189.85(5)^\circ$ . This reflects weak coordination of each of two cadmium atoms to an acetone oxygen atom ( $\text{Cd-O} = 2.688(9) \text{ \AA}$ ). The Cd-Fe distances are within experimental error all equal at  $2.562(3) \text{ \AA}$ . The major distortion from octahedral symmetry about the  $\text{Fe}(\text{CO})_4$  groups is a bending of the axial carbonyl ligands toward the ring centroid and away from the vector perpendicular to the plane containing the metal atoms. The result is an average C-Fe-C angle of  $154.7(4)^\circ$  for these groups. The acetone can be removed from the lattice with minimal changes in the metal-metal bonding geometry. The base-induced cleavage reaction for this

Group II system is similar to the previously reported cleavage of  $[R_2MFe(CO)_4]_2$  molecules where M = Ge, Sn, Pb.

Support: NSF-MRL, NSF, PRI, Sloan and Dreyfus

METAL-METAL BOND CLEAVAGE REACTIONS. THE CRYSTAL AND MOLECULAR STRUCTURE OF (2,2' -BIPYRIDYL)CADMIUMTETRACARBONYLIRON, (2,2' -BIPYRIDYL)CdFe(CO)<sub>4</sub>

Richard D. Ernst, Tobin J. Marks and James A. Ibers  
[J. Am. Chem. Soc. 99, 1977]

The oligomeric derivative of CdFe(CO)<sub>4</sub>, (2,2' -bipyridyl)CdFe(CO)<sub>4</sub> crystallizes from hot 1, 2, 4-trichlorobenzene as a trimer with the stoichiometry  $[(bipy)CdFe(CO)_4]_3 \cdot \frac{3}{4}C_6H_3Cl_3$ . The crystals belong to the tetragonal space group  $S_4^1-P\bar{4}$  with eight six-membered metal-metal bonded rings and six solvent molecules in a unit cell of dimensions  $a = b = 29.049(10) \text{ \AA}$ ,  $c = 13.241(5) \text{ \AA}$ ,  $V = 11.170 \text{ \AA}^3$ . Full matrix least-squares refinement yielded a final value of the conventional R index (on F) of 0.066 for 5643 reflections having  $F_o^2 > 3\sigma(F_o^2)$ . The molecular structure consists of nearly planar rings of alternating cis-Fe(CO)<sub>4</sub> and (bipy)Cd units. The ring is distorted from ideal D<sub>3h</sub> to approximate C<sub>2</sub> symmetry by compression along a C<sub>2</sub> axis in the plane of the ring. All Fe-Cd distances are equal within experimental error [2.640(7) Å]. The Cd-Fe-Cd angles vary from 138.81(15)° to 148.40(15)°, and the Fe-Cd-Fe angles from 94.78(14)° to 102.04(16)°. The iron coordination geometry is significantly distorted from an octahedral one toward a tetrahedral one in which cadmium atoms cap two of the faces. There is evidence for a weak semibridging interaction between carbonyl carbon and cadmium atoms. The Cd-Fe bonding in  $[(bipy)CdFe(CO)_4]_3$  appears to be more ionic than in  $[CdFe(CO)_4]_4$ .

Support: NSF-MRL, NSF, PRI, Sloan and Dreyfus

ARYLDIAZO COMPLEXES. SYNTHESIS AND STRUCTURE OF A FIVE-COORDINATE COMPLEX POSSESSING A "HALF DOUBLY BENT" ARYLDIAZO LIGAND AND AN INTERMEDIATE COORDINATION GEOMETRY,  $[IrCl(N_2C_6H_5)(P(CH_3)(C_6H_5)_2)_3][PF_6]$

Martin Cowie, Barry L. Haymore and James A. Ibers  
[J. Am. Chem. Soc. 98, 1976]

The complex  $[IrCl(N_2C_6H_5)(P(CH_3)(C_6H_5)_2)_3][PF_6]$  has been prepared with the specific intent of inducing the aryldiazo ligand into a geometry intermediate between the previously observed singly and doubly bent geometries.

This has been accomplished by employing ligands of intermediate bulk ( $\text{P}(\text{CH}_3)(\text{C}_6\text{H}_5)_2$ ) to distort the coordination geometry of the Ir atom from its electronically favored geometry. The structure of this iridium-aryldiazo complex has been determined crystallographically and consists of discrete cations and anions. The cation is five-coordinate with a highly distorted geometry about the metal which cannot be adequately described by an idealized geometry. The intermediate coordination geometry about the iridium atom is mirrored by the geometry of the aryldiazo ligand which is intermediate between singly and doubly bent. Some relevant metrical parameters are: Ir-N(1), 1.835(8) Å; N(1)-N(2), 1.241(11) Å; N(2)-C(11), 1.421(11) Å; Ir-N(1)-N(2), 155.2(7)°; N(1)-N(2)-C(11), 118.8(8)°. The hexafluorophosphate anion is disordered. The compound crystallizes from acetone in space group  $\text{C}_2^2-\text{P2}_1$  with  $a = 15.767(7)$  Å,  $b = 15.583(7)$  Å,  $c = 9.002(4)$  Å,  $\beta = 91.67(2)^\circ$  and  $Z = 2$ . The pseudo-mirror-symmetry of the cation caused great difficulty in the solution of the structure, as it was very difficult to differentiate the correct atomic positions from the mirror-related images. The correct solution was obtained by excluding those solutions which resulted in highly irregular bond angles and distances and in unreasonably short nonbonded contacts. Based on 7134 reflections with  $F_o^2 \geq 3\sigma(F_o^2)$ , the structural data were refined by full-matrix, least-squares methods to R indices of  $R = 0.046$  and  $R_w = 0.072$ . The synthesis, spectra, and reaction chemistry of the complex are discussed.

Support: NSF-MRL and National Research Council of Canada

BLUE COPPER PROTEINS: SYNTHESIS, SPECTRA AND STRUCTURES  
OF  $\text{Cu}^{\text{I}}\text{N}_3(\text{SR})$  AND  $\text{Cu}^{\text{II}}\text{N}_3(\text{SR})$  ACTIVE SITE ANALOGUES

Jeffery S. Thompson, Tobin J. Marks and James A. Ibers  
[Proc. Nat. Acad. Sci., USA, in press]

The reaction of  $\text{Cu}(\text{SR})$  or  $[\text{Cu}(\text{SR})][\text{ClO}_4]$  derivatives,  $\text{SR} = p\text{-nitro-benzenethiolate}$  or  $O\text{-ethylcysteinate}$ , with potassium hydrotris-(3,5-dimethyl-1-pyrazolyl)borate produces redox pairs of the stoichiometry  $\text{Cu}^{\text{I}}\text{N}_3(\text{SR})$  and  $\text{Cu}^{\text{II}}\text{N}_3(\text{SR})$ . These complexes are the first well-defined synthetic approximations to the proposed  $\text{N}_3\text{S}$  binding sites of blue (type 1) copper electron transfer proteins. The new compounds were investigated by a variety of chemical and spectral (optical, resonance Raman, electron paramagnetic resonance) techniques; the complex  $\text{K}[\text{Cu}(\text{HB}(3,5\text{-Me}_2\text{pz})_3)(p\text{-NO}_2\text{C}_6\text{H}_4\text{S})] \cdot 2 \text{ acetone}$  was also studied by single crystal x-ray diffraction methods. The spectrochemical characteristics of the  $\text{Cu}^{\text{I}}\text{N}_3(\text{SR})$  species are in large part similar to the



native system and thus provide some perspective regarding the origin of the unique type 1 spectral parameters and electron transfer properties.

Support: NSF-MRL

SINGLE-CRYSTAL ELECTRON NUCLEAR DOUBLE RESONANCE STUDIES  
OF SILVER(II) AND COPPER(II) TETRAPHENYLPORPHYRINS

Theodore G. Brown, Jeffrey L. Petersen, George P. Lozos,  
James R. Anderson and Brian M. Hoffman  
[Inorg. Chem. 16, 1977]

The importance of understanding the bonding in planar transition ion complexes such as the metalloporphyrins has led us to undertake a comparative study of silver(II) and copper(II) tetraphenylporphyrins (TPP) through the use of electron nuclear double resonance (ENDOR) on oriented, dilute single crystals. These are the first such studies on these systems, and the enhanced resolution available from ENDOR uniquely permits us to map out the odd-electron distribution within these molecules, to compare the M-N bonding in the two systems, and gives information about their geometric configurations as well.

Support: NSF-MRL, NSF and NIH

JAHN-TELLER EFFECTS IN METALLOPORPHYRINS  
AND OTHER FOURFOLD SYMMETRIC SYSTEMS

Brian M. Hoffman and Mark A. Ratner  
[Submitted for publication]

The Jahn-Teller (J-T) effect in systems of four-fold symmetry is well known to differ from that in all other point groups with respect to the nature of the J-T active normal modes of vibration. The present report addresses some previously unnoticed features which are of intrinsic importance in recognizing and understanding the unique manifestations of quadrate symmetry in both the static and dynamic Jahn-Teller effects. We first consider the nature of the static J-T potential surfaces when coupling to and strains in two modes,  $b_1$  and  $b_2$ , are included in the Hamiltonian.

The second part of this paper is devoted to an examination of the dynamic J-T effect in four-fold systems. Utilizing both perturbation theory and numerical solution to the Schrödinger equation, we examine the spin-Hamiltonian parameters for a metalloporphyrin  $^3E_u$  triplet state and discuss some dynamical processes, including reorientation of the system between minima, spin-lattice

relaxation, and the dependences of these phenomena on the nature and magnitude of the off-diagonal terms in the Hamiltonian. There emerge from this analysis several signal differences between the Jahn-Teller effect for a doubly degenerate state in four-fold systems and in the more usual cubic or tetrahedral situation.

Support: NSF-MRL

APPLICATIONS OF MODEL HAMILTONIANS TO THE ELECTRON DYNAMICS  
OF ORGANIC CHARGE TRANSFER SALTS

Mark A. Ratner, John R. Sabin and Samuel B. Trickey  
[The Uncertainty Principle and the Foundations  
of Quantum Mechanics, Wiley, 1977]

Many of the charge-transfer salts based on planar aromatic organic electron-acceptor molecules, such as tetracyanoquinodimethan or chloranil, crystallize in segregated stacks of donor and acceptor molecules. These stacks provide large overlap of valence orbitals, and as a result the salts can become rather good conductors, though the conductivity is usually activated due to disorder. To describe magnetic excitations in these systems, the Heisenberg (1926, 1928) model has been applied quite successfully (Soos, 1974). In particular, salts have been observed which exhibit both delocalized and localized spin excitations, depending on the magnitude of the Heisenberg exchange integral  $J$ . The electrical properties of these systems can be discussed in terms of modified Hubbard (1963) or Pariser-Parr-Pople (Parr, 1963; Lindenberg and Öhrn, 1968, 1973) models, which have been shown (Van Vleck, 1966; Anderson, 1963, Lindenberg and Öhrn, 1968) to be equivalent (to second order) to the Heisenberg (1926, 1928; Dirac, 1929) model.

We shall discuss the general nature of the excitations in these systems, certain experimental results and the numerical estimation of tunnelling, exchange and repulsion parameters. Comments about vibronic effects and geometry dependence will also be included. Finally, questions of dimensionality are considered very briefly, in connection with the low-temperature phase transitions which these systems undergo. Similarities to other molecular systems are indicated.

Support: NSF-MRL



# FIRST-PRINCIPLES PSEUDOPOTENTIAL IN THE LOCAL DENSITY FUNCTIONAL FORMALISM

Alex Zunger, Sid Topiol and Mark Ratner  
[Submitted for publication]

A first principles approach to the pseudopotential method is developed in the local density formalism (LDF). It is shown that due to the locality of the exchange-correlation operator in the LDF, the present pseudopotential method is exactly equivalent to a frozen core approximation. As an example, tests on the carbon atom potential are given. Comparison of the energy eigenvalues and total energy differences obtained in accurate self-consistent numerical solutions of the all-electron problem with those of the pseudopotential problem reveals an error smaller than  $10^{-3}$  a.u. for a very wide range of electronic configuration and excitation states. Charge density observables such as moments of  $r$  and x-ray scattering factors are obtained with accuracy of better than 0.1%. Applications to large-scale electronic structure calculations as well as comparison of the results with the empirical pseudopotential scheme are discussed.

Support: NSF-MRL and NSF

## THE USE OF PSEUDOPOTENTIALS WITHIN LOCAL-DENSITY FORMALISM CALCULATIONS FOR ATOMS: SOME RESULTS FOR THE FIRST ROW

Sid Topiol, Alex Zunger and M. A. Ratner  
[Chem. Phys. Lett., in press]

The use of a pseudopotential to replace the core electron density within electronic structure calculations of Kohn-Sham type is proposed. An heuristic derivation of such a potential is given. Within the local exchange-correlation scheme, the pseudopotential employed is precisely equivalent to solving a frozen-core problem; this is quite different from the situation encountered in using pseudopotentials in Hartree-Fock calculations, where additional approximations are involved. Numerical results for several excited and ionic states of first row atoms are given; the errors due to the frozen core are less than  $10^{-3}$  Hartree.

Support: NSF-MRL and NSF

A NEW, SIMPLE *ab initio* PSEUDOPOTENTIAL FOR USE IN FSGO CALCULATIONS:  
APPLICATION TO SOME LITHIUM COMPOUNDS

Sid Topiol, A. A. Frost, J. W. Moskowitz and M. A. Ratner  
[J. Chem. Phys. 65, 1977]

A new model potential designed for use within an FSGO framework is proposed. Results of calculation using this new model for Li compounds are in good agreement with all-electron FSGO results.

Support: NSF-MRL and NSF

PSEUDOPOTENTIAL CALCULATIONS: SOME ELECTRONIC PROPERTIES OF ZINC DICHLORIDE

Mark A. Ratner, Jules W. Moskowitz and Sid Topiol  
[Chem. Phys. Lett. 46, 1977]

*Ab-initio* calculations are performed for the  $\text{ZnCl}_2$  molecule, employing recently-developed pseudopotential methods. Two separate calculations are discussed, one treating the d-electrons explicitly, the other including the d's in the core. The description of the valence region seems quite satisfactory, with only negligible errors arising from the use of the pseudopotential. Comparison is made to the photoelectron spectrum, and to the  $\text{ZnF}_2$  molecule.

Support: NSF-MRL and NSF

INTRAMOLECULAR ELECTRON TRANSFER IN SIMPLE MODEL SYSTEMS:  
A PROPAGATOR STUDY

Mary Jo Ondrechen and Mark A. Ratner  
[J. Chem. Phys. 66, 1977]

The probability of site-to-site intramolecular electron or hole transfer as a function of time in simple model systems is calculated. Systems studied are the hydrogen molecule, allyl cation, and cyclopropenium ion, in the Hubbard model. We employ the method of electron propagators, using both exact and approximate (molecular orbital and valence bond) ground state wavefunctions. We conclude that the molecular orbital wavefunction affords a good description of the transfer process for a wide variety of systems. The utility of our approach for the calculation of electron transfer rates in which purely electronic effects are dominant is stressed.

Support: NSF-MRL

INTRAMOLECULAR ELECTRON TRANSFER: SIMPLE THEORY OF PURELY ELECTRONIC EFFECTS

Mark A. Ratner and Mary Jo Ondrechen  
[Mol. Phys. 32, 1976]

Within a given simple model hamiltonian of extended Hückel, Hubbard or CNDO type, we derive, using perturbation theory, an expression for the effective transfer rate of an electron or hole from one region within the molecule to another. Vibronic interactions, though crucial to the real, observed rate process, are ignored for present purposes; rather, attention is focused on comparative electronic effects. Perturbation theory is used to derive relations for effective transfer integrals. Application to mixed valence dimeric systems as well as to substituted biphenyl derivatives is suggested. Brief comparison with other treatments is outlined.

Support: NSF-MRL

THE SCREENED INDO (INDO/S) MODEL: APPLICATION TO  
PHOTOELECTRON SPECTRUM OF BENZONITRILE

Karsten Krogh-Jespersen and Mark Ratner  
[J. Chem. Phys. 65, 1977]

A screened INDO model, which we previously developed for analysis of optical spectra and excited-state properties of organic compounds, is applied to the prediction of photoelectron spectra. Results are quite satisfactory for benzene, and an assignment based on Koopman's theorem allows complete assignment, including previously unassigned peaks, in the benzonitrile molecule.

Support: NSF-MRL

IONIC AND MIXED CONDUCTORS FOR ENERGY STORAGE AND CONVERSION SYSTEMS

D. H. Whitmore  
[J. Crystal Growth, in press]

Experimental information is reviewed on the structures and the ionic transport properties of a number of solids which are predominantly ionic conductors possessing unusually mobile selected ionic species. The structural criteria for finding fast ionic diffusivity in such solid phases (fast ion conductors) is discussed and the current status of the theory of optimized ionic conduction in solid electrolyte materials is reviewed.

Recent data on selected materials which exhibit tunnel or layer structures, within which significant charge transport occurs due to the motion of both ionic and electronic species (mixed conductors), is also discussed. Emphasis is placed here on those mixed conductors which might find application as cathode materials in secondary cells.

Support: NSF-MRL, ARPA-MRL and ERDA

TEMPERATURE DEPENDENT RAMAN SPECTRA OF THE ORDERED  
AND DISORDERED PHASES OF  $\text{Ag}_2\text{HgI}_4$  AND  $\text{Cu}_2\text{HgI}_4$

D. R. Creig, G. C. Joy III and D. F. Shriver  
[J. Chem. Phys., in press]

Raman spectra of  $\text{Ag}_2\text{HgI}_4$  were collected over the temperature range  $8^\circ$  to  $470^\circ\text{K}$ . The ordered phase of  $\text{Ag}_2\text{HgI}_4$  exhibits strong temperature dependent damping of the  $85\text{ cm}^{-1}$  mode. The reduced Raman spectra of the disordered phases of both  $\text{Ag}_2\text{HgI}_4$  and  $\text{Cu}_2\text{HgI}_4$  are found to be temperature dependent. This unusual temperature dependence is attributed to the combined influence of anharmonicity, multiphonon processes, and the correlation time for ion hopping. An estimate of the latter was obtained from the line broadening data. Based on polarized scattering data obtained on very small crystals, symmetry assignments are made for some of the Raman bands of  $\text{Ag}_2\text{HgI}_4$ .

Support: NSF-MRL

PRESSURE DEPENDENT RAMAN SPECTRA OF THE FAST ION CONDUCTORS  
 $\text{Ag}_2\text{HgI}_4$  AND  $\text{Cu}_2\text{HgI}_4$

D. Creig, D. F. Shriver and J. R. Ferraro  
[J. Chem. Phys. 66, 1977]

Pressure dependent Raman data indicate that modes associated with CuI and AgI stretching are highly anharmonic. This result indicates that further studies of anharmonicity in superionic conductors are warranted because a highly anharmonic potential may be important in providing a low energy barrier for ion motion. In contrast with previous conductivity data the high pressure Raman spectra strongly indicate that no structural phase change occurs in the vicinity of 4 kbar for  $\text{Ag}_2\text{HgI}_4$  and the Raman data also provide clues to the structure of the high pressure phases.

Support: NSF-MRL



CONDUCTIVITY AND RAMAN SPECTROSCOPY OF NEW INDIUM(I) AND THALLIUM(I)  
IONIC CONDUCTORS.  $\text{In}_4\text{CdI}_6$ ,  $\text{In}_2\text{ZnI}_4$  AND  $\text{Tl}_2\text{ZnI}_4$ ,  
AND THE RELATED COMPOUND  $\text{Tl}_4\text{CdI}_6$

R. L. Ammlung, D. F. Shriver, M. Kamimoto and D. H. Whitmore  
[J. Solid State Chem. 21, 1977]

The new compound  $\text{Tl}_2\text{ZnI}_4$  has been prepared and characterized by Raman spectroscopy, powder x-ray diffraction, elemental analyses, and a partial binary phase diagram. The compounds  $\text{In}_4\text{CdI}_6$ ,  $\text{Tl}_4\text{CdI}_6$ , and  $\text{In}_2\text{ZnI}_4$ , for which phase diagrams are available in the literature, were characterized by Raman spectroscopy and their identity confirmed by elemental analyses and x-ray powder diffraction. Each of these materials, except  $\text{Tl}_4\text{CdI}_6$ , undergoes a sharp order-disorder phase transition at elevated temperatures, that can be detected by the measurement of Raman spectra as a function of temperature. Conductivity measurements as a function of temperature, using both reversible and blocking electrodes, reveal a high ionic conductivity in the disordered, high-temperature phase. This work suggests that indium(I) and thallium(I) ionic conductors may exist, analagous to some well-known double salt conductors based on simple silver(I) and copper(I) halides. In addition, the present study demonstrates the usefulness of Raman spectroscopy in the characterization of heavy-metal ionic conductors.

Support: NSF-MRL, ERDA and NSF

RAMAN SCATTERING FROM THE SUPERIONIC CONDUCTOR SILVER TETRAIODOMERCURATE(II)  
AND OTHER RELATED COMPOUNDS

D. R. Greig  
[Ph.D. Thesis, June, 1977]

The Raman scattering from the superionic conductor  $\text{Ag}_2\text{HgI}_4$  has been studied in detail and additional data was collected on some related compounds. Oriented single crystal spectra were collected on  $\beta\text{-Ag}_2\text{HgI}_4$  which allowed partial assignments of the symmetry types of the bands. The mercury-iodide symmetric stretch is assigned at  $122\text{ cm}^{-1}$ , and silver-iodide modes between  $80$  and  $106\text{ cm}^{-1}$ .

The effect of temperature on the Raman spectrum of  $\text{Ag}_2\text{HgI}_4$  was studied between  $8$  and  $470^\circ\text{K}$ . The silver-iodide modes between  $80$  and  $106\text{ cm}^{-1}$  broaden considerably at very low temperatures (below  $100^\circ\text{K}$ ), and this is believed to be due to high anharmonicity of the silver ion potential well. The order-disorder phase transition at  $323^\circ\text{K}$  shows a dramatic change in the Raman



spectrum; all of the bands broaden considerably, and the low frequency region simplifies to one peak at ca.  $17\text{ cm}^{-1}$  with a shoulder at ca.  $30\text{ cm}^{-1}$ . In addition, a shoulder at  $142\text{ cm}^{-1}$  appears that has no counterpart in the  $\beta$ -phase spectrum. Various possible mechanisms for the broadening are discussed, with the dominant contribution believed to be a relaxation of the  $\vec{k}=0$  selection rule, thereby allowing light scattering from the entire Brillouin zone. In addition, it is felt that there is a significant contribution from time correlation effects since the mobile ions may be hopping on a time scale similar to the vibrational time scale. Disorder induced broadening is observed in amorphous solids, where it has been shown that the Raman spectrum may be "reduced" by Bose-Einstein and harmonic oscillator factors to arrive at an approximate density of states spectrum. This analysis has been applied to  $\alpha\text{-Ag}_2\text{HgI}_4$  and  $\alpha\text{-Cu}_2\text{HgI}_4$  which results in a rather similar density of states for the two materials.

High pressure spectra for  $\text{M}_2\text{HgI}_4$  ( $\text{M}=\text{Ag}, \text{Cu}, \text{Tl}$ ) were collected in a diamond anvil cell. The silver salt appears to have at least five distinct structural phases in the 0 to 10 kbar and 25 to  $100^\circ\text{C}$  region. The  $\alpha$ -phase undergoes a transition at ca. 6 kbar to a new phase that exhibits strong, narrow bands, which is consistent with the report that this phase exhibits poor ionic conductivity. The copper salt does not show any phase transitions at room temperature between 0 and 28 kbar, thereby allowing the bands to be tracked over a large pressure range. The copper-iodide mode at  $86^{-1}$  shows a much greater sensitivity to pressure than any other mode, which gives another indication of high anharmonicity of the mobile ion potential well.

Finally, the possibility of using Raman line broadening and Rayleigh line enhancement as a screening technique for superionic conductors is discussed. A number of examples of this application are given, and it is believed that this technique could be quite valuable, particularly for the order-disorder type superionic conductors.

Support: NSF-MRL - Advisor: D. F. Shriver

ELECTRICAL AND OPTICAL PROPERTIES OF THE SEMICONDUCTOR ALLOY  $\text{In}_{1-x}\text{Tl}_x\text{Te}$

C. A. Gaw and C. R. Kannewurf

[San Diego Meeting of the American Physical Society  
March, 1977]

Electrical and optical properties of the semiconductor alloy system  $\text{In}_{1-x}\text{Tl}_x\text{Te}$  for compositions  $x = 0.1, 0.2$  and  $0.5$  are reported. From electrical conductivity, optical absorption and photoconductivity data on single crystal samples the energy gap is shown to narrow in a linear fashion from the semiconductor composition  $x = 0.5$  to the semimetal binary composition  $\text{InTe}$ . Optical absorption data on the body-centered tetragonal composition at  $x = 0.5$  show indirect band gaps in the range  $0.74$  to  $0.92$  eV; electrical conductivity data indicate a somewhat lower energy gap. For each composition the electrical conductivity and Hall effect from  $77^\circ$  to  $300^\circ\text{K}$  are presented. The photoconductive spectral response of these compositions is shown at  $77^\circ\text{K}$ . The peak photoresponse is at  $1.3 \mu\text{m}$  for the  $x = 0.5$  composition and moves farther out in the infrared as  $x$  decreases from  $0.5$ . Potential application of the narrow gap compositions for infrared photodetectors is discussed.

Support: NSF-MRL

OPTICAL DISPERSION AND ELECTRICAL TRANSPORT STUDIES  
OF IRON INTERCALATED ZIRCONIUM DISLENIDE

Mark T. Ratajack

[Ph.D. Thesis, June, 1977]

The intercalation system  $\text{Fe}_x\text{ZrSe}_2$  has been found to exist in two distinct phases; a semiconducting phase for  $0 \leq x < 1/3$  and a metallic phase for  $x \approx \frac{1}{2}$ . The structure of the semiconducting phase is a variation of the  $\text{CdI}_2$  -  $\text{NiAs}$  intermediate type with octahedral coordination of Se atoms about both Fe and Zr atoms. The metallic phase is found to crystallize with six formula units per unit cell in a structure in which the Fe atoms are in octahedral holes while the Zr atoms are trigonal prismatically coordinated by Se atoms.

A study of the far infrared reflectance spectra of the semiconducting phase of this system has been performed. The dispersion analysis was performed by means of computer programs which analyze the spectra by both Kramers-Kronig and Lorentzian oscillator techniques. From the oscillator model it was possible to extract information regarding the effect of iron intercalation upon the bonding character of the material. A single reststrahlen band was observed at  $\omega_{\text{TO}} = 102 \text{ cm}^{-1}$  for the unintercalated host and

no additional modes were observed as a result of iron intercalation. The single Lorentzian oscillator strength and damping were found to increase with iron concentration and the electronic (high frequency) polarizability showed a linear increase with  $x$ . As a result, the iron intercalation was observed to increase the macroscopic effective charge and hence the ionicity of the compound.

The features of the  $\text{Fe}_x\text{ZrSe}_2$  system can be explained by a rigid band model in which the  $\text{ZrSe}_2$  host lattice determines the basic band structure and the Fe nonbonding levels remain localized. To verify this model, electrical conduction studies were employed to determine the activation energies of the Fe levels. These studies indicate that the Fe levels lie within a conduction band for the metallic phase and within the forbidden gap of the host  $\text{ZrSe}_2$  for the semiconducting phase. An analysis of the temperature dependence of the resistivity for the semiconducting phase has shown that the Fe levels extend over a narrow range of energy approximately 0.12 eV below the bottom of the conduction band. Further analysis of these results indicates that the mobility is independent of the intercalate iron concentration.

Support: NSF-MRL - Advisor: C. R. Kannewurf

#### ELECTRICAL CONDUCTION STUDIES OF Fe INTERCALATED $\text{ZrSe}_2$

M. T. Ratajack, J. F. Revelli, J. B. Wagner and C. R. Kannewurf  
[San Diego Meeting of the American Physical Society,  
March, 1977]

The  $\text{Fe}_x\text{ZrSe}_2$  system has been found to exist in two distinct phases; a semiconducting phase for  $x < 0.3$  and a metallic phase for  $x \approx 0.5$ . The conductivity of the semiconducting phase increases with Fe concentration and is characterized by an exponential temperature dependence with a compositionally independent activation energy of approximately 0.06 eV. The metallic phase exhibits a power law temperature dependence of conductivity. These results are interpreted to mean that the intercalation of Fe results in impurity-like levels which lie within the forbidden gap of the host  $\text{ZrSe}_2$  for the semiconducting phase (octahedral Zr) and within the conduction band for the metallic phase (trigonal prismatic Zr), accounting for the observed behavior.

Support: NSF-MRL



BAND STRUCTURE AND LATTICE INSTABILITY OF  $\text{TiSe}_2$

Alex Zunger and A. J. Freeman  
[Submitted for publication]

The energy band structure of  $\text{TiSe}_2$ , determined in the local density approach yields a semi-metal (band overlap  $0.20 \pm 0.05$  eV) with holes at  $\Gamma$  and electron pockets only at L. The dimensions of the electron pocket indicate the presence of  $7-8 \times 10^{20}$  carriers/cm<sup>3</sup> in excellent agreement with both transport and angular resolved photo-emission data. The observed charge density wave is attributed to characteristic "volume" effects, i.e., nesting of parallel electron-hole bands at  $E_F$  separated by the  $\Gamma$ -L zone boundary wave vector.

Support: NSF-MRL, AFOSR and ERDA

SELF-CONSISTENT NUMERICAL BASIS SET LINEAR-COMBINATION-OF-ATOMIC-ORBITALS  
INVESTIGATION OF THE ELECTRONIC STRUCTURE AND PROPERTIES OF  $\text{TiS}_2$

Alex Zunger and A. J. Freeman  
[Phys. Rev. B, June, 1977]

A fully-self-consistent numerical basis set LCAO calculation of the electronic structure of  $\text{TiS}_2$  is reported using the method described previously. The calculated band structure differs considerably from those previously obtained by non-self-consistent muffin-tin models. Comparison with experiment shows the calculated optical properties for energies below 16 eV and the various characteristics of the valence and conduction bands to agree very well with optical absorption and electron energy loss data as well as with photoemission, x-ray absorption and appearance potential spectra. A small indirect gap (0.2 - 0.3 eV) occurs at the points M and L in the Brillouin zone with a larger direct gap (0.8 eV) at  $\Gamma$ . We suggest that the characteristic semi-metallic large g-value observed experimentally originates from a near coincidence of the band gap with the enhanced spin-orbit splitting which is consistent with the soft x-ray data and our band model. The bonding mechanism in  $\text{TiS}_2$  is discussed in detail; it is shown by a direct calculation of the self-consistent charge density and the transverse effective charge that the system is predominantly covalent with small static ionic character and large dynamic ionicity. In contrast with muffin-tin  $X\alpha$  models, the bonding is found to be largely due to Ti 4s4p to S 3p bonds and a much weaker Ti 3d to S 3p bond. The effects of muffin-tin approximation and self-consistency are discussed in detail. Extrapolations of these results to the case of  $\text{TiSe}_2$  is made and the possible origin



of its charge density wave is discussed.

Support: NSF-MRL, AFOSR and ERDA

GENERALIZED ELECTRONIC SUSCEPTIBILITY AND CHARGE-DENSITY WAVES  
IN 1 T-TaS<sub>2</sub> AND 1 T-TaSe<sub>2</sub>

H. W. Myron, J. Rath and A. J. Freeman  
[Phys. Rev. b 2, 1977]

Generalized susceptibilities,  $\chi^0(\vec{q})$ , have been obtained for the 1 T polymorphs of both TaS<sub>2</sub> and TaSe<sub>2</sub> from their Korringa-Kohn-Rostoker band structures. Peaks are found which correspond to the charge-density-wave (CDW) nesting vectors found by Wilson, Di Salvo and Mahajan and appear to confirm the role of electronically driven instabilities as the origin of the observed CDW in these metals.

Support: NSF-MRL

LOCAL DENSITY FORMALISM APPROACH TO COHESIVE PROPERTIES  
OF SOLIDS: DIAMOND, BN AND LiF

Alex Zunger and A. J. Freeman  
[Intern. J. Quantum Chem. Symp. 11, 1977]

Predictions of the local density formalism approach to cohesive properties of covalently bonded solids (diamond and cubic BN) and prototype ionic system (LiF) are described using results of our recently developed fully self-consistent numerical basis set LCAO-DVM approach. Comparisons with restricted Hartree-Fock results and experiment for cohesive energies and equilibrium lattice constants are presented. Some of the principal bonding mechanisms in these crystals are discussed in terms of the contributions of local exchange and correlation to the binding and the charge redistribution relative to the non-interacting atoms.

Support: NSF-MRL, NSF and AFOSR

DEFECT STATE MODEL FOR LOCALIZED EXCITATIONS IN LiF

Alex Zunger and A. J. Freeman  
[Phys. Lett. 60, 1977]

We find that a defect state treatment of localized excitations in LiF within the local density functional formalism accounts remarkably well for the observed experimental (core plus optical gap) excitations--in contrast to the failure of the one-electron band model. We show that when electron relaxation, self-interaction and charge polarization effects are taken into account by treating the excitation as a localized point defect, the improved band model predicts the correct exciton and interband states.

Support: NSF-MRL and AFOSR

Ab initio SELF-CONSISTENT STUDY OF THE ELECTRONIC STRUCTURE  
AND PROPERTIES OF CUBIC BORON NITRIDE

Alex Zunger and A. J. Freeman  
[Submitted for publication]

We present the results of a first-principles fully self-consistent study of the electronic properties of cubic boron nitride in the local density formalism using our previously published numerical basis set LCAO scheme. The resulting band structure shows considerable disagreement with previously published orthogonalized plane wave, augmented plane wave, and pseudopotential studies. A detailed study of the ground state properties of the system, such as x-ray scattering factors, cohesive energy, equilibrium lattice constant, and their behavior under pressure, yields very good agreement with available experimental data. Reasonably good agreement is obtained for excited state properties determined by optical and x-ray absorption measurements. The bonding characteristics in this prototype of III-V compounds are discussed in detail and compared with results of our previous study of its isoelectronic homopolar analog, diamond, and with studies on the hexagonal graphite-like modification of BN.

Support: NSF-MRL and AFOSR

SELF-CONSISTENT NUMERICAL-BASIS-SET LINEAR-COMBINATION-OF-ATOMIC-ORBITALS  
MODEL FOR THE STUDY OF SOLIDS IN THE LOCAL DENSITY FORMALISM

Alex Zunger and A. J. Freeman  
[Phys. Rev. B 15, 1977]

A new approach to the fully self-consistent solution of the one-particle equations in a periodic solid within the Hohenberg-Kohn-Sham local-density-functional formalism is presented. The method is based on systematic extensions of non-self-consistent real-space techniques of Ellis, Painter and collaborators and the self-consistent reciprocal-space methodologies of Chaney, Lin, Lafon and co-workers. Specifically, our approach combines a discrete variational treatment of all potential terms (Coulomb, exchange and correlation) arising from the superposition of spherical atomiclike overlapping charge densities, with a rapidly convergent three-dimensional Fourier series representation of all the multicenter potential terms that are not expressible by a superposition model. The basis set consists of the exact numerical valence orbitals obtained from a direct solution of the local-density atomic one-particle equations and (for increased variational freedom) virtual numerical atomic orbitals, charge-transfer (ion-pair) orbitals, and "free" Slater one-site functions. The initial crystal potential consists of a non-muffin-tin superposition potential, including nongradient free-electron correlation terms calculated beyond the random-phase approximation. The usual multicenter integrations encountered in the linear-combination-of-atomic-orbitals tight-binding formalism are avoided by calculating all the Hamiltonian and other matrix elements between Bloch states by three-dimensional numerical Diophantine integration. In the first stage of self-consistency, the atomic superposition potential and the corresponding numerical basis orbitals are modified simultaneously and nonlinearly by varying (iteratively) the atomic occupation numbers (on the basis of computed Brillouin-zone averaged band populations) so as to minimize the deviation,  $\Delta\rho(\vec{r})$ , between the band charge density and the superposition charge density. This step produces the "best" atomic configuration within the superposition model for the crystal charge density and tends to remove all the sharp "localized" features in the function  $\Delta\rho(\vec{r})$  by allowing for intra-atomic charge redistribution to take place. In the second stage, the three-dimensional multicenter Poisson equation associated with  $\Delta\rho(\vec{r})$  through a Fourier series representation of  $\Delta\rho(\vec{r})$  is solved and solutions of the band problem are found using a self-consistent criterion on the Fourier coefficients of  $\Delta\rho(\vec{r})$ . The observables include the total crystal ground-state energy, equilibrium lattice constants, electronic pressure, x-ray scattering factors,

and directional Compton profile. The efficiency and reliability of the method is illustrated by means of results obtained for some ground-state properties of diamond; comparisons are made with the predictions of other methods.

Support: NSF-MRL

#### GROUND-STATE ELECTRONIC PROPERTIES OF DIAMOND IN THE LOCAL-DENSITY FORMALISM

Alex Zunger and A. J. Freeman  
[Phys. Rev. B 15, 1977]

We use our previously reported method for solving self-consistently the local-density one-particle equations in a numerical-basis-set linear combination of atomic orbitals expansion to study the ground-state charge density, x-ray structure factors, directional Compton profile, total energy, cohesive energy, equilibrium lattice constant, and behavior of one-electron properties under pressure of diamond. Good agreement is obtained with available experiment data. The results are compared with those obtained by the restricted Hartree-Fock model: the role of electron exchange and correlation on the binding mechanism, the charge density, and the momentum density is discussed.

Support: NSF-MRL

#### GROUND AND EXCITED STATE PROPERTIES OF LiF IN THE LOCAL DENSITY FORMALISM

Alex Zunger and A. J. Freeman  
[Submitted for publication]

The band structure, charge density, x-ray scattering factor (and their behavior under pressure), equilibrium lattice constant, and cohesive energy of the prototype ionic solid LiF were determined using our recently developed self-consistent numerical basis set (non-muffin-tin) LCAO method, within the local density formalism (LDF). The details of the bonding and the effects of exchange and correlation on the electronic structure are discussed with reference to the conventional picture of ionic bonding. Remarkable good agreement is found with the observed data for the ground state properties of the system. Contrary to the results of previous band studies, the conventional band structure approach to excitation energies (i.e., identifying them with the band eigenvalue differences) is found to fail completely in accounting for the observed data in the entire x-ray and optical spectral region when fully self-consistent solutions of the LDF one-particle equation with no further



approximation to the crystal potential, are obtained. It is found that in the presence of some spatial localization of the initial or final crystal states, the spurious self-interaction terms, as well as the polarization and orbital relaxation self-energy effects are of a similar order of magnitude as the Koopmans'-like interband terms. In order to treat these effects within the LDF self-consistently, we describe the excitation processes as transitions involving point defect-like states in the solid calculated by a supercell method in which the excitation energies are determined as total-energy differences between (separately calculated) excited and ground state configurations. The excited state is represented as a superlattice of locally excited sites using large (8 and 16 atom) unit cells, each containing a single excited site. We find, in the self-consistency limit, that a small but finite degree of spatial localization of the excited states exists even for valence excitations, inducing thereby self-interaction as well as self-energy relaxation and polarization effects. The LDF model is found to account very well for both interband and exciton transitions over the entire spectral region (12-695 eV) and to yield definite predictions regarding the exciton band widths and series limits.

Support: NSF-MRL, NSF, AFOSR and ERDA

# ROLE OF ELECTRONIC STRUCTURE ON OBSERVED PHONON ANOMALIES OF TRANSITION-METAL CARBIDES

Michèle Gupta and A. J. Freeman  
[Phys. Rev. B 14, 1976]

The possible role of electronic structure on observed phonon anomalies in high-temperature superconducting transition-metal carbides is studied by means of accurate *ab initio* calculations of the conduction electron response function. From augmented-plane-wave determinations of the electronic band structure, density of states, and Fermi surface of NbC and TaC, the wave-vector-dependent generalized susceptibility,  $\chi(\vec{q})$ , is calculated in the constant-matrix-element approximation. For both NbC and TaC,  $\chi(\vec{q})$  has strong maxima at precisely those  $\vec{q}$  values at which soft modes were observed by Smith and Gläser. Maxima in  $\chi(\vec{q})$  are predicted for other directions. The locus of these  $\vec{q}_{\text{max}}$  values can be represented by a warped cube of dimension  $\sim 1.2(2\pi/a)$  in momentum space--in striking agreement with the soft-mode surface proposed phenomenologically by Weber. In sharp contrast, the  $\chi(\vec{q})$  calculated for both ZrC and HfC--for which no phonon anomalies have been observed--fall off in all symmetry directions away from the zone center. In agreement with Phillips, we thus

interpret the phonon anomalies in the transition-metal carbides as due to an "overscreening" effect resulting from an anomalous increase of the response function of the conduction electrons.

Support: NSF-MRL

DIRECT CORRELATION OF OBSERVED PHONON ANOMALIES AND MAXIMA IN THE  
GENERALIZED SUSCEPTIBILITIES OF TRANSITION METAL CARBIDES

Michèle Gupta and A. J. Freeman  
[Superconductivity in d- and f-Band Metals (1976)  
Edited by D. H. Douglass, Plenum Pub. Corp.]

The generalized susceptibility,  $\chi(\vec{q})$ , of both NbC and TaC determined from APW energy band calculations show large maxima to occur at precisely those  $\vec{q}_{\max}$  values at which soft phonon modes were observed by Smith. Maxima in  $\chi(\vec{q})$  are predicted for other directions. The locus of these  $\vec{q}_{\max}$  values can be represented by a warped cube of dimension  $\sim 1.2(2\pi/a)$  in momentum space--in striking agreement with the soft mode surface proposed phenomenologically by Weber. In sharp contrast, the  $\chi(\vec{q})$  calculated for both ZrC and HfC--for which no phonon anomalies have been observed--fall off in all symmetry directions away from the zone center. We thus interpret the phonon anomalies in the transition metal carbides as due to an "overscreening" effect resulting from an anomalous increase of the response function of the conduction electrons.

Support: NSF-MRL, NSF, AFOSR and ERDA

ELECTRONIC STRUCTURE AND PROPERTIES OF EuO AND EuS  
IN THE MOLECULAR-CLUSTER APPROXIMATION

E. Byrom, D. E. Ellis and A. J. Freeman  
[Phys. Rev. B 14, 1976]

Molecular-cluster models are developed to describe ground-state properties of EuO and EuS in the Hartree-Fock-Slater one-electron approximation. Spin-polarized  $(EuX_6)^{0-}$  complexes are examined using both neutral- and ionic-model potentials which incorporate a part of the effect of the crystalline environment. Self-consistent calculations are made for  $(EuO_6)^{10-}$ . From the charge and spin densities, the transferred hyperfine field at the O site in EuO is found to be  $-8 \pm 2$  kG and a small solid-state bonding effect is predicted for the neutron magnetic form factor. The pressure dependence of the charge density at the Eu nucleus in EuS is determined as a function of bond length

in the  $(\text{EuS}_6)^{10-}$  cluster and used to obtain from the experimental data an isomershift calibration constant  $\alpha = -0.48 \text{ a}_0^3 \text{ mm/sec}$ . The one-electron energy levels of the  $(\text{EuO}_6)^{10-}$  cluster are found to be in good agreement with the augmented-plane-wave results of Cho when both calculations are performed with similar model potentials. The extension to self-consistency leads to significant energy-level rearrangement which indicates the importance of final-state relaxation and Coulomb correlation effects in the interpretation of experimental spectra.

Support: NSF-MRL

MOMENTUM DENSITIES AND COMPTON PROFILES OF DIAMOND,  
SILICON AND SILICON CARBIDE

A. Seth and D. E. Ellis  
[J. Phys. C 10, 1977]

Momentum densities and Compton profiles were calculated for the tetrahedral semiconductors diamond, silicon carbide and silicon, making use of approximate Hartree-Fock-Slater crystal wavefunctions. Reasonable agreement is found with available experimental data and also with the calculations of Wepfer, Euwema, Surrat and Wilhite on diamond. Anisotropies of momentum densities and Compton profiles are analysed by means of spherical harmonic expansions. Although the spherical components are remarkably similar when scaled according to lattice momentum  $2\pi/a$ , the anisotropic components of the three crystals show distinctive features.

Support: NSF and AFOSR

CHEMICAL BONDING AND X-RAY EMISSION SPECTRA ANALYSIS  
FOR NIOBIUM CARBIDE, NITRIDE AND OXIDE

Michèle Gupta, V. A. Gubanov and D. E. Ellis  
[J. Phys. Chem. Solids 38, 1977]

A molecular orbital description of  $(\text{NbX}_6)^{n-}$  clusters with  $X = \text{C}, \text{N}$  and  $\text{O}$  has been obtained in the Hartree-Fock-Slater model. Effects of spin polarization and self-consistent iterations on energy levels and charge distribution are explored; comparison is made to band structure results. The calculated x-ray emission spectra are in reasonably good agreement with experiment.

Support: NSF and AFOSR

ENERGY BANDS AND BONDING IN  $\text{LaB}_6$  AND  $\text{YB}_6$

P. F. Walch, D. E. Ellis and F. M. Mueller  
[Phys. Rev. B 15, 1977]

Energy bands of the "covalent metal"  $\text{LaB}_6$  have been calculated by a discrete variational method in the Hartree-Fock-Slater model. We find that the basic topology of the bands and the predicted Fermi surface are rather insensitive to the atomic configuration assumed in constructing the potential. The proposed Fermi surface is consistent with the basic features of published experimental de Haas-van Alphen data; it is not consistent with the hypothesis of magnetic breakdown which has been invoked to explain the finer details. A study of selected valence-band and conduction-band wave functions supports the conclusion that La-B bonding is more important than La-La bonding in explaining the metallic behavior of  $\text{LaB}_6$ . The total density of states and the inter-band joint density of states for several bands are calculated and the results are compared to x-ray and optical data. Preliminary calculations of the energy bands of  $\text{YB}_6$  are presented; the similarity of these bands to those of  $\text{LaB}_6$  cannot be explained by simple density-of-states arguments.

Support: NSF-MRL

MOLECULAR CLUSTER THEORY OF CO CHEMISORPTION ON A NICKEL(100) SURFACE

D. E. Ellis, E. J. Basrands, Hirohiko Adachi and F. W. Averill  
[Surface Science, 1977]

Self-consistent Hartree-Fock-Slater molecular cluster models for the chemisorption of carbon monoxide on a (100) transition metal surface are presented. Energy levels and charge distribution for the  $\text{CO:Ni}_5$  cluster in  $C_{4v}$  symmetry are obtained, and the variation of binding energies with height of the CO molecule above the surface of nickel is studied in detail. Comparison is made with experimental binding energy spectra and with the multiple-scattering results of Batra and Bagus. The redistribution in energy of free-atom valence levels is studied by means of local-densities-of-states diagrams.

Support: NSF and NASA



RARE-EARTH ORTHOVANADATES: COVALENCY, CHEMICAL BONDING AND OPTICAL SPECTRA

V. A. Gubanov, D. E. Ellis and A. A. Fotiev  
[J. Struc. Chem, 1977]

Investigations of electronic structure and optical spectra were made for yttrium orthovanadate, and for rare-earth orthovanadates  $RVO_4$ , where  $R = Ce, Nd, Eu, Tb, Dy, Gd$  and  $Yb$ . The Hartree-Fock-Slater model was used in conjunction with a numerical discrete variational method to calculate energy levels and wavefunctions for molecular clusters  $(VO_4)^{3-}$  and  $(RO_8)^{13-}$  found in the orthovanadate crystal lattice. Analysis of the MO charge and spin densities reveals a significant involvement of rare-earth 4f orbitals in chemical bonding, through hybridization of R-5p and mixing with O-2p atomic orbitals. The MO energy level diagrams provide a satisfactory semiquantitative interpretation of the experimental excitation, reflection, and luminescence spectra. Energy transfer from the vanadate ion to the rare-earth ion is understood in terms of covalent mixing between metal and shared O-2p orbitals for neighboring  $(VO_4)^{3-}$  and  $(RO_8)^{13-}$  clusters. The relative luminescent efficiency of some rare-earth elements is explained on the basis of the calculated energy level diagrams.

Support: AFOSR

MOMENT-POLARIZED RELATIVISTIC POTENTIALS

D. E. Ellis  
[J. Phys. B, 1977]

Exchange potentials are considered in a Dirac-Slater local density approximation, with the aim of simultaneously treating orbital polarization and relativistic effects in open-shell systems. A simple moment-polarized scheme analogous to the spin-unrestricted non-relativistic theory is developed, and illustrated by application to diatomic FeO.

Support: NSF

ELECTRONIC STRUCTURE AND LATTICE INSTABILITY OF METALLIC  $\text{VO}_2$

Michele Gupta and A. J. Freeman  
[Phys. Rev. B, 1977]

A first principles energy band study of the metallic rutile phase of  $\text{VO}_2$ , using a general crystal potential and an expansion of the Bloch functions in a linear combination of atomic orbitals, is reported. The results are compared with previous work and experimental optical, x-ray absorption and emission, and x-ray photoelectron spectroscopy data. We obtain a large density of states at the Fermi energy; the Fermi surface is found to be determined by the two lowest d bands, at the bottom of the " $t_{2g}$ " manifold which is split by the orthorhombic field; the lowest band Fermi surface possesses some nesting features corresponding to a nesting vector  $\vec{q} = \Gamma R$ . A calculation of the generalized susceptibility in the constant matrix elements approximation shows the existence of a maximum at the zone boundary R. We suggest that the formation of a charge density wave with wave vector  $\vec{q} = \Gamma R$ , accompanied by a periodic lattice distortion is thus possible; the subsequent condensation of phonons at the point R could then explain the crystallographic phase transition observed at  $T = 339$  K.

Support: NSF-MRL, AFOSR and ERDA

Thrust Area Research

Support:  
NSF-MRL Program

FATIGUE OF METALS AND ALLOYS

Faculty:

M. Meshii, Professor, Materials Science and Engineering, Group Leader  
M. E. Fine, Professor, Materials Science and Engineering  
T. Mura, Professor, Civil Engineering  
L. H. Schwartz, Professor, Materials Science and Engineering  
J. Weertman, Professor, Materials Science and Engineering  
J. R. Weertman, Assistant Professor, Materials Science and Engineering

Research Staff:

K. Hamada, Visiting Scholar, Civil Engineering  
Y. Hamada, Visiting Scholar, Civil Engineering  
M. Uemura, Research Associate, Materials Science and Engineering  
A. K. Vasudevan, Research Associate, Materials Science and Engineering  
K. J. Kim, Visiting Scholar, Materials Science and Engineering

Graduate Students:

C. R. Aita, Materials Science and Engineering  
D. L. Anton, Materials Science and Engineering  
C. E. Atchley, Materials Science and Engineering  
R. R. Castles, Engineering Science and Applied Mathematics  
R. T. Chen, Materials Science and Engineering  
P. C. H. Cheng, Civil Engineering  
A. H. D. Chiou, Materials Science and Engineering  
B. Ditchek, Materials Science and Engineering  
D. Gan, Materials Science and Engineering  
T. S. Gross, Materials Science and Engineering  
N. Hsieh, Materials Science and Engineering  
Y. Izumi, Materials Science and Engineering  
Y. H. Kim, Materials Science and Engineering and Civil Engineering  
C. Y. Kung, Materials Science and Engineering  
K. P. Liaw, Materials Science and Engineering  
R. G. Pahl, Materials Science and Engineering  
D. J. Quesnel, Materials Science and Engineering  
T. Saegusa, Materials Science and Engineering  
W. H. Schlosberg, Materials Science and Engineering  
S. Stock, Materials Science and Engineering  
C. Vilman, Civil Engineering

Personnel Who Have Left:

C. R. Aita, U. S. Gypsum, Inc., Des Plaines, Illinois  
C. E. Atchley, present situation not known  
P. C. H. Cheng, Fluor Pioneer, Inc., Chicago, Illinois  
K. Hamada, returned to Japan  
D. J. Quesnel, University of Rochester, Rochester, N. Y.

Degrees Granted:

C. R. Aita, Ph.D., August, 1977  
P. C. H. Cheng, Ph.D., June, 1977  
D. J. Quesnel, Ph.D., August, 1977

Other Sponsorship:

NSF-MRL, National Science Foundation, Materials Research Laboratory  
AFOSR, Air Force Office of Scientific Research  
AISI, American Iron and Steel Institute  
Alcoa, Alcoa Foundation Fellowship  
Cabell, Cabell Fellowship  
Inland Steel  
NSF, National Science Foundation  
ONR, Office of Naval Research

Introduction

Fatigue of metals and alloys has been known to engineers and scientists for 150 years. Nevertheless, fatigue is still the major cause of failure of engineering materials. Although the strength of engineering materials has been improved significantly in the last few decades, a corresponding improvement in fatigue resistance has been disappointingly limited. The monotonic strength is relatively well understood in terms of dislocation theory and the microstructure of metals and alloys; on the contrary, the fatigue strength is still very poorly understood. The method most commonly used to quantify the fatigue behavior of engineering materials is the plot of stress amplitude,  $S$ , versus the number of cycles to failure,  $N$ . The fatigue strength is often represented by this  $S$ - $N$  curve. However, it is now understood that a number of processes are involved in fatigue and that each is expected to have a different dependence on structure, stress, strain, temperature, environment, etc., and to take place by a different mechanism. Therefore, fatigue research must be multifaceted: each process must be identified and its dependence on the variables must be determined. A close relationship between theoretical and experimental investigations is essential. The theoretical formulation needs a continual input of new information on the characterization and detailed mechanism of the fatigue processes. The experimental studies are often guided by the theoretical predictions. Fatigue research requires a multidisciplinary approach; expertise in mechanical testing, electron microscopy, x-ray diffraction, physical metallurgy, dislocation theory, and continuum mechanics is essential.



Fatigue research must maintain a balance between materials most suitable for the identification of mechanisms and materials which possess high strength. The limitation in fatigue strength is particularly critical in high monotonic strength materials. Recent investigations have shown that fatigue processes can be quite different in low and high strength materials.

The Fatigue Thrust Group has been conducting research with these considerations in mind and the projects are, therefore, coordinated to achieve maximum efficiency. Recently, the following points have been emphasized:

- 1) Plastic deformation behavior under cyclic stress: How does the cyclic plastic deformation differ from monotonic deformation, what is the corresponding dislocation behavior, and how does the microstructure affect the cyclic deformation and the dislocation motion under cyclic stress?
- 2) Initiation of fatigue cracks: How does cyclic deformation result in crack initiation? How is the crack initiation affected by microstructures? Can we predict the crack initiation from a standard test?
- 3) Fatigue crack propagation: Can crack propagation rates be determined from material parameters (e.g., cyclic yield stress,  $\sigma'_y$ , cyclic plastic work,  $U$ , etc.) and the stress condition? The identification of crack tip plastic zones, their measurement and the identification of fatigue crack propagation mechanics and the overloading effect are being studied.

A recent extension of the theory of fracture mechanics by Professor J. Weertman permits, for the first time, a first principles calculation of the fracture criterion for materials which undergo small scale plastic yielding prior to fracture. The fracture stress can be predicted solely from a knowledge of the stress-strain curve and the true surface energy.

Theories of the rate of fatigue crack growth propagation,  $dc/dN$ , predict that  $dc/dN$  at constant stress intensity amplitude,  $\Delta K$ , varies inversely with the cyclic yield stress,  $\sigma_y$ , and the plastic work required per unit area of crack advance,  $U$ . The theories of Professor Weertman and Professor Mura and Dr. Lin in this area also pointed out the importance of  $U$  as one of the rate controlling factors, but this has not been demonstrated experimentally. Recently Professor M. E. Fine and coworkers have measured  $U$  for three steels and four aluminum alloys. These results agree with the theories of Weertman and Mura and Lin and demonstrated the prominent role that  $U$  plays in controlling  $dc/dN$ .

An important principle for increasing the fatigue strength of metals has been developed by Professor M. E. Fine and coworkers. Steels aged to produce a bimodal precipitate structure, i.e., a coherent precipitate and a larger carbide, had a much greater resistance to the initiation of fatigue cracks compared to a structure consisting of carbides alone, both steels being at the same strength level.

Professor Schwartz has studied the effects of the mechanically induced austenite-martensite transformation on the crack growth rate and the plastic work required per unit area of crack advance,  $U$ , in iron-nickel and iron-manganese cryogenic steels. The amount of retained austenite was varied by heat treatments and determined by the Mössbauer effect before and after failure.

Professor J. R. Weertman has been studying void formation during high temperature fatigue and was able to correlate the void formation sites with serrations in grain boundaries in high purity copper. The observation explains why the void formation during fatigue is considerably faster than that predicted by the existing theory of void growth.

Professor Mura is currently working on a theory of fatigue employing continuum mechanics and thermodynamics. The theory will explain why repeated loadings cause failure in materials at the stress level at which the materials would not fail for static loadings.

Professor Meshii has been investigating the cyclic creep behavior of iron, iron-carbon alloys, and 7050 high strength aluminum alloys. The specific interest is in the cyclic creep acceleration (CCA). The temperature and stress dependence of CCA have been determined and the role of the alloy elements in causing CCA is now known. The relationship between the state of dispersion of the alloy elements and the effect on CCA is being investigated.

The residual stress distribution and its evolution during cyclic deformation has been investigated by Professors Quesnel, Meshii, and Cohen in cold-rolled HSIA steel. At a high strain amplitude, the initial distribution is quickly displaced by a new distribution, characteristic of the given cyclic deformation. It is found that the distribution and orientation dependence of the residual stress reverses this sign during each cycle.

The following abstracts of reports have been prepared from the research activities of the Fatigue Thrust Group and represent some of the accomplishments described above during the 1976-1977 academic year.

## THE RESPONSE OF HIGH STRENGTH LOW ALLOY STEEL TO CYCLIC PLASTIC DEFORMATION

D. J. Quesnel and M. Meshii  
[Mat. Sci. and Eng., in press]

The low cycle fatigue behavior of a niobium-bearing HSLA steel has been investigated at room temperature at an applied total strain rate of  $\dot{\epsilon} = 10^{-2} \text{ s}^{-1}$ . Specimens are examined in the as-hot-rolled condition, the cold-rolled 50% condition and the annealed condition. It has been shown that cyclic saturation is not always obtained in HSLA steels and further that this transient portion of the stress response to constant strain amplitude cycling may be represented by a power law. The cyclic hardening rate thus defined is independent of cycling and shows a smooth variation with strain amplitude. The behavior is substantially different for the three specimen treatments with the exception that each treatment suggests cyclic softening at sufficiently low strain amplitudes. The cyclic stress-strain curves obtained by incremental step method are presented along with companion specimen cyclic stress-strain curves obtained at 1, 10 and 50 percent of crack initiation life. It is found that the number of cycles to crack initiation does not depend strongly on the specimen condition. The energy associated with crack initiation is examined experimentally for this HSLA steel. The results agree quite well with an empirical derivation of this quantity based on the Coffin-Manson relation and the power law cyclic stress-strain relation. It appears that for broad classes of engineering materials, the hysteretic energy associated with crack initiation rises sharply with decreasing strain amplitude.

Support: NSF-MRL

## INFLUENCE OF CARBON ON THE STATIC AND CYCLIC CREEP BEHAVIORS OF ALPHA IRON

D. K. Shetty and M. Meshii  
[Submitted for publication]

Plastic deformation of  $\text{ZrH}_2$  treated iron and iron with a controlled amount of carbon is examined under constant load and repeated loading respectively. The pure iron exhibits cyclic stress acceleration behavior under cyclic loading but the magnitude of creep enhancement is not large and is relatively insensitive to applied stress, a result in contrast to the behavior of f.c.c. metals. The presence of carbon, even in small concentration (65 at. ppm) enhances the relative cyclic stress acceleration when the specimens are aged after carburization. In carburized and quenched specimens, on the

other hand, both static as well as cyclic creep is suppressed. The observed difference in cyclic creep behavior is correlated to the difference in the nature and distribution of carbon and the relative ease of pinning of dislocations by the carbon atoms.

Support: NSF-MRL

#### CYCLIC CREEP OF PURE IRON

A. K. Vasudevan and M. Meshii

Cyclic creep behavior of  $ZrH_2$  purified (1133°K/48 hrs) Ferrovac-E iron is studied by varying the peak stress, temperature, unloading time and frequency. At 255°K, the cyclic creep deceleration was observed prior to cyclic creep acceleration (CCA). At 295°K, only CCA was observed at higher stress levels. The ratio of cyclic to static creep rates increased with peak stress and creep time. The most interesting property observed at both these temperatures is that cyclic creep at higher stress levels approached a constant creep rate which increased with stress ( $\sim 5 \times 10^{-8}$  to  $\sim 2 \times 10^{-6}$  sec<sup>-1</sup>). At 350°K, an additional effect due to interstitial impurities reduced the static creep rate significantly with respect to the cyclic creep rate at the low creep rate range, producing a greater CCA.

Support: NSF-MRL

#### EFFECT OF CARBON ON CYCLIC CREEP OF IRON

A. K. Vasudevan and M. Meshii

In order to study the effects of interstitial solutes on cyclic creep behavior, pure iron specimens were carburized to give  $\sim 80$  at. ppm carbon. Two heat treatments, as-quenched and furnace cooled + aged at 200°C for 12 hrs were employed. While the overall cyclic and static behaviors were similar for both heat treatments at a given stress level, the aged alloy showed relatively greater cyclic creep acceleration (CCA) than the quenched alloy at 295°K. In particular, the CCA was observed to be significant at lower stress levels than at higher stress levels, when the results were compared at a constant creep time. At 255°K, the differences between the static and cyclic creep behaviors were relatively small. The observed CCA in the dilute Fe-C alloy appeared to be dependent on the diffusion of the carbon atoms.

Support: NSF-MRL



# THE CHARACTERIZATION OF CYCLIC CREEP BEHAVIOR OF 7050 ALUMINUM ALLOY

Herng-Der Chiou and M. Meshii

The cyclic unloading of creep stress can increase or decrease the creep rate drastically. The cyclic creep acceleration (CCA) generally occurred at high stress levels and the cyclic creep deceleration (CCD) took place at low stress levels in pure f.c.c. metals such as aluminum and copper. The CCA has been interpreted in terms of static and dynamic recovery processes, while the CCD has been explained by relating to an unloading yield point behavior. The present work extends the cyclic creep study to the high strength 7050 aluminum alloy to examine the effects of microstructure on cyclic behavior. In the as-quenched alloy at 295°K, CCA was observed above the yield stress. However, in the aged alloy at 295°K, CCA was observed only below the yield stress and CCD was found above it. At 198°K, the critical stress (the stress at which CCA changes to CCD) became higher than the yield stress. These results can be interpreted in terms of the work-hardening behavior and structure changes that may occur during cyclic creep.

Support: NSF-MRL

## ON THE EFFECTS OF INTERCRITICAL TEMPERING ON THE IMPACT ENERGY OF Fe-9Ni-0.1C

K. J. Kim and L. H. Schwartz  
[Submitted for publication]

The effects of intercritical tempering on the impact energy of Fe-9Ni-0.1C have been investigated. The Charpy V-notch energy at all test temperatures between 77°K and 300°K increased with increasing precipitated and retained austenite up to concentrations of austenite of  $\approx 14$  pct. and then decreased. Evidence for a mechanically induced austenite  $\rightarrow$  martensite transformation in the plastic zone preceding the crack tip was obtained using Mössbauer effect scattering from the fracture surface. The contribution to the impact energy from this localized TRIP mechanism is shown to be negligible compared to the scavenging effect of the austenite, removing deleterious impurities from the martensite and increasing its toughness. The decrease in impact energy for austenite concentrations in excess of  $\approx 14$  pct. is attributed to the development of a nearly continuous network of austenite in interlath and prior austenite boundaries. In the plastic zone ahead of the crack, this

network is transformed into brittle untempered martensite providing a low energy path for the advancing crack.

Support: AISI and NSF-MRL

AN ANALYSIS OF THE KINETICS OF SPINODAL DECOMPOSITION  
IN Cu-10w/oNi-6w/oSn

B. Ditchek and L. H. Schwartz  
[Submitted for publication]

New data on the amplitude ( $A$ ) and wavelength ( $\lambda$ ) growth with time ( $t$ ) for the sideband alloy Cu-10 w/oNi-6 w/oSn is presented. The amplitude and wavelength are derived from an analysis of the integrated intensity and position of the x-ray diffraction (200) satellites. It is shown that the  $\log A$  vs  $\log t$  curve displays the expected S shaped transformation curve. The  $\log \lambda$  vs  $\log t$  curve displays a constant region at small times followed by a coarsening regime. The theory of spinodal decomposition formulated by Cahn provides a closed form expression for the kinetics of the early stages only. Hence his linearized theory can explain only the small amplitude part of the S transformation curve and the region in which the wavelength remains constant. Recently Tsakalakos obtained an approximate analytical expression for the growth of a symmetric wave which extends Cahn's treatment to the late and coarsening stages. He found

$$A(t) = A_c(\beta, \beta_c(o)) \tanh(A_o(\beta) \exp(R(\beta)t))$$

where  $\beta_c(o)$  is the critical wavenumber and  $R(\beta)$  is the amplification factor defined by Cahn. It is shown that in general the wavenumber which maximizes  $A(t)$  displays both the constant and coarsening regimes of the  $\log \lambda$  vs  $\log t$  curve. In addition the amplitude of this wavenumber displays the S shaped transformation curve. From a comparison of the data on Cu-10 w/oNi-6 w/oSn with the predictions of the Tsakalakos expression the degree of decomposition during the quench and  $R(\beta)$  can be determined. The comparison confirms the spinodal nature of the transformation in Cu-10 w/oNi-6 w/oSn.

Support: NSF-MRL

EFFECTS OF TENSILE OVERLOADS ON CRACK CLOSURE AND CRACK  
PROPAGATION RATES IN 7050 ALUMINUM

R. D. Brown and J. Weertman  
[Submitted for publication]

It has been suggested that the crack closure concept can account for the retardation in crack growth rate following removal of tensile overloads. To test this possibility, measurements of effective stress were made on center notched cracked specimens during tests in which tensile overloads were applied. A comparison of the changes in crack growth rate and in effective stress following removal of the overload indicates that the crack growth rate reaches a minimum value before the effective stress does, indicating that the closure concept cannot account for the decrease in crack growth rate. Additional evidence for the inability of crack closure to account for the retardation in crack growth rate is provided by specimens run at a high mean stress and then overloaded. No crack closure is observed when there is a high mean stress present, yet the crack growth rate does decrease by an amount about the same as that observed at low mean stresses where crack closure is present. Measurements of closure stress and effective stress were obtained from load-displacement curves recorded using an extensometer mounted across the crack on the specimen centerline. This procedure also enabled us to measure the distance over which the crack faces were in contact when the stress was at its minimum value in the stress cycle. The length of crack closed reached a minimum value later than did either the crack growth rate or the effective stress. It occurred when the crack tip had propagated nearly across the plastic zone created by the application of the overload.

Support: NSF-MRL

MEAN STRESS EFFECTS ON CRACK PROPAGATION RATE AND CRACK CLOSURE  
IN 7050-T76 ALUMINUM ALLOY

R. D. Brown and J. Weertman  
[Submitted for publication]

High strength aluminum alloys that are cyclically loaded in tension are known to show increased fatigue crack propagation rates when the mean stress is increased. It has been suggested that this increase in growth rate may be due to a lower crack closure stress. A smaller closure stress results in a higher effective fatigue crack propagation stress. Measurements of the closure stress were made using an extensometer placed across the crack in

order to study the effects of crack closure on the fatigue crack growth rate. The closure stress was determined from the change in slope of load-displacement curves. The growth rate data at various mean stresses were plotted as a function of effective stress intensity factor. In all tests the cyclic stress amplitude was 80 MPa. For specimens run at mean stress levels of 44 MPa and 70 MPa the crack faces were found to close, but on increasing the mean stress to above 120 MPa no closure was observed. The growth rate data from specimens run at mean stresses from 44 MPa to 120 MPa coincided when plotted vs effective stress intensity factor but that crack growth rates for a mean stress of 226 MPa were higher than those obtained at lower mean stresses. We concluded that effects other than crack closure also influence the crack growth rate. Much greater scatter was found in the fatigue crack growth rates of our thicker specimens (5.6 mm thick) than in our thinner specimens (2.5 mm thick). Indirect measurements of the length over which the crack faces were closed showed that the length closed decreased sharply with increasing mean stress. At a mean stress of 44 MPa the length closed at minimum stress was several millimeters, while at 70 MPa it had been reduced to less than 1 mm.

Support: NSF-MRL

#### FRACTURE MECHANICS: A UNIFIED VIEW FOR GRIFFITH-IRWIN-OROWAN CRACKS

J. Weertman

[Submitted for publication]

A unified picture of fracture mechanics is proposed in this paper for small scale yielding conditions (a small plastic zone at a crack tip). For a Griffith crack in a brittle material two equivalent fracture criteria that give the same results can be used. One is an energy argument that uses the true surface energy  $\gamma$  of a solid. The other is based on the intensity of the stress singularity at a crack tip. If the stress singularity is intense enough the stresses at the crack tip can break the solid apart and create surfaces of energy  $\gamma$ . The generalization of the Griffith crack theory to plastic small scale yielding has used only the energy argument. In the generalization the true surface energy is replaced with an effective surface energy that presumably has its origin in plastic work. The physical factor that determines the magnitude of this plastic work surface energy has never been determined. The intensity of the stress singularity at the actual tip of the



crack (rather than the attainment of some stress or strain value within the interior of the plastic zone) has never been used as a fracture criterion before. To have a unified picture of fracture mechanics this criterion should be used and shown to be equivalent to the energy criterion. In this paper it is proposed that the stress strain curve to use in small scale fracture theory is one that is elastic to a yield stress  $\sigma_0$ , is plastic up to a stress of the order of the theoretical strength  $\sigma_T \approx \mu/10$ , where  $\mu$  is the shear modulus), and then is elastic again to infinite stress and strain.

It is shown how to calculate the true stress intensity factor  $K_t$  and the plastic zone parameters for any stress-strain curve for a Mode III crack (a shear crack in anti-plane strain). Because of plastic blunting the true stress intensity factor  $K_t$  is smaller than the stress intensity factor  $K$  of a brittle crack. ( $K = \sigma_a(\pi a)^{\frac{1}{2}}$  for a crack of length  $2a$  in an infinite plate of infinite width subjected to an applied stress  $\sigma_a$ .) The condition of fracture is found after setting  $K_t = K_{cb}$  where  $K_{cb}$  is the critical value of  $K$  for a crack in a perfectly brittle solid. However, the equation  $K_t = K_{cb}$  is not necessarily the fracture equation. Two classes of solids must be distinguished in obtaining a fracture equation. One is a material (called a plastically hard one) that, when no fracture occurs, absorbs more plastic work energy in its plastic zone per unit zone length than the Griffith elastic energy release rate. The other (called plastically soft) absorbs less energy until the moment a Lüders zone propagates outward from the crack tip. The theory can be used to give a very simple explanation of environmental effects in fracture phenomenon. The theory offers support to fatigue crack propagation theories that are based on accumulated energy arguments.

Support: NSF-MRL

#### THEORY OF INTERNAL STRESS FOR CLASS I HIGH TEMPERATURE CREEP ALLOYS

J. Weertman  
[Acta Met., in press]

The internal stress for Class I alloys--the alloys that obey a third power law steady state creep rate--is calculated for two dimensional dislocation models. It is found that if no frictional stress is present, the internal stress is only a small fraction of the applied stress. For an Al-5.5 at.% Mg alloy it is suggested that the temperature dependent frictional

stress that has been measured by Ahlquist and Nix and by Kuchařová, Saxl and Čadek might be produced by a stress induced order microcreep mechanism that is enhanced by the increased magnesium concentration near dislocations. This mechanism, however, does not control the creep rate. The rate controlling mechanism is likely to be either Friedel's, as suggested by Kuchařová et al., or the Cottrell-Jaswon microcreep mechanism.

Support: NSF-MRL

THEORY OF ENHANCED HIGH TEMPERATURE CYCLIC CREEP  
IN POLYCRYSTALLINE MATERIAL

J. Weertman and W. V. Green  
[J. Nuclear Materials, in press]

A theory of high temperature cyclic stress creep rate enhancement is developed that is based on the mechanism of the athermal generation of self interstitial atoms. It is first shown that interstitial atoms cannot be generated athermally at a fast enough rate to affect the creep rate under a constant stress. Under cyclic stressing it may be possible for athermally-generated interstitial atoms to produce an enhanced creep rate. The effect can only be important in the high temperature region from about  $1/3$  to  $1/2$  the melting temperature of the material and then only for fine-grained material that deforms in double or multiple slip. The predicted effect is larger the higher is the frequency of the cyclic stress. This creep rate enhancement effect should be taken into account in the design and material selection of the first-wall material of fusion reactors that operate in pulsed modes, such as reactors using lasers.

Support: ERDA

CREEP LAWS FOR THE MANTLE OF THE EARTH

J. Weertman  
[Submitted for publication]

The analyses of glacial rebound data by Cathles and by Peltier and Andrews have led them to the conclusion that the flow law of the mantle of the Earth is Newtonian and that the viscosity is essentially a constant ( $10^{22}$  poise) throughout the mantle. In this paper it is concluded that no large

strain, steady-state creep process in mantle rock can account for a Newtonian, constant viscosity mantle. It is suggested that small strain, transient creep and not steady-state creep is involved in the isostatic rebound phenomenon. Since convective motion in the mantle involves large creep strains, conclusions about the effective viscosity of mantle rock undergoing such flow that is based on isostatic rebound data are likely to be wrong. If Post's and Carter and Mercier's laboratory results of the stress dependence of the grain size in a mantle type rock are representative of the actual grain sizes in the mantle, power law creep is almost certainly the creep law that governs convective flow in the mantle.

Support: NSF-RANN

#### INFLUENCE OF GRAIN BOUNDARY MORPHOLOGY ON VOID FORMATION

T. Saegusa and J. R. Weertman

This paper describes a study of the effect of stress concentrations on the early stages of development of grain boundary voids formed during high temperature fatigue. A recent theory of cavity growth, based on diffusional processes, predicts that cavities produced by cyclic loading  $\sigma_0 \sin \omega t$  should grow at a rate which differs from the rate under static loading  $\sigma_0$  by a factor  $\approx \sigma_0 \Omega / kT$ . This factor is  $\ll 1$ , yet material stressed in fatigue cavitates at least as readily as in creep. It has been suggested that serrations in grain boundaries produce high stress concentrations normal to the boundaries during gb sliding. In the case of sharp serrations and high frequency of cycling, high normal stresses may be set up near the serration peaks. A detailed investigation has been carried out to correlate the sites of early void formation with respect to gb morphology in high purity Cu cycled at about 1000 cpm at  $1/2 T_m$ . In the early states of fatigue the majority of voids form near serration peaks. The effect of serration development, subgrain boundaries, and frequency of cycling on cavity siting will be described.

Support: NSF

#### VOID GROWTH SUPPRESSION BY DISLOCATION IMPURITY ATMOSPHERES

Johannes Weertman and W. V. Green  
[Am. Soc. for Testing and Materials, 1976,  
Special Technical Publication 611]

A detailed calculation is given of the effect of an impurity atmosphere on void growth under irradiation damage conditions. Norris has proposed that such an atmosphere can suppress void growth. We have found the hydrostatic stress field of a dislocation that is surrounded by an impurity atmosphere and from it have calculated the change in the effective radius of a dislocation line as a sink for interstitials and vacancies. The calculation of the impurity concentration in a Cottrell cloud takes into account the change in hydrostatic pressure produced by the presence of the cloud itself. It is assumed that the hydrostatic pressure field of an impurity atom exists over a radial distance larger than the radius of the impurity atom. It is found that void growth is eliminated whenever dislocations are surrounded by a condensed atmosphere of either oversized substitutional impurity atoms or interstitial impurity atoms. A condensed atmosphere will form whenever the average impurity concentration is larger than a critical concentration.

Support: ERDA

#### CRYSTALLOGRAPHIC FATIGUE FRACTURE IN COPPER SINGLE CRYSTALS

R. Yeske and J. Weertman  
[Met. Trans. A, 8A, 1977]

In an examination of crystallographic effects on fatigue crack growth in pre-stressed copper single crystals, crystallographic facets were observed on the fracture surface. The conditions of facet formation and their effect on crack growth rate are discussed.

Support: ONR



CREEP RATE ENHANCEMENT THEORY FOR IRRADIATED  
SUBSTITUTIONAL SOLID SOLUTION ALLOYS

Johannes Weertman and Walter V. Green  
[Met. Trans. A, 8A, 1977]

A new theory of creep rate enhancement under energetic particle irradiation is developed in this paper. The theory is applicable only to substitutional solid solution alloys in which a diffusion controlled dislocation drag-mechanism (a microcreep mechanism) determines the creep rate. If the dislocation lines are the dominant sinks for point defects, the predicted enhanced creep rate is proportional to the first power of the applied stress. If voids are the dominant point defect sinks then the predicted enhanced creep rate is proportional to the third power of the stress. In both cases the predicted enhanced creep rate is only very weakly dependent upon the temperature.

Support: ERDA

FLUID FLOW THROUGH A LARGE VERTICAL CRACK IN THE EARTH'S CRUST

J. Weertman and S. P. Chang  
[J. Geophys. Res. 82, 1977]

The crack profile and the stress intensity factors for a two-dimensional crack with fluid flowing through it are determined for flow rates applicable to geothermal heat extraction. The entrance and exit portals for the fluid are placed away from the tips of the crack. For vertical cracks of half heights greater than 50 m that have fluids of the viscosity and density of water flowing through them at physically practical velocities it is found that the crack profile and stress intensity factors are essentially the same as those of a crack in which the fluid is stationary.

Support: NSF-RANN

PENETRATION DEPTH OF CLOSELY SPACED WATER-FREE CREVASSES

J. Weertman  
[J. Glaciology 18, 1977]

An approximate, analytic solution is found for the profile of a water-free crevasse in a field of closely spaced crevasses. The depth of penetration of the crevasses into the glacier is found. If the fracture strength of ice

is taken to be zero, the penetration depth is equal to the value found by Nye and is independent of the crevasse spacing. This conclusion is in disagreement with results reported recently by R. A. Smith. If the fracture strength of ice is taken to be finite, the penetration depth is reduced if the spacing between crevasses is reduced.

The results of the analysis can be applied to other crack problems. In particular, it can be applied to thermal secondary cracking that it is hoped occurs when cooling fluid flows through the cracks created by hydraulic fracture for the purpose of extracting geothermal heat from hot, dry rock masses.

Support: NSF-RANN

AN EQUIVALENT INCLUSION METHOD FOR A THREE-DIMENSIONAL  
LENS-SHAPED CRACK IN ANISOTROPIC MEDIA

T. Mura and P. C. Cheng  
[Fracture 3, 1977]

Micro cracks in materials sometimes take a three-dimensional lens-shape. In this paper crack opening displacements, crack extension forces, stress concentration factors for  $a_3 \neq 0$  and stress intensity factors for  $a_3 = 0$  are developed through the use of the equivalent inclusion method for an isolated three-dimensional lens-shaped crack under simple tension and pure shear, where  $a_3$  is the smallest principal axis of the ellipsoid.

Support: NSF-MRL

EIGENSTRAINS IN LATTICE THEORY

T. Mura  
[Proc. Symp. on Continuum Models of  
Discrete Systems, in press]

In lattice theory (e.g., Born and Huang, 1954, Maradudin, 1963) a change of potential energy caused by a deformation is expressed by a function of atomic displacements measured from a perfect lattice state. For harmonic approximation the potential energy is expressed by a quadratic form of the atomic displacement components. The coefficients of the polynomial are chosen such that a uniform displacement (rigid motion) does not create any potential energy of deformation. The potential energy, however, does not vanish when a

part of the material is displaced plastically and reformed into a perfect crystal. When a perfect crystal is deformed into another perfect crystal accompanying only a plastic shape change, no change of potential energy is expected. Therefore the classical lattice theory should be modified so that the potential energy does vanish for such a plastic deformation. A similar question about the incompleteness of the classical lattice theory was already raised by M. Kuriyama (1967) from a different standpoint.

It is shown in this paper that such a difficulty in the classical lattice theory simply can be eliminated when the concept of eigenstrains in continuum mechanics is introduced into the lattice theory. The general name of eigenstrain is given for thermal expansion strain, phase transformation strain, plastic strain, misfit strain, etc. In continuum mechanics the eigenstrain has played an important role in analysis of elastic fields caused by line and point imperfections, inclusions, inhomogeneities, etc. The introduction of the concept of eigenstrains into lattice theory provides similar advantages and eliminates the above mentioned difficulty in classical lattice theory.

Examples of the proposed theory are shown for a uniformly moving screw dislocation, a dynamically created vacancy, and a uniformly moving mode III crack.

Support: NSF-MRL and AROD

#### FATIGUE BEHAVIOUR OF PRECIPITATION-HARDENING MEDIUM C STEELS CONTAINING Cu

S. Ikeda, T. Sakai and M. E. Fine  
[J. Mat. Sci. 12, 1977]

The presence of Cu precipitates counteracts the cyclic softening present in ordinary quenched and tempered steels. This is expected to result in an increase in fatigue limit. The fatigue crack propagation rate ( $dc/dN$ ) at constant  $\Delta K$  in the Cu-C steels was shown to depend on heat treatment and carbon content. To maximize yield strength and minimize  $|da/dN|_{\Delta K}$  for tempering at 500°C, one must choose a low C content and temper for a short time;  $|da/dN|_{\Delta K}$  in 0.28 wt.% C-1.45 wt.% Cu tempered for 13 min was one-third that for 0.45 wt.% C-1.45 wt.% Cu tempered for 200 min. There is also an advantage in adding Cu while simultaneously lowering the C content. The  $dc/dN$  data are discussed in terms of the yield strength and the energy to form a unit area of fatigue crack,  $U$ , which was measured using foil strain gauges. The quantity

$(|dc/dN|_{\Delta K} \sigma_y'^2 U)$ , where  $\sigma_y'$  is the cyclic yield stress, was found to be nearly constant. In the 0.28 wt.% C-1.45 wt.% Cu alloy, short aging times at 500°C resulted in greater resistance to initiation of cracks at notches for low  $\Delta K$ s than long aging times.

Support: AISI

PLASTIC WORK DURING FATIGUE CRACK PROPAGATION IN A HIGH STRENGTH  
LOW ALLOY STEEL AND IN 7050 AL-ALLOY

S. Ikeda, Y. Izumi and M. E. Fine  
[Engineering Fracture Mechanics 9, 1977]

Theoretically and empirically a fatigue crack propagation rate equation of the form

$$\frac{dc}{dN} \propto \frac{(\Delta K)^4}{\mu \sigma^2 U}$$

is indicated where  $\mu$  is the shear modulus,  $\sigma$  is an appropriate measure of the alloy's strength, and  $U$  is the energy to make a unit area of fatigue crack. The local stress-strain curves in the plastic zone around a propagating fatigue crack were determined using tiny foil strain gages. The areas in the hysteresis loops were integrated over the plastic zone for a unit area of crack advance to give an approximate value for  $U$ . The non-hysteretic plastic work was neglected in this calculation but its contribution to the total plastic work in the plastic zone near the crack tip is small.

Support: NSF-MRL and AFOSR

SOME RECENT RESULTS ON FATIGUE CRACK INITIATION AND PROPAGATION OF AL ALLOYS

M. E. Fine, C. Y. Kung, Y. Izumi and K. P. Liaw  
[106th AIME Annual Meeting, March, 1977]

Initiation of fatigue cracks in electropolished notches is being studied using a 400X long-working distance objective metallurgical microscope mounted directly on an MTS machine. Studies in 2024 aluminum alloy have related fatigue crack initiation to the inclusion size and persistent slip bands. At low stress amplitudes the fatigue cracks form on inclusions. The probability a given inclusion nucleates a fatigue crack decreases very rapidly as the inclusion dimensions decrease from 5  $\mu$ m. At high stress amplitudes, the cracks nucleate on persistent slip bands.



The fatigue crack propagation rate in unalloyed aluminum is 50 or more times faster at 300°K and at 77°K. This effect is not related to atmosphere, specimen thickness, or prior plastic deformation of the samples. It is due to a difference in the dislocation structure which results from cyclic straining. Dislocation cells form at room temperature while dislocation tangles form at 77°K. The latter results in a much higher value for the plastic work required to propagate a fatigue crack.

Support: AFOSR

THE HYSTERETIC PLASTIC WORK AS A FAILURE CRITERION IN A  
COFFIN-MANSON TYPE RELATION

J. S. Santner and M. E. Fine  
[Scripta Met. 11, 1977]

The changes in  $\Delta\sigma$  and  $\Delta\epsilon_p$  with cycling in constant strain amplitude tests which occur in certain alloys would seem to mitigate against the use of  $\Delta\epsilon_p$  as the independent variable in a Coffin-Manson type plot in materials which don't saturate (i.e.,  $\Delta\sigma$  varies continuously with  $N$ ). Since  $\Delta W_p$ , the hysteretic plastic work, is nearly invariant with cycling ( $\Delta\epsilon_p$  and  $\Delta\sigma$  are inversely related),  $\Delta W_p$  is a more logical parameter to use in these cases.

A Coffin-Manson type plot was made for the three aluminum base alloys using  $\Delta \bar{W}_p$ , the arithmetic average hysteretic energy per loop, and  $2N_i$ , the number of reversals to fatigue crack initiation. A simple power law describes the relationship with a regression correlation confidence limit of 0.98. Similar results have been reported elsewhere for different aluminum alloys with both notched and unnotched specimens. The single straight line which results when  $\log (\Delta \bar{W}_p)$  vs  $\log (2N_i)$  plots are made is in contrast to the two linear segments which result when  $\log (\Delta \epsilon_p/2)$  is plotted vs  $\log (2N_i)$  for these and a number of other aluminum alloys. Interestingly, the data for all three alloys fall on the same straight line.

Support: AFOSR

## ROLE OF PLASTIC WORK IN FATIGUE CRACK PROPAGATION IN METALS

Y. Izumi, M. E. Fine and T. Mura  
[106th AIME Annual Meeting, March, 1977]

Many theoretical and semi-empirical treatments of the rate of fatigue crack propagation,  $dc/dN$ , have shown that it is inversely related to the plastic work energy required for a unit area of fatigue crack,  $U$ . In the present work, the total plastic deformation at the crack tip was calculated using a two dimensional stress distribution around a crack including work hardening parameter assuming the antiplane longitudinal shear solution holds. Then the plastic work per cycle,  $\Delta W$ , was set equal to  $U\Delta C$  where  $\Delta C$  is the crack advance for one cycle. The equation obtained is  $|dc/dN|_{\Delta K} \propto 1/U \sigma_y^2 \mu$  where  $\sigma_y$  is the cyclic yield stress and  $\mu$  is the shear modulus. This equation is similar to that based on other criteria. A technique was developed in this laboratory for measuring  $U$  by determining stress-strain curves in the plastic zone around the tip of the crack using tiny foil strain gages. Measurements of  $U$  in a series of aluminum based and nickel based alloys and steels have been made. The results to date confirm the importance of  $U$  as a rate determining parameter for the growth of fatigue cracks. Preliminary results indicate that introducing a dispersed phase, such as  $\theta$  particles in binary Al-Cu alloys, to decrease the inhomogeneity of the plastic deformation increases  $U$  and decreases  $dc/dN$ .

Support: AFOSR

## THE STRENGTH AND TOUGHNESS OF A CERAMIC REINFORCED WITH METAL WIRES

J. G. Zwissler, M. E. Fine and G. W. Groves  
[J. Am. Ceram. Soc., in press]

Composites consisting of fine stainless steel fibres of 6, 12 or 25  $\mu m$  diameter in a matrix of wüstite were prepared by hot-pressing. The fracture stress of unnotched beams and the critical stress intensity factor for crack initiation in notched beams were measured and both increased linearly with volume fraction of fibre. Part of these improvements were attributed to the action of yielding fibres which bridged the crack surfaces. Plastic deformation of fibres at the crack tip was thought to also play a role. There were large increases in the total work of fracture, largest for the 25  $\mu m$  fibre, which were accounted for by the work done in fracturing crack-bridging fibres. For long cracks bridged by fibres over a substantial length, the critical

applied stress intensity factor for further crack propagation increased strongly with increasing bridged crack length and the form of this increase could be accounted for by considering the negative stress intensity factor due to the closure forces exerted on the crack by the bridging fibres.

Support: AFOSR and INCO Fellowship

THE ELASTIC FIELD CAUSED BY A GENERAL ELLIPSOIDAL INCLUSION  
AND THE APPLICATION TO MARTENSITE FORMATION

T. Mura, T. Mori and M. Kato  
[J. Mech. Phys. Solids 24, 1976]

The elastic field throughout an ellipsoidal inclusion in an indefinitely-extended anisotropic material is investigated when an eigenstrain (a stress-free transformation strain) is periodically distributed throughout the inclusion. This is an extension of the results obtained by J. D. Eshelby (1961) for uniform eigenstrains and by R. J. Asaro and D. M. Barnett (1975) for polynomial eigenstrains.

The solution is applied to the evaluation of elastic strain energies of a disc-shaped martensite with alternating twins and of a spherical precipitate with a banded structure. The significant amount of the elastic strain energies explains the necessity of the supercooling of austenite steel for the martensitic transformation to occur.

Support: NSF-MRL and NSF

INTERACTION AMONG INTERSTITIAL SOLUTE ATOMS IN IRON AND TETRAGONAL ORDERING

T. Mori, Paul C. Cheng and T. Mura  
[Proceedings of the First JIM International Symposium  
on "New Aspects of Martensitic Transformation," 1977]

The elastic energy due to the presence of interstitial atoms in iron has been calculated on the basis of continuum elasticity with a sphere-in hole model by taking into account elastic anisotropy. When interstitial atoms are randomly distributed in a crystal, the elastic energy has been shown to take a minimum due to the elastic interaction among the interstitial atoms, if all the interstitial atoms occupy the single sublattice. The critical temperature for the spontaneous ordering has been calculated. The elastic energy has also been computed when interstitial atoms, represented by nitrogen atoms in iron,

are periodically distributed. It has been found that the arrangement corresponding to the  $\text{Fe}_{16}\text{N}_2$  structure gives the lowest elastic energy.

Support: NSF-MRL and NSF

#### THE ELASTIC FIELD OUTSIDE AN ELLIPSOIDAL INCLUSION

T. Mura and P. C. Cheng  
[Submitted for publication]

The elastic field outside an ellipsoidal inclusion is investigated. No particular restrictions are imposed to eigenstrain distributions throughout the inclusion and to the anisotropy of elastic media for matrices. The solution is expressed in the form of integrals defined on a sub-space of a unit sphere. Since the integrands of these integrals have no singularities, the numerical calculation on a computer can easily be performed.

Support: NSF, Army and NSF-MRL

#### STRESS FIELD OF A PLANAR ELLIPTICAL DISLOCATION LOOP

E. N. Mastrojannis, T. Mura and L. M. Keer  
[Phil. Mag. 35, 1977]

The stress field produced by a dislocation loop of arbitrary shape in an infinite anisotropic medium has been expressed as line integrals of Green's function along the dislocation loop by Mura (1963). This note presents explicit results, which have been obtained by integration of the line integrals mentioned, for the stress components in the plane of a planar elliptical dislocation loop in an unbounded isotropic elastic medium.

#### PLASTIC WORK DURING FATIGUE CRACK PROPAGATION IN A HIGH STRENGTH LOW ALLOY STEEL AND IN 7050 AL-ALLOY

S. Ikeda, Y. Izumi and M. E. Fine  
[Engineering Fracture Mechanics 9, 1977]

Theoretically and empirically a fatigue crack propagation rate equation of the form

$$\frac{dc}{dN} \propto \frac{(\Delta K)^4}{\mu \sigma^2 U}$$



is indicated where  $\mu$  is the shear modulus,  $\sigma$  is an appropriate measure of the alloy's strength, and  $U$  is the energy to make a unit area of fatigue crack. The local stress-strain curves in the plastic zone around a propagating fatigue crack were determined using tiny foil strain gages. The areas in the hysteresis loops were integrated over the plastic zone for a unit area of crack advance to give an approximate value for  $U$ . The non-hysteretic plastic work was neglected in this calculation but its contribution to the total plastic work in the plastic zone near the crack tip is small.

Support: NSF-MRL and AFOSR

Thrust Area Research

Support:  
NSF-MRL Program

METALS, ALLOYS AND INTERMETALLIC COMPOUNDS

Faculty:

- D. E. Ellis, Professor, Physics and Astronomy and Chemistry,  
Group Leader
- J. O. Brittain, Professor, Materials Science and Engineering
- A. J. Freeman, Professor, Physics and Astronomy
- W. P. Halperin, Assistant Professor, Physics and Astronomy
- J. E. Hilliard, Professor, Materials Science and Engineering
- C. R. Kannewurf, Professor, Electrical Engineering
- J. B. Ketterson, Professor, Physics and Astronomy
- D. H. Whitmore, Professor, Materials Science and Engineering

Research Staff:

- P. Cristea, Visiting Scholar, Materials Science and Engineering
- D. H. Dye, Postdoctoral Associate, Physics and Astronomy
- R. P. Gupta, Research Associate, Physics and Astronomy
- N. Karnezos, Postdoctoral Fellow, Physics and Astronomy
- J. R. Willhite, Postdoctoral Associate, Materials Science and Engineering

Graduate Students:

- G. A. Benesh, Physics and Astronomy
- Y. Ochiai, Materials Science and Engineering
- T. Tsakalakos, Materials Science and Engineering

Personnel Who Have Left:

- E. Byrom, Department of Radiology, University of Illinois at the Medical  
Center, Chicago, Ill.
- N. Karnezos, Visiting Professor, Illinois Institute of Technology,  
Chicago, Ill.
- T. Tsakalakos, Assistant Professor, Rutgers University, New Brunswick,  
N. J.
- J. R. Willhite, Gould Inc., Rolling Meadows, Ill.

Degrees Granted:

- T. Tsakalakos, Ph.D., June, 1977

Other Sponsorship:

NSF-MRL, National Science Foundation, Materials Research Laboratory  
AFOSR, Air Force Office of Scientific Research  
AROD, Army Research Office, Durham  
ERDA, Energy Research and Development Administration  
ICRA, International Copper Research Association  
NSF, National Science Foundation

Introduction

This newly reorganized thrust group brings together faculty, research associates and students already active in electronic structure and properties studies of metals, alloys and intermetallic compounds. Our objective is to focus a variety of experimental and theoretical approaches onto specific materials in order to obtain a more profound understanding of relations between microscopic theory, spectroscopic properties and transport properties of metallic systems.

The intermetallic compounds with cesium chloride structure are of particular interest to this group. Professor Brittain's group has shown, for example, that stoichiometric NiAl is an ordinary paramagnet and that reported transport anomalies were due to ppm amounts of magnetic transport metal impurities. Using resistivity, magnetoresistance and NMR techniques they have studied the influence of magnetic impurities and deviations from stoichiometry on transport properties of  $\text{Ni}_x\text{Al}_{1-x}$  and  $(\text{NiAl})_x\text{M}_x$  systems. Theoretical studies have been made by Professor Ellis and coworkers on these systems, using molecular cluster methods. Self-consistent spin polarized Hartree-Fock-Slater models have been employed to study electronic energy levels and densities of states, charge densities and distribution of magnetization around transition metal sites.

The B32 lattice or Zintl structure provides another interesting example of cubic AB compounds, for which NaTl is the prototype. The crystal structure can be viewed as two interlocking diamond lattices, so that each atom has four neighbors of A type and four neighbors of B type, leading to interesting controversies about the nature of bonding and conduction electron composition. Experimental studies on LiAl have been made in Professor Brittain's group, using resistivity and NMR data to study diffusion and charge transport mechanisms. Molecular cluster and energy band studies for this material have been carried out by the theorists.

Professor Kannewurf is involved in optical and transport measurements of related alloy systems. A strong effort in materials preparation, particularly in growth of high purity single crystal specimens, is under way.

The relative role of one-electron and correlation effects in spectroscopic and transport properties of metals has been of interest to Professor Freeman. A series of studies on the shape of soft x-ray absorption and emission bands in "simple" metals suggests that many body effects have been overestimated in many cases. The augmented plane wave method was used to calculate energy bands and wave functions, from which the transition-strength matrix elements were calculated. It was found that structure in the density of states and matrix elements is responsible for several observed peaks in the x-ray structure, making it possible to focus on remaining discrepancies as possible many-body effects.

The generalized susceptibility function which measures the response of electrons to an external perturbation is central to the understanding of many physical phenomena in solids. Here again one-electron models of  $\chi(\vec{q})$  provide an important test of band theory, as shown in the recent work on Sc metal by Professor Freeman and associates. Further applications concerning the surface susceptibility of a simple metal have been made.

Professor Hilliard's group has been active in developing composition-modulated alloys in the form of thin foils. They have discovered an enhanced elastic modulus in gold-nickel, copper-nickel and copper-palladium foils. The modulus enhancement decreases with increasing composition-modulation wavelength, and for greater than  $\sim 3$  nm the modulus is the same as that for homogeneous foils. Interdiffusion in these foils has been studied by measuring the decay rate of x-ray diffraction satellite intensities. Further studies of these very interesting materials is under way.

Professor Ketterson has used the de Haas-van Alphen technique to measure Fermi surface properties in Nb, Au, AuGa and other materials. This technique probably provides the most precise comparison possible between experimental one-electron properties and theory. The study of cyclotron effective masses, g-factors, and magnetic breakdown effects is invaluable for tests of the validity of band theory models, and in providing inputs for improving those models. The use of dHvA scattering rates in determining the magnitude and anisotropy of conduction electron scattering in real (defective) materials now provides a challenge to theories of the defect state.



Professor Halperin is using static susceptibility (SQUID) and NMR techniques to probe the electronic properties of small metallic particles, beginning with Pt powders. The effect of the surface of such particles upon the conduction electron gas is being studied, using NMR linewidths. The surface electronic structure, which may well be different from that of the bulk metal, can in principle be studied by NMR on adsorbed species such as hydrogen or  $^3\text{He}$  although intensity problems must be solved. Volume effects on electronic structure are being studied by static susceptibility and NMR Knight shift and  $T_1$  measurements.

Professors Halperin and Ketterson are also involved in a search for new superconducting elements, at ultralow temperatures. Lithium is of particular interest, since pseudopotential calculations predict a superconducting bcc phase, and extrapolation to understanding (possibly) superconducting states of metallic hydrogen would be aided. Work on Pd and other noble metals is aimed at the possible occurrence of p-wave pairing in the superconducting state, which could be stabilized by spin fluctuations.

Professor Whitmore's group has constructed a gamma-ray Compton scattering spectrometer, which is in the final stages of testing. We expect to obtain direction-dependent Compton profiles for CoGa and several other alloys for comparison with theoretical calculations of momentum densities. Interesting possibilities for extracting Fermi surface properties from Compton scattering data are being explored.

#### ELECTRICAL RESISTIVITY OF NiAl

T. Yoshitomi, Y. Ochiai and J. O. Brittain  
[Solid State Commun. 20, 1976]

Resistivity-temperature measurements on annealed near stoichiometric NiAl showed the absence of a resistivity minimum and confirms that the reported anomalous transport properties are an extrinsic effect not observed in high purity NiAl. Thermal treatments on NiAl designed to affect the order did not produce a resistivity-temperature minimum.

Support: NSF-MRL

NMR SPIN LATTICE RELAXATION RATE IN NiAl DUE TO 3-d IMPURITIES

J. R. Willhite, L. B. Welsh and J. O. Brittain  
[AIP Conf. Proc. (USA) No. 29, 233, 1976]

The  $\text{Al}^{27}$  NMR spin lattice relaxation in stoichiometric NiAl due to the magnetic 3-d impurities Cr, Mn and Fe have been studied. The recovery of the NMR signal following a saturation train is exponential in time. The impurity induced relaxation rate ( $T_1^{-1}_{\text{imp}}$ ) is linear in impurity concentration for  $c \leq 500$  ppm. The magnetic field dependence of the rate is  $T_1^{-1}_{\text{imp}} = (A + GH)^{-1}$  for  $1.5 \leq H \leq 15$  kOe and  $T_1^{-1}_{\text{imp}}$  is temperature independent for  $1.5 \leq T \leq 4.2$  K. Measured values of the impurity magnetization and of the impurity broadening of the host NMR linewidth are used to interpret  $T_1^{-1}_{\text{imp}}$  using the model of energy diffusion in the nuclear spin system to the impurity.

Support: NSF-MRL

RESISTIVITY MEASUREMENTS ON INTERMETALLIC COMPOUND  $\beta'$ - $\text{Ni}_{48}\text{Al}_{52}$   
WITH 3d TRANSITION METAL IMPURITIES

Y. Ochiai and J. O. Brittain  
[J. of Physics F: Metal Physics - Accepted for publication]

Electrical resistivity measurements have been made on the intermetallic compound  $\beta'$ - $\text{Ni}_{48}\text{Al}_{52}$  with additions of 500 ppm 3d transition metals. The comparison of the present results with those of  $\beta'$ - $\text{Ni}_{50}\text{Al}_{50}$  with the same 3d metal additions has clearly revealed a local environment effect on the local moment formation.

Support: NSF-MRL

ELECTRICAL RESISTIVITY AND MAGNETORESISTANCE  
OF  $(\text{NiAl})_{1-x}\text{M}_x$ , M = 3d TRANSITION METALS

T. Yoshitomi, Y. Ochiai and J. O. Brittain  
[J. Phys. Chem. Solids 38, 1977]

Transport properties were investigated in  $(\text{NiAl})_{1-x}\text{M}_x$ , M = 3d transition metals, in order to examine the extrinsic nature of NiAl. Experimental results are well described by the s-d exchange (Kondo) theory from which exchange energy J, Kondo temperature  $T_K$ , and spin value S were estimated. A comparison between our results and the results from dilute alloys is made.

Support: NSF-MRL

MAGNETIC IMPURITY STATES OF Fe DOPED INTERMETALLIC COMPOUND  $\beta'$ -Ni<sub>x</sub>Al<sub>100-x</sub>

Y. Ochiai and J. O. Brittain  
[Solid State Commun. 22, 1977]

Resistivity measurements were made on the Fe doped intermetallic compound  $\beta'$ -Ni<sub>x</sub>Al<sub>100-x</sub> (x = 46.9 to 51.5 at.%). No resistivity minimum was observed for x ≤ 49.0 while for x ≥ 49.5, a clear resistivity minimum was observed. We interpret the previously reported Kondo-like phenomena on the discontinuous local moment formation.

Support: NSF-MRL

<sup>7</sup>Li SELF DIFFUSION IN LiAl--AN NMR STUDY

J. R. Willhite, N. Karnezos, P. Cristea and J. O. Brittain  
[J. Phys. Chem. Solids 37, 1976]

The self diffusion of <sup>7</sup>Li in near stoichiometric LiAl has been investigated by observing the <sup>7</sup>Li and Al<sup>27</sup> NMR relaxation rates. The diffusivity for a <sup>7</sup>Li atom is determined to be  $D = 9 \times 10^{-6} \exp(-0.12 \text{ eV}/kT) \text{ cm}^2/\text{sec}$ . Both the <sup>7</sup>Li and Al<sup>27</sup> rates show the effects of quadrupole relaxation. The electric field gradients from the moving defects in LiAl are a factor of  $37 \pm 5$  stronger at the Al nuclei suggesting covalent character to the bonding.

Support: NSF-MRL

MOLECULAR CLUSTER STUDIES OF BINARY ALLOYS: LiAl

D. E. Ellis, G. A. Benesh and E. Byrom  
[Submitted for publication]

The electronic structure of the ordered Zintl phase of LiAl has been studied in a molecular cluster model within the framework of the Hartree-Fock-Slater theory. Li<sub>5</sub>Al<sub>4</sub> and Al<sub>4</sub>Li<sub>5</sub> clusters were embedded in a potential field representative of the alloy environment; energy levels and wavefunctions were obtained by self-consistent iteration. Density-of-states and charge density results are used to interpret NMR and electrical conductivity studies. The case of a single Li-vacancy was also treated, and discussed in light of positron annihilation data.

Support: NSF-MRL

BAND THEORY OF K-EDGE TRANSITIONS IN Li

R. P. Gupta, A. J. Freeman and J. D. Dow  
[Phys. Lett. 59A, 1976]

APW band calculations of the soft x-ray K absorption and emission spectra of Li are used to discuss the extent to which various conflicting theories and measurements of absorption, emission, electron-energy-loss, and photoemission can be reconciled.

Support: NSF-MRL, NSF and AFOSR

BAND-STRUCTURE CONTRIBUTIONS TO X-RAY EMISSION AND ABSORPTION SPECTRA  
AND EDGES IN MAGNESIUM

Raju P. Gupta and A. J. Freeman  
[Phys. Rev. Lett. 20, 1976]

The soft-x-ray  $L_{2,3}$  emission and absorption spectra of Mg metal have been determined by means of high-resolution ab initio augmented-plane-wave calculations. The inclusion of transition-matrix elements calculated from the augmented-plane-wave wave functions changes the sharp structure found in the joint density of states, yields an  $L_{2,3}$  emission spectrum in good agreement with experiment, and indicates that band-structure effects play an important role in the observed x-ray threshold shape.

Support: NSF-MRL

ROLE OF BAND STRUCTURE ON THE X-RAY EDGE-SHAPE IN Na METAL

R. P. Gupta and A. J. Freeman  
[Phys. Lett. 59A, 1976]

Marked structure found in an APW study of both the density of states and transition matrix elements contributing to the emission/absorption spectra of Na emphasizes the need for including band structure effects in all x-ray edge analyses.

Support: NSF-MRL



ROLE OF MATRIX ELEMENTS IN THE THEORETICAL DETERMINATION  
OF GENERALIZED SUSCEPTIBILITIES IN METALS

Raju P. Gupta and A. J. Freeman  
[Phys. Rev. B 13, 1976]

The role of matrix elements in the calculation of the generalized susceptibilities  $\chi(\vec{q})$  of metals is discussed using the results of an augmented-plane-wave energy-band calculation for the eigenvalues and eigenfunctions of Sc metal. The inclusion of the oscillator strength matrix elements is found to significantly alter the structure obtained for  $\chi(\vec{q})$  in the constant-matrix-element approximation. The effects of local-field corrections on the phonon anomaly in Sc and the observed magnetic ordering of dilute rare-earth Sc alloys are described; in the latter case, a crude estimate of this effect is found to restore a (broad) peak in  $\chi(\vec{q})$  at  $\vec{q} \approx [0,0,0.5(\pi/c)]$ , in good agreement with experiment.

Support: NSF-MRL

THE SURFACE SUSCEPTIBILITY OF A SIMPLE METAL

R. L. Kautz, A. J. Freeman and B. B. Schwartz  
[Phys. Lett. 57A, 1976]

The magnetic surface response of a simple metal to a uniform field is calculated for a jellium model of a metal surface. We find a positive surface contribution to the measured susceptibility of finite samples.

Support: NSF

CONDUCTION ELECTRON POLARIZATION, MAGNETIZATION DENSITIES  
AND NEUTRON MAGNETIC FORM FACTORS IN METALS

A. J. Freeman  
[Physica B, Proc. Conf. on Itinerant Electron Magnetism,  
Oxford, England, 1976]

Itinerant vs localized descriptions of 3d, 4f and 5f electron states is discussed. Recent energy band determinations of conduction electron polarization and magnetization densities and predictions of neutron magnetic form factors in metals are described. Comparisons of theory with experiment show good agreement and confirm the range of validity of the energy band description.

Support: NSF, AROSF and ERDA

MAGNETIC FIELD INDUCED CONDUCTION ELECTRON POLARIZATION, MAGNETIZATION DENSITY, AND NEUTRON MAGNETIC FORM FACTOR OF Pt METAL

T. J. Watson-Yang, A. J. Freeman and D. D. Koelling  
[Submitted for publication]

Results are presented of a detailed relativistic augmented plane wave (RAPW) study of the magnetic field induced conduction electron polarization, magnetization density, and neutron magnetic form factor of Pt metal. We find that the spherical part of the total induced spin density is very localized spatially and almost entirely d-like in character, with the band 6 contribution differing substantially from its counterpart in Pd metal. The spin only estimate of the Weiss-Freeman asymmetry parameter is large (93%  $t_{2g}$  and 7%  $e_g$ ). Our predicted Fermi surface dimensions for both the electron and hole surfaces (and the suitably enhanced effective masses) show excellent agreement with the recent measurements of Dye et al.

Support: NSF and ERDA

CORRELATION OF PHONON ANOMALIES IN Pd AND Pt WITH MAXIMA IN THE GENERALIZED SUSCEPTIBILITY

T. J. Watson-Yang and A. J. Freeman  
[Am. Phys. Soc. Meeting, February, 1977]

The generalized susceptibility,  $\chi(\vec{q})$ , in Pd and Pt for  $\vec{q}$  along the [100], [110], [111], and [120] directions was determined from their APW and RAPW energy band structure, respectively, using the tetrahedron scheme of Rath and Freeman. Peaks in  $\chi(\vec{q})$  for  $\vec{q}$  along [110] are found at  $\vec{q}$  values ( $0.65 \pi/a$  for Pd and  $0.75 \pi/a$  for Pt) which are close to the phonon anomalies observed in the  $T_1$  branch by Miller et al. Significant peaks in  $\chi(\vec{q})$  are also found in the [111] direction and weaker peaks in the [120] direction. Experiments are suggested to test the prediction of weak phonon anomalies arising from the [111] peaks at  $q = 0.65 \pi/a$  for Pt.

Support: AFOSR, NSF and ERDA

ELECTRONIC STRUCTURE, FIELD-INDUCED MAGNETIZATION DENSITY  
AND NEUTRON MAGNETIC FORM FACTOR OF PALLADIUM

T. J. Watson-Yang, B. N. Harmon and A. J. Freeman  
[J. Magnetism and Magnetic Materials 2, 1976]

The magnetic field induced magnetization density and neutron magnetic form factor of Pd metal is obtained from an ab initio APW energy band study of its electronic structure and properties. The magnetization consists of the spin density calculated for states on the Fermi surface and a much smaller orbital contribution. The solid state wavefunctions are found to yield a spatial localization of the spin density which is greater than that of the very contracted Hartree-Fock density of the free  $\text{Pd}^{2+}$  ion. The theoretical magnetic form factor, which is dominated by the contribution of the fifth band, is found to be in excellent agreement with the measurements of Cable, Wollan, Felcher, Brun and Hornfeldt.

Support: NSF, AFOSR and ERDA

THE SURFACE SUSCEPTIBILITY OF A SIMPLE METAL

R. L. Kautz, A. J. Freeman and B. B. Schwartz  
[Phys. Lett. 57A, 1976]

The magnetic surface response of a simple metal to a uniform magnetic field is calculated for a jellium model of a metal surface. We find a positive surface contribution to the measured susceptibility of finite samples.

Support: NSF

ENHANCED ELASTIC MODULUS IN COMPOSITION-MODULATED  
GOLD-NICKEL AND COPPER-PALLADIUM FOILS

W. M. C. Yang, T. Tsakalakos and J. E. Hilliard  
[J. Appl. Phys. 48, 1977]

The biaxial elastic modulus  $Y_{[111]}$  has been measured by bulge testing in Au-Ni and Cu-Pd foils containing short-wavelength one-dimensional composition modulations produced by vapor deposition. As compared with homogeneous foils of the same average composition, the modulated foils exhibited an appreciable increase in modulus--from 0.21 to 0.46 TPa for Au-Ni, and from 0.27 to 1.31 TPa for Cu-Pd. For the latter system, the increase was found to be proportional to the square of the amplitude of the modulation. The

enhancement of the modulus decreased with increasing wavelength and for wavelengths greater than 3 nm the modulus was the same as that for homogeneous foils. It was also observed that the deformation was non-Hookian; the slope of the stress-strain curves decreased with increasing strain.

Support: NSF-MRL and AROD

#### ENHANCED ELASTIC MODULUS IN COMPOSITION-MODULATED COPPER-NICKEL FOILS

T. Tsakalakos and J. E. Hilliard

The biaxial elastic modulus  $Y_{[111]}$  has been measured by bulge testing in Cu-Ni foils containing short-wavelength one-dimensional composition modulations produced by vapor deposition. As with two other systems previously studied, Au-Ni and Cu-Pd, a marked increase (approximately a factor of three) was observed in the elastic modulus of foils having modulations with wavelengths  $< 3$  nm.

It is proposed that this increase is due to a change in the band structure resulting from the new Brillouin zones produced by the composition modulation.

Support: NSF-MRL

#### INTERDIFFUSION IN COMPOSITION-MODULATED COPPER-GOLD THIN FILMS

Wayne M. Paulson and John E. Hilliard  
[J. Appl. Phys. 48, 1977]

Vapor-deposited Cu-Au thin films were produced containing composition modulations with wavelengths between 8 and 26 Å. The modulations produced satellite peaks in the x-ray diffraction patterns. Amplification factors and the corresponding diffusion coefficients were obtained by measuring the decay rate of the satellite intensities. The amplification factor reached a maximum at 17 Å and decreased at both shorter and longer wavelengths. Interdiffusion coefficients between  $10^{-21}$  and  $10^{-19}$  cm<sup>2</sup>/sec were measured over the temperature range 200-260°C. The effective diffusion coefficient is linearly dependent on the function  $B^2(\lambda)$  for  $\lambda > 10$  Å. From the wavelength dependence of the measured diffusivities, a gradient-energy coefficient of  $-4.7 \times 10^{-6}$  erg/cm was obtained and is in good agreement with theoretical estimates.



These experimental results were compared with the predictions from a proposed model for diffusion on cubic lattices.

Support: ICRA

#### INTERDIFFUSION IN COMPOSITION-MODULATED COPPER-NICKEL THIN FILMS

T. Tsakalakos and J. E. Hilliard  
[Submitted for publication]

Interdiffusivities were measured in vapor-deposited Cu-Ni foils containing [111] composition modulations with wavelengths between 0.8 and 5 nm. The interdiffusivities in the range of 375-450°C, measured from the decay rate of x-ray diffraction satellite intensities, were in good agreement with an extrapolation of existing high temperature data obtained with conventional diffusion specimens. The effective diffusion coefficient  $D_B$  at 400°C as a function of the dispersion relation  $B^2(h)$  showed a minimum, in contrast with the behavior of several other systems investigated so far. A new formulation of  $D_B$  in powers of  $B^2$  was developed and six interatomic potentials were calculated from short range order parameters which yielded a minimum in  $D_B$  at approximately 1.6 nm as was observed experimentally. Screening singularities showed up in the  $D_B$  by the appearance of a sharp peak at a wavelength 2.5 nm.

Support: NSF-MRL

#### ANALYTICAL SOLUTION TO CAHN'S NON-LINEARIZED DIFFUSION EQUATION

T. Tsakalakos and J. E. Hilliard

A one-dimensional analytic solution has been obtained to Cahn's non-linearized diffusion equation. The solution correctly predicts the anomalous kinetic behavior of the intensities of the second and third order x-ray diffraction satellites during the annealing of Cu-Ni composition-modulated foils. It is also in agreement with numerical solutions obtained by de Fontaine. A theoretical treatment has also been made of the later stages of spinodal decomposition which yields an approximate  $(\text{time})^{1/3}$  dependence for the growth of wavelengths.

Support: NSF-MRL

A DE HAAS-VAN ALPHEN STUDY OF NIOBIUM: FERMI SURFACE, CYCLOTRON  
EFFECTIVE MASSES, AND MAGNETIC BREAKDOWN EFFECTS

D. P. Karim, J. B. Ketterson and G. W. Crabtree  
[Submitted for publication]

The Fermi surface of niobium has been investigated using the de Haas-van Alphen effect. Data were taken at temperatures as low as 0.3 K and in fields as high as 130 kG. An on-line minicomputer was used to Fourier transform the digitized signals. Many new extremal area data have been obtained including oscillations associated with the previously unobserved  $\Gamma$ -centered hole octahedron and  $\Gamma$  and N centered orbits on the so-called jungle gym. An additional set of signals has been observed near [100] which are thought to be a result of magnetic breakdown between the second zone octahedron and third zone jungle gym. A separate low frequency signal was observed and is believed to be a result of magnetic breakdown induced quantum interference oscillations. Anisotropies of the cyclotron effective mass have been determined for many orbits on all three of the Fermi surface sheets. Finally, the area data has been used to parameterize the Fermi surface in terms of scattering phase shifts in a KKR band structure formalism

Support: ERDA and NSF

ANISOTROPY OF CONDUCTION ELECTRON g-FACTOR IN Au  
USING THE DE HAAS-VAN ALPHEN EFFECT

G. W. Crabtree, L. R. Windmiller and J. B. Ketterson  
[AIP Conference Proceedings 34, 1977]

Conduction electron g-factors in Au were measured by an absolute amplitude technique. The gain of the field modulation detection system was calibrated and absolute amplitudes were deduced from the size of the measured signal. g-factors were derived using measurements of the frequency, mass, and Dingle temperature and values of the curvature factor from both KKR phase shift and Fourier series parameterizations of the surface. The measured g factors show a large anisotropy, from a low of  $\sim 1.2$  on the neck at  $\langle 111 \rangle$  to a high of  $\sim 2.4$  for belly and dogsbone orbits.

Support: ERDA

CONDUCTION ELECTRON SCATTERING IN QUENCHED AND ANNEALED GOLD

Y. K. Chang, G. W. Crabtree and J. B. Ketterson  
[Phys. Rev., July, 1977]

The anisotropy of the conduction electron scattering due to vacancies and stacking fault tetrahedra (SFT) in quenched and subsequently annealed gold single crystals has been studied by measuring the de Haas-van Alphen (dHvA) Dingle (scattering) temperatures,  $T_D$ , for a large number of cyclotron orbits. The samples were quenched from 900°C into ice water, and were later annealed at 23°C and 40°C. We find that the dHvA scattering rates,  $(1/\tau)_{\text{dHvA}}$ , due to both vacancies and SFT are much larger than those obtained from resistivity measurements,  $(1/\tau)_\rho$ . The ratio of the [111] neck to belly orbital scattering rate rises from 1.0 for vacancies to 3.5 for SFT. This is attributed to the stronger and longer range strain field associated with the larger defects. We have calculated the local lifetimes  $\tau(\vec{k})$  from the measured  $T_D$  and found a large scattering anisotropy with the strongest scattering arising from the [100] region.

Support: ERDA

DE HAAS-VAN ALPHEN MEASUREMENTS AND PHASE SHIFT ANALYSIS  
OF ELECTRONIC SCATTERING ANISOTROPY IN AuGa

D. H. Dye, J. B. Ketterson, D. H. Lowndes  
G. W. Crabtree and L. R. Windmiller  
[J. Low Temp. Phys. 26, 1977]

Measurements of the electronic scattering anisotropy due to dilute concentrations of gallium in gold have been carried out using the de Haas-van Alphen effect. These measurements have been analyzed using the partial wave approach, and the results have been compared with those for other noble metal-heterovalent impurity systems.

Gallium, which has a valence difference of 2 with respect to gold, exhibits a much smaller change in lattice constant upon alloying than any of the other noble metal-heterovalent impurity systems studied to date. The results reported here indicate that the Friedel phase shifts for AuGa are considerably different from those for the other systems, in which impurity-induced strain is expected to play a larger role. The phase shifts for AuGa indicate that the Coulomb potential is effectively screened within a relatively short distance of the impurity site.

Support: NSF-MRL, NSF and ERDA

Thrust Area Research

Support:  
NSF-MRL Program

POLYMER PROCESSING AND PROPERTIES

Faculty:

- W. W. Graessley, Professor, Chemical Engineering and Materials Science and Engineering, Group Leader
- J. O. Brittain, Professor, Materials Science and Engineering
- S. H. Carr, Associate Professor, Materials Science and Engineering and Chemical Engineering
- B. Crist, Jr., Assistant Professor, Materials Science and Engineering and Chemical Engineering

Research Staff:

- Y. Aoki, Visiting Scholar, Materials Science and Engineering
- H. Rachapudy, Postdoctoral Research Fellow, Chemical Engineering

Graduate Students:

- Y. Aoki, Materials Science and Engineering
- C. Claiborne, Materials Science and Engineering
- J. T. Coates, Materials Science and Engineering
- R. J. Comstock, Materials Science and Engineering
- L. Dossin, Chemical Engineering
- P. Engler, Materials Science and Engineering
- W. R. Even, Materials Science and Engineering
- J.-C. Hser, Materials Science and Engineering
- R. Judd, Chemical Engineering
- E. Menezes, Materials Science and Engineering
- D. S. Pearson, Chemical Engineering
- M. Pucci, Materials Science and Engineering
- V. R. Raju, Chemical Engineering
- W. E. Rochefort, Chemical Engineering
- G. G. Smith, Chemical Engineering
- S. I. Stupp, Materials Science and Engineering
- G. Wissler, Materials Science and Engineering

Personnel Who Have Left:

- Y. Aoki, Sony Corp., Tokyo, Japan
- J. T. Coates, Kendall Co., Barrington, Illinois
- S. I. Stupp, Assistant Professor, Biological Materials, Dental School, Northwestern University, Chicago, Illinois

Degrees Granted:

- Y. Aoki, Ph.D., June, 1977
- J. T. Coates, M.S., June, 1977
- S. I. Stupp, Ph.D., August, 1977



Other Sponsorship:

American Can Company  
EXXON  
NSF, National Science Foundation  
ONR, Office of Naval Research  
PI, Plastics Institute of America  
PRF-ACS, Petroleum Research Fund, American Chemical Society  
WPM, Walter P. Murphy Fund

Introduction:

The properties of polymeric materials depend on several factors. The regularity of local molecular structure governs, for example, the inherent ability of the chains to crystallize. The large scale molecular structure (molecular weight, molecular weight distribution, branching) governs melt flow properties and the long range structural coherence required for mechanical strength. The thermal and flow histories (processing procedures) govern the orientation of chains and the morphological characteristics of the solid. Commercially useful products are made by the adjustment and balancing of these factors and are graded for the most part by experience and some qualitative generalizations. The objective of the Polymer Processing and Properties Thrust Group is to develop a more fundamental understanding of the relationships and how they combine to control properties.

Work is proceeding along two principal lines. The first deals with crystallizable polymers. The approach is to study processing phenomena with a set of crystallizable polymers, hydrogenated polybutadienes, which can be synthesized with known and simple molecular structure. Unlike commercial polyethylene, which otherwise they closely resemble, these model polymers have narrow distributions of molecular weight. They are therefore ideally suited for fundamental studies of flow-induced crystallization, a common aspect of commercial melt processing, and molecular orientation produced by deformation in the solid state. The influence of molecular weight distribution can be studied using blends of these materials. Current work in the groups of Professors Graessley and Crist deals with synthesis and the molecular and solid state characterization of the model polymers. Professor Carr's group is developing experimental procedures, using commercial polymers at present, to study flow-induced crystallization and crystallization from the oriented glassy state.

The second line deals with polymer blends. A relatively new method, the thermally stimulated discharge current (TSC) technique, is being used in Professor Brittain's group to study low temperature relaxation processes in polycarbonate, polysulfone and their blends. Several relaxation peaks have been resolved which appear as single broad peaks in conventional mechanical and dielectric relaxation measurements. These peaks exhibit quite different sensitivities to thermal and mechanical history. Moreover, the response of blends appears not to be the simple sum of contributions from individual plus component phases. Some mutual solubility is indicated by the observation of important changes in both mechanical properties and TSC behavior when very small amounts of the second component are added to either pure component. Supporting structural studies on polycarbonate are being conducted by Professor Crist's group.

#### STUDIES OF HYDROGENATED POLYBUTADIENES AS MODEL CRYSTALLIZABLE POLYMERS

H. Rachapudy, V. R. Raju, W. E. Rochefort,  
G. G. Smith and W. W. Graessley

Samples of polybutadiene with molecular weights from  $10^3$  to  $10^6$  and narrow molecular weights distributions ( $\bar{M}_w/\bar{M}_n < 1.1$ ) have been prepared. Hydrogenation converts them to saturated hydrocarbon polymers which closely resemble polyethylene. If hydrogenation can be conducted without disruption of the large scale structure of the chains the polymers will retain a narrow distribution of molecular weights and should be suitable as models for studying the properties of crystallizable polymers. Among several hydrogenation methods we have found two which leave the large scale structure virtually unchanged. Both involve heterogeneous catalysts (Ni on Kieselguhr and Pd on calcium carbonate) and high pressures (ca. 500 psi  $H_2$ ).

In melt rheology these hydrogenated polybutadienes are very similar to fractions of linear polyethylene. In the solid state they more closely resemble branched polyethylene. These characteristics are no doubt related to the presence of approximately 20 ethyl branches/1000 main chain carbon atoms, associated with the presence of vinyl side groups in the parent polymer.

Samples of model star polybutadienes are currently being prepared and hydrogenated to study the influence of long branches on both rheological and solid state properties.

Support: NSF-MRL and NSF

ON-LINE VISCOMETRY COMBINED WITH GEL PERMEATION CHROMATOGRAPHY  
I. INSTRUMENTAL CALIBRATION AND TESTING WITH LINEAR POLYMERS

Won S. Park and William W. Graessley  
[J. Polymer Sci. 15, 1977]

Gel permeation chromatography (GPC) was combined with flow time measurements on the eluant to provide both the distribution of hydrodynamic volumes and the distribution of intrinsic viscosities in linear polymers. Standard polystyrene samples were used to establish a universal hydrodynamic volume calibration as well as the zone spreading and viscometer transfer line tailing parameters. Viscometry data are particularly helpful in establishing the zone spreading parameters and the calibration curve at very high molecular weights. The results were applied to measurements on samples of linear polybutadiene and polyvinyl acetate. Agreement between values of  $\bar{M}_w$  from GPC with those obtained by light scattering confirmed the universal calibration principle.

Support: NSF-MRL

ON-LINE VISCOMETRY COMBINED WITH GEL PERMEATION CHROMATOGRAPHY  
II. APPLICATION TO BRANCHED POLYMERS

Won S. Park and William W. Graessley  
[J. Polymer Sci. 15, 1977]

Gel permeation chromatography (GPC) combined with on-line flow time measurements have been applied to the analysis of branching in polymers. Three sets of branched polymers were examined: polybutadienes lightly cross-linked by high energy radiation, a styrene-divinyl benzene copolymer and several of its fractions, and polyvinyl acetates branched by polymer transfer reactions during polymerization. The reduction in intrinsic viscosity due to branching was determined for each GPC fraction of the polybutadiene samples. The branching frequency in these fractions was known from other information, so the results were used to establish a relationship between viscosity ratio  $G$  and the theoretical size ratio  $g$ . This relationship was then used to calculate the distribution of branching and  $\bar{M}_w$  in the styrene copolymers and the polyvinyl acetates. The results were compared with independent information on these polymers. The agreement was generally good.

Support: NSF-MRL

## STRUCTURE AND PROPERTIES OF SEMICRYSTALLINE POLYMERS

G. Wissler and B. Crist

Experiments on two crystalline polymers which are also the subjects of research projects of other members of the Polymer Processing Thrust Group are under way. These involve poly(4,4' - isopropylidenediphenylene carbonate), the polycarbonate investigated by Professor Brittain by TSD, and the narrow molecular weight distribution hydrogenated polybutadienes (HPB) prepared by Professor Graessley.

The polycarbonate has been crystallized by evaporating a solution in methylene chloride at room temperature or by annealing the quenched glass at 190°C for periods up to four weeks. Both solution cast and bulk crystallized samples exhibit multiple melting peaks in the region of 217 - 247°C. X-ray diffraction patterns show that the width of the 020,  $\bar{2}10$  doublet is much narrower in the bulk crystallized material.

HPB samples with molecular weights ranging from 5,100 to 189,000 have been examined with a number of techniques. The higher molecular weight polymers (MW > 20,000) solidify as clear films, with a density of 0.905 g/cm<sup>3</sup>; the peak melting temperature by DSC is 100°C. At lower molecular weights, the density (crystallinity) increases, as does the melting temperature. The density and melting point of the HPB's are anomalously low when compared to high-pressure polyethylenes or ethylene- $\alpha$ -olefin copolymers having similar branch concentrations.

Support: NSF-MRL

## CHEMICAL ORIGIN OF THERMALLY STIMULATED DISCHARGE CURRENTS IN POLY(ACRYLONITRILE)

S. I. Stupp and S. H. Carr  
[J. Polymer Sc., Polymer Physics Edition]

Thermally stimulated discharge has been used in the past to diagnose and estimate the magnitude of electrical polarization in polymers. Nevertheless, molecular characterization of operative phenomena by this technique alone is often a difficult task. In the present work, infrared attenuated total reflection spectroscopy has been used to investigate the origin of thermally stimulated discharge currents near 200°C in externally unpolarized films of poly(acrylonitrile)(PAN). Spectroscopic analysis of thermally degraded films reveals some unsaturation of the PAN backbone and possibly the



generation of cyanide ions. Opposite surfaces in a solvent-cast film give rise to different spectra, indicating a gradient in chemical degradation products across the film thickness. Data suggest that non-uniform generation of charged species and unsaturated bonds gives rise to internal potentials in PAN. The origin of thermally stimulated currents in PAN near 200°C is thus believed to be associated with the onset of chemical degradation.

Support: ONR

#### MICROMECHANICAL FRACTURE ANALYSIS OF AMYLOSE

W. R. Even and S. H. Carr  
[Submitted for publication]

Amylose films were prepared with two distinctly different microstructures, and these specimens were subsequently tensile tested at different levels of moisture content. Measurement of the strain energy release rate,  $G_I$ , was approached from three separate methods. Two of these methods, the J-integral and stress intensity analyses, are based on bulk tensile properties. The third method involves direct calculation of the work expended in producing the microplastic zone at the crack tip. Birefringence measurements were used in mapping the magnitude and shape of the plastic zones. Although the semicrystalline material would not lend itself to the bulk tensile analyses,  $G_I$  values were obtained via the optical analysis. The  $G_I$  values derived from the optical analysis correlate well with those from bulk measurements, and the fracture toughness of amylose proves to be comparable to that of other engineering polymers. Surprisingly, moisture content within the range investigated herein has no great effect on the strain energy release rate. This insensitivity is attributed to active interaction between the absorbed water and the amylose macromolecules.

Support: NSF

#### THERMALLY STIMULATED DISCHARGE CURRENTS FROM POLYACRYLONITRILE

R. J. Comstock, S. I. Stupp and S. H. Carr  
[J. Macromol. Sci.-Phys. B13(1), 1977]

Electrical polarizations in as-cast and electrically polarized films of stretched and unstretched polyacrylonitrile have been measured with the thermally stimulated discharge technique. Preferential orientation of nitrile

side groups in polarized specimens is inferred from birefringence and x-ray diffraction experiments, but the contribution of observed persistent electrical polarization appears to be small. The major contribution is concluded as being due to trapped space charges, some part of which may be associated with residual solvent molecules. Small ordered regions within polyacrylonitrile are expected to play a role in development of each contribution to final persistent electrical polarization.

Support: ONR

#### GEL CHROMATOGRAPHY OF ELASTIN

J. T. Coates  
[M.S. Thesis]

Reconstituted elastin has been shown to have a specific relationship between mechanical properties and molecular weight distribution. A method of separating the different polypeptides derived from partially hydrolyzed elastin was developed using column gel permeation chromatography. Significant differences between chains obtained at early stages of solubilization by boiling oxalic acid solutions are reported. These differences lie in the distributions of molecular size and amino acid content. A selective hydrolysis pattern is proposed based on models of structure in native elastin.

Support: Bio-medical Engineering Center, Northwestern University  
Advisor: S. H. Carr

#### THERMALLY STIMULATED DISCHARGE CURRENT STUDIES ON LOW-TEMPERATURE RELAXATIONS IN POLYCARBONATE

Y. Aoki and J. O. Brittain  
[J. Appl. Polymer Sci. 20, 1976]

The  $\beta$ -relaxation in polycarbonate has been investigated by the thermally stimulated discharging current (TSC) technique. The polarization of the  $\beta$ -peak in polycarbonate is shown to be uniform. Two broad peaks centered at 130° and 200°K were observed. Furthermore two single relaxation processes were resolved for the lower temperature peak. The high temperature peak was also resolved into two peaks, however, only one of them was a single relaxation process. The individual peaks satisfied the dipolar theory and the three peaks are associated with activation energies of 0.24, 0.27 and 0.47

eV and temperature of the peak maxima were 121°, 131° and 193°K, respectively. The mechanism attributed to each peak is discussed and does not appear to contradict the results of conventional dielectric and mechanical relaxation and NMR measurements on the  $\beta$ -relaxation in polycarbonate.

Support: NSF-MRL

THERMALLY STIMULATED DISCHARGE CURRENT STUDIES ON THE EFFECT  
OF THERMAL TREATMENT ON THE STRENGTH OF POLYCARBONATE

Y. Aoki and J. O. Brittain  
[J. Polymer Sci. 15, 1977]

It is well known that polycarbonate annealed at 80 - 130°C undergoes gradual changes in mechanical properties. Annealing below T<sub>g</sub> (~ 150°C) results in a decrease in impact resistance and an increase in strength. Polycarbonate has three single relaxation processes and some distributed relaxation processes in the temperature range between 100°K and 250°K (the  $\beta$  transition region). The effect of thermal pretreatment on the relaxation processes of polycarbonate has been investigated by the thermally stimulated discharge current technique. Partial heating, peak cleaning and theoretical fitting have been performed and the activation parameters associated with the relaxation processes have also been calculated to assist in the analysis of the relationship between the effect of annealing and structural motions in polycarbonate.

Support: NSF-MRL

THERMALLY STIMULATED DISCHARGE CURRENT STUDIES ON POLYCARBONATE,  
POLYSULFONE, AND THEIR BLENDS

Yoshio Aoki  
[Ph.D. Thesis]

The relaxation process in polymeric materials has been a subject of great interest in advancing our knowledge and understanding of the behavior of molecular motions in polymeric materials. The use of mechanical and dielectric relaxations to characterize polymeric materials has come into prominence and has advanced our understanding of their molecular behavior. In general, however, these techniques have been unable to provide the desired characterization of polymeric materials due mainly to the inability to

associate specific relaxation mechanisms with the observed relaxation spectra. The investigation of relaxation processes in polymeric materials via mechanical or dielectric techniques is complicated by the fact that several relaxation processes generally coexist at about the same temperature. Relaxation processes in most polymers are distributed in activation energies and/or natural frequencies. Therefore, the contribution of different relaxation mechanisms can be distinguished in the dispersion curve only if the corresponding relaxation times differ appreciably. Furthermore, the dielectric measurements by the alternating field method has another complication when there is a non-vanishing electric conductivity within the material, because it builds up a space charge on the interfaces between a sample and the electrodes which can stimulate an additional polarization mechanism superimposed upon the true dispersions.

Some of the complications and shortcomings associated with the use of mechanical and dielectric relaxation techniques to study polymeric materials was minimized, if not eliminated entirely by use of the recently developed "Thermally Stimulated Discharge Current (TSC) Method."

This dissertation presents thermally stimulated discharge current measurements on polycarbonate, polysulfone, and their blends. These materials are of commercial prominence due to their relatively high glass transition and their superior ductility and impact strength below  $T_g$ . The toughness of these polymers has been attributed to molecular motions of the main chain at temperatures below  $T_g$ . These motions are evidenced by the broad  $\beta$ -relaxation processes in these materials. Mechanical and dielectric properties of the  $\beta$ -relaxation in those materials have been extensively studied. Most of these measurements have been done at medium or high frequencies and showed a broad  $\beta$ -peak. However, TSC measurements are made at very low frequencies. This extension of the scope of dielectric measurements is important and facilitates the interpretation of relaxation mechanisms in dielectrics.

Dielectric relaxation measurements at the very low frequency ( $3 \times 10^{-2} \sim 6 \times 10^{-4}$  Hz) were carried out on polycarbonate and showed that the equivalent frequency of our TSC measurement was about  $1.2 \times 10^{-3}$  Hz in the  $\beta$ -peak region in polycarbonate. The  $\beta$ -relaxations in polycarbonate and polysulfone were investigated by the TSC technique. Two broad peaks centered at  $\sim 140^\circ$  and  $\sim 200^\circ\text{K}$  were observed in these materials and the polarization of the  $\beta$ -peaks was shown to be uniform.



It was found that there were at least four kinds of relaxation processes in the  $\beta$ -peak in polycarbonate, polysulfone, and their blends. The low temperature side of the  $\beta$ -peak was associated with the polar group, while the high temperature side was associated with the phenyl groups in the main chain of these materials. The decreased impact resistance and the increased strength in polycarbonate after annealing below  $T_g$  were mainly due to the decreased mobility of the phenyl groups and further ordering of the chains involving the movements of the phenyl groups in this material.

Chain backbone motion in polycarbonate was investigated by the TSC technique. A prominent peak was found at about 50°C below  $T_g$  from cold rolled polycarbonate. The results indicated an evidence of the chain backbone motion below  $T_g$  in polycarbonate.

The TSC studies on PCO/PSO blends revealed a definite compositional dependence. A phase inversion occurred for these blends at the 60 wt/o PSO and at this composition the TSC was almost equal to the sum of the weight fractions of their component. The result suggested that the polarization in the blend at the phase inversion was mainly due to molecular motion associated with dipole moments. Addition of small quantities of PSO to PCO resulted in a large increase in the activation energy.

Support: NSF-MRL - Advisor: J. O. Brittain

#### LIGHT AND X-RAY SCATTERING BY POLYMER GLASSES

C. Clairborne, R. Judd and B. Crist

The nature of the large (ca. 2000 Å) heterogeneities in polymer glasses is being investigated by the scattering of light and x-rays. Experiments to date have been to perfect the technique of preparing samples of poly(methyl methacrylate) and polystyrene from chemically pure, dust-free monomer. We have noticed that polymerization conditions, especially the polymerization temperature, greatly affect the homogeneity of the resulting polymer. Preliminary examination of commercial polymers has shown that the concentration of large scattering centers (probably dust) is non-uniform over volume elements of a few cubic millimeters. The preparation of polymers free from such extrinsic structures will enable us to examine any basic heterogeneities or structures characteristic of the glassy material.

Support: NSF

## MOLECULAR ASPECTS OF RUBBER ELASTICITY

D. S. Pearson, L. Dossin and W. W. Graessley

Both the equilibrium and dynamic mechanical properties of rubber depend on the structure of the network which forms when the polymer is crosslinked. The classical theories attribute elasticity to the reduction of configurational entropy of the network strands as the rubber is stretched. The modulus calculated from these theories is smaller in many cases than observed experimentally, sometimes by a factor of ten or more. Some evidence indicates that the difference is caused by chain entanglement: a physical coupling between network strands which increases the effective concentration of junctions in the network. Experimental studies to test this hypothesis are under way on two systems: polybutadiene and ethylenepropylene copolymers. Samples of both polymers with narrow molecular weight distributions have been prepared and characterized, and networks have been formed by radiation-induced crosslinks. Data on network structure, solvent swelling and stress-strain behavior in tension are now being gathered. Preliminary results indicate that the equilibrium modulus is proportional to the sum of the network junction concentration and the concentration of trapped entanglements.

Support: EXXON and PRF-ACS

## TIME DEPENDENT STRESS IN SHEARING FLOWS OF POLYMER SYSTEMS

E. Menezes and W. W. Graessley

The rheological properties of polymer liquids are commonly characterized by measurements of steady state stresses developed during simple shear flows and time dependent stresses in the linear viscoelastic regime. Although useful in themselves, such measurements are not sufficient to distinguish among various generalized theories of viscoelasticity. Stress of development after the start of steady shear flow and stress relaxation after the flow is stopped are both potentially useful in this regard. We have recently completed a study of start-up and relaxation using a specially modified commercial instrument, the Weissenberg Rheogoniometer. We are now incorporating a mini-computer into the experiments which will allow us to gather and process data more efficiently. Precision of the measurements will also be improved, and we will be able to extend our studies to other types of non-linear transient experiments.

Support: NSF

Support:  
NSF-MRL Program

GENERAL MATERIALS RESEARCH: PART I

Faculty:

K. W. Singwi, Professor, Physics and Astronomy  
R. P. Van Duyne, Associate Professor, Chemistry  
E. Weitz, Assistant Professor, Chemistry  
G. D. Wong, Assistant Professor, Physics and Astronomy  
C.-W. Woo, Professor, Physics and Astronomy

Research Staff:

H.-h. Chou, Physics and Astronomy  
A. K. Gupta, Postdoctoral Fellow, Physics and Astronomy  
P. Jena, Postdoctoral Fellow, Physics and Astronomy

Graduate Students:

M. A. Lee, Physics and Astronomy  
M. R. Suchanski, Chemistry

Degrees Granted:

M. A. Lee, Ph.D. August, 1977  
M. R. Suchanski, Ph.D., June, 1977

Sponsorship:

NSF-MRL, National Science Foundation, Materials Research Laboratory  
ACS-PRF, American Chemical Society, Petroleum Research Fund  
ANL, Argonne National Laboratory  
NATO, North American Treaty Organization  
NSF, National Science Foundation  
Research Corporation  
Sloan, Alfred P. Sloan Foundation

Introduction

The General Materials Research is divided into two sections. Section I includes research projects which were supported under the MRL program as individual projects and includes the collaborative research efforts of Professors Singwi and Wong on the Electronic Structure of Point Defects in Metals and Electron Hole Droplets. The research of Professors Van Duyne, Weitz, Wong and Woo on Resonance Raman Spectroscopy, Energy Transfer in Matrix Isolated Molecules, Optical Properties of Semiconductors and Statistical Mechanical Calculations for Liquid Crystals, respectively, are included.

NONLINEAR ELECTRON-DENSITY DISTRIBUTION AROUND POINT DEFECTS  
IN SIMPLE METALS. I. FORMULATION

A. K. Gupta, P. Jena and K. S. Singwi  
[Submitted for publication]

A modification, which is exact in the limit of long wavelength, of the nonlinear theory of Sjölander and Stott of electron distribution around point defects is given. This modification consists in writing a nonlinear integral equation for the Fourier transform  $\gamma_{12}(q)$  of the induced charge density surrounding the point defect, which includes a term involving the density derivative of  $\gamma_{12}(q)$ . A generalization of the Pauli-Feynman coupling-constant-integration method, together with the Kohn-Sham formalism, is used to exactly determine the coefficient of this derivative term in the long-wavelength limit. The theory is then used to calculate electron-density profiles around a vacancy, an eight-atom void, and a point ion. The results are compared with those of (i) a linear theory, (ii) Sjölander-Stott theory, and (iii) a fully self-consistent calculation based on the density-functional formalism of Kohn and Sham. It is found that in the case of a vacancy, the results of the present theory are in very good agreement with those based on Kohn-Sham formalism, whereas in the case of a singular attractive potential of a proton, the results are quite poor in the vicinity of the proton, but much better for larger distances. A critical discussion of the theory vis a vis the Kohn-Sham formalism is also given. Some applications of the theory are pointed out.

Support: NSF-MRL, NSF and ANL

NONLINEAR ELECTRON-DENSITY DISTRIBUTION AROUND POINT DEFECTS  
IN SIMPLE METALS. II. APPLICATIONS

P. Jena, A. K. Gupta and K. S. Singwi  
[Submitted for publication]

Electron distribution around point defects (vacancies, voids, and impurities) in a number of simple metals has been calculated using linear and generalized nonlinear-response theories and compared with that obtained from a self-consistent calculation based on the density-functional formalism of Hohenberg, Kohn, and Sham. Using these electron-density profiles, positron lifetimes, and angular correlation between annihilation photons in vacancies and small voids are calculated. We have also computed the distribution of



electric-field gradients due to several impurities in Al. The results are compared with experiment.

Support: NSF-MRL, NSF and ANL

#### ELECTRONIC STRUCTURE OF HYDROGEN IN SIMPLE METALS

P. Jena and K. S. Singwi  
[Submitted for publication]

Based on the Hohenberg-Kohn-Sham formalism, a fully self-consistent calculation of the electron density distribution around a proton in the metallic density range is presented. The calculation takes into account the first gradient correction to the exchange-correlation potential, hitherto treated only in the local density approximation. Very shallow bound states are found to exist for all metallic densities ( $r_s = 2.07-5$ ) considered. The physical picture regarding the electronic structure of a proton in the metallic density range is that of an extended  $H^-$  ion accompanied by an equally extended compensating hole in the uniform electron gas. Assuming that a positive muon ( $\mu^+$ ) constitutes a heavy impurity in an electron gas, the Knight shift at  $\mu^+$  site as a function of electron density ( $r_s$ ) has also been calculated and the results are compared with experiment.

Support: NSF-MRL and ANL

#### ELECTRON-HOLE DROPLETS IN GERMANIUM IN THE HIGH STRESS LIMIT

B. J. Feldman, H.-h. Chou and George K. Wong  
[Submitted for publication]

We have measured the density, binding energy, and phase diagram of electron-hole droplet at a uniform  $\langle 111 \rangle$  uniaxial stress of  $13.1 \text{ kg/mm}^2$ . Our results are in good agreement with the theoretical calculations of P. Vashishta, S. G. Das and K. S. Singwi.

Support: NSF-MRL, Research Corp. and Sloan

OBSERVATION OF "HOT" ELECTRON-HOLE DROPLETS  
IN GERMANIUM UNDER UNIFORM  $\langle 111 \rangle$  STRESS

H.-h. Chou, George K. Wong and B. J. Feldman  
[Submitted for publication]

We have observed "hot" free excitons and electron-hole droplets in Ge when the stress induced splitting between the conduction-band ellipsoids is larger than the Fermi energy of electrons. Our results show that both "hot" and "cold" electrons co-exist in the same electron-hole droplet. We have also measured the total lifetime of "hot" EHD which is in good agreement with an intervalley relaxation process by electron-electron scattering.

Support: NSF-MRL, Research Corporation and Sloan

OPTICAL-FIELD-INDUCED REFRACTIVE INDICES AND ORIENTATIONAL RELAXATION TIMES  
IN A HOMOLOGOUS SERIES OF ISOTROPIC SUBSTANCE

E. G. Hanson, Y. R. Shen and George K. Wong  
[Phys. Rev. 14, 1976]

We have measured the optical Kerr constant and the orientational relaxation times of seven p,p'-di-n-alkoxyazoxybenzene homologous compounds as functions of temperature in the isotropic phase. The observed critical behaviors near isotropic-nematic transitions agree well with the predictions from the Landau-de Gennes model. Various characteristic parameters of the homologs are deduced from the experiment. Their variations with increase of methylene groups in the alkyl chain are discussed. Our results suggest that neither the mean-field theory of Maier and Saupe nor the Landau expansion of free energy is a good approximation for quantitative description at the isotropic-nematic transition.

Support: NSF-MRL

RESONANT EXCITONIC CONTRIBUTIONS TO NONLINEAR OPTICAL SUSCEPTIBILITIES OF CdS

H.-h. Chou and George K. Wong  
[Phys. Rev. Letters 37, 1976]

We have observed resonant excitonic contributions to the nonlinear optical susceptibilities of CdS when the fundamental frequency was tuned through exciton resonances. We show that our data are in good agreement with quantum-mechanical calculations while the anharmonic oscillator model gives

incorrect resonance denominators. We also show that selection rules for exciton contributions are different depending on whether the fundamental frequency or generated second-harmonic frequency is in resonance with exciton states.

Support: NSF-MRL and Sloan

#### STATISTICAL MECHANICAL CALCULATIONS FOR LIQUID CRYSTALS

Michael A. Lee and Chia-Wei Woo  
[Submitted for publication]

A molecular theory of liquid crystals is developed within the framework of statistical mechanics for classical liquids. Coupled Bogoliubov-Born-Green-Kirkwood-Yvon (BBGKY) equations are derived and solved for anisotropic systems of molecules interacting via a pairwise, orientation-dependent potential. Solutions representing isotropic and nematic phases are obtained. Among the quantities calculated are the temperature- and density-dependent orientational order parameters. Besides serving as a prototype calculation, what is presented here also provides a theoretical backbone in which the mean field approximation can be better understood.

Support: NSF-MRL and NSF

#### AN INFORMATION THEORETIC DERIVATION OF POPULATION DISTRIBUTIONS FOR VIBRATIONAL STATES IN LASER EXCITED SYSTEMS

R. K. Huddleston and Eric Weitz  
[J. Chem. Phys. 66, 1977]

Information theory has been shown to provide a simple means of deriving population distributions in vibrationally excited systems where rapid vibration-vibration energy transfer occurs. The implications of the distributions obtained with respect to temperature of different modes, decay of vibrational populations and the possibility of vibrationally induced reactions are discussed. Non-equilibrium vibrational distributions are most pronounced when the heat bath temperature is much lower than the vibrational temperature of the modes of the system. This is expected to occur in vibrationally excited matrix isolated molecules.

Support: ACS-PRF, NATO and NSF-MRL

RESONANCE RAMAN SPECTROSCOPY OF TTF-TCNQ

Mary R. Suchanski  
[Ph.D. Thesis]

Well resolved resonance Raman (RR) spectra ( $200\text{ cm}^{-1}$  to  $1800\text{ cm}^{-1}$ ) have been obtained for the one-dimensional organic metal tetrathiafulvalene tetracyanoquinodimethane (TTF-TCNQ) in the form of powders dispersed in KBr and as vapor deposited thin films. Interpretation of the RR spectra has been carried out by comparison with the RR spectra of  $\text{TCNQ}^{\cdot-}$  and  $\text{TTF}^{\cdot+}$  generated electrochemically in solution. The degree of charge transfer in TTF-TCNQ has been estimated as  $0.56 \pm .11$  by comparison of the C=C stretching frequency in TCNQ derivatives with that in TTF-TCNQ. Since only one Raman band is observed corresponding to each TCNQ intramolecular normal mode we conclude that the TCNQ in TTF-TCNQ is best represented as a delocalized  $\text{TCNQ}^{\cdot-56}$  moiety on the RRS time scale of ca.  $10^{-14}$  to  $10^{-13}$  sec.

Support NSF-MRL and NSF - Advisor: R. P. Van Duyne



GENERAL MATERIALS RESEARCH: PART II

Faculty:

J. B. Cohen, Professor, Materials Science and Engineering  
A. J. Freeman, Professor, Physics and Astronomy  
W. P. Halperin, Assistant Professor, Physics and Astronomy  
J. A. Ibers, Professor, Physics and Astronomy  
J. B. Ketterson, Professor, Physics and Astronomy  
T. J. Marks, Associate Professor, Chemistry  
M. Meshii, Professor, Materials Science and Engineering  
E. Weitz, Assistant Professor, Chemistry  
D. H. Whitmore, Professor, Materials Science and Engineering  
G. K. Wong, Assistant Professor, Physics and Astronomy  
C.-W. Woo, Professor, Physics and Astronomy

Research Staff:

P. Bardhan, Postdoctoral Fellow, Materials Science and Engineering  
W. Jakubowski, Visiting Scholar, Materials Science and Engineering  
K. Kojima, Postdoctoral Research Associate, Materials Science and Engineering  
D. N. Lowy, Postdoctoral Fellow, Physics and Astronomy  
I. Muscutariu, Visiting Scholar, Physics and Astronomy  
L. Senbetu, Postdoctoral Fellow, Physics and Astronomy  
L. Shen, Visiting Scholar, Physics and Astronomy  
S. Y. Shen, Postdoctoral Fellow, Physics and Astronomy  
Y. M. Shih, Visiting Scholar, Physics and Astronomy

Graduate Students:

S. Bhattacharya, Physics and Astronomy  
I.-S. Chuang, Chemistry  
G. T. Fujimoto, Chemistry  
P. Georgopoulos, Materials Science and Engineering  
G. W. Grynkewich, Chemistry  
M. R. James, Materials Science and Engineering  
D. G. Kalina, Chemistry  
S. Kobayashi, Materials Science and Engineering  
M. A. Lee, Physics and Astronomy  
Y. R. Lin-Liu, Physics and Astronomy  
J. Nagakawa, Materials Science and Engineering  
J. Ni, Materials Science and Engineering  
S. Y. Shen, Physics and Astronomy  
D. R. Stojakovic, Chemistry  
J. S. Thompson, Chemistry  
C. J. Umrigar, Physics and Astronomy  
W. A. Wachter, Chemistry

Degrees Granted:

M. A. Lee, Ph.D., August, 1977  
D. R. Stojakovic, Ph.D., August, 1977

Sponsorship:

AFOSR, Air Force Office of Scientific Research  
ANL, Argonne National Laboratory  
Dreyfus, Camille and Henry Dreyfus Foundation  
ERDA, Energy Research and Development Administration  
NATO, North Atlantic Treaty Organization  
NIH, National Institute of Health  
NSF, National Science Foundation  
ONR, Office of Naval Research  
PRF, Petroleum Research Fund  
Research Corporation  
Sloan, Alfred P. Sloan Foundation

Introduction

This section of the General Materials Research includes individually non-MRL funded research projects. However, the research described made significant use of the Central Facilities or the space of the Materials Research Center or received indirect support from the MRL program.

A STRUCTURAL STUDY OF THE ALLOY  $\text{Cu}_3\text{Au}$  ABOVE ITS CRITICAL TEMPERATURE

P. Bardhan and J. B. Cohen  
[Acta Crystallographica A32, 1976]

Absolute measurements of the diffuse intensity in a volume in reciprocal space have been made at six temperatures ranging from  $2^\circ\text{C}$  above  $T_c$  to  $930^\circ\text{C}$ . The Warren short-range order parameters were obtained after correcting for the intensity due to atomic displacements in a more complete manner than in earlier studies. As a result the short-range order parameters are considerably smaller than in these earlier investigations. The (previously disputed) specific heat anomalies in  $\text{Cu}_3\text{Au}$  above  $T_c$  and the  $\text{LL}_2$  phase have been shown to be associated with unusual changes in diffuse X-ray scattering vs temperature. From studies of the scattering distributions, computer simulation and pair potentials obtained with the Warren short-range order parameters, the anomaly at  $600^\circ\text{C}$  appears to be due to the disappearance of  $\text{DO}_{22}$ -like fluctuations, whereas above  $850^\circ\text{C}$ ,  $\text{CuPt}$ -like fluctuations develop. There are premonitory effects just above  $T_c$ ; there is a large increase in the Debye-Waller factor, in the total

intensity due to quadratic terms in atomic displacements, and an apparent change in the sign of average first-neighbor displacement. The long-range oscillations in the interatomic potentials determined from the diffuse-scattering data fit the Friedel potential only approximately. The electron-to-atom ratio in  $\text{Cu}_3\text{Au}$  was found to be  $\sim 0.97$ , in agreement with results on Cu alloys by other methods.

Support: NSF

#### STUDY OF THE PRECISION OF X-RAY STRESS ANALYSIS

M. R. James and J. B. Cohen

[Denver Conf. on Advances in X-Ray Analysis 20, 1976]

Software is described for complete computer control of residual stress measurements. One program (that incorporates either the two tilt method, the  $\sin^2\psi$  procedure, or the Cohen-Marion technique) has been developed for use with either a normal detector or a position sensitive detector. The operator inputs the desired error in stress and various instrumental parameters that determine systematic errors. The counting strategy to obtain the total error is then determined by the software.

Employing this automated system, an investigation of a parabolic fit to the top of a diffraction profile indicates that a three point fit is satisfactory only for sharp profiles. Surprisingly, with a standard detector for fixed total time of data accumulation, the  $\sin^2\psi$  procedure gives better precision than the two tilt method.

A position sensitive detector system exhibited excellent precision in replicate residual stress measurements. Errors of  $\pm 6000$  psi were obtained on samples having broad diffraction profiles in only 30 seconds.

It was also found that sample displacement is less important for stationary slit geometry than with the parafocusing technique. Parallel beam geometry shows minimal effects due to sample displacement (as is well known) but the precision of the residual stress measurement decreases because this procedure broadens the diffraction profile.

Design parameters for a portable unit based on these results are discussed.

Support: ONR

ROLE OF CRYSTALLOGRAPHY

Sidney C. Abrahams and Jerome B. Cohen  
[Phys. Today 29, 1976]

Contemporary crystallographic techniques for examining the structures of solids and their excitations and defects use generators ranging from new miniature x-ray tubes to synchrotrons and pulsed-neutron sources.

Support: NSF

THE DEFECT STRUCTURE AND DEBYE WALLER FACTORS VS COMPOSITION IN  $\beta\text{-Ni}_{1-x}\text{Al}_{1+x}$

P. Georgopoulos and J. B. Cohen  
[Scripta Met. 11, 1977]

The  $\beta\text{-NiAl}$  phase has a range of composition, extending from 45 at pct to approximately 60 at pct Ni. The first phase diagram, accepted to this date with only slight modifications, was determined by Bradley and Taylor. At the stoichiometric composition the  $\beta\text{-NiAl}$  phase was shown to be a fully ordered CsCl structure (Strukturbericht notation B2) with Ni atoms occupying the corners and Al atoms the centers of the unit cell. Measurements of lattice parameter and density as a function of composition suggested defect structures in off stoichiometric alloys: for compositions above 50% Ni, excess Ni atoms replace Al on the Al sublattice, but below 50% Ni, vacancies are introduced on the Ni sublattice. To confirm this, Bradley and Taylor measured the integrated intensities of powder diffraction lines on film and compared them with calculations for different types of defects. While agreement was indeed found for these defect structures, only three peaks were employed. In fact, there has been some debate as to whether a small amount of Al is tolerated on the Ni sublattice, because some authors find a maximum in the lattice parameter slightly off stoichiometry while others find it at stoichiometry. Fraser et al. have suggested that this difference may be due to the formation of surface films of  $\text{NiAl}_2\text{O}_4$  on powder particles depleting the bulk of Al; chemical analysis would give the total Ni and Al, but the lattice parameter from the  $\beta$  phase would be for a phase richer in Ni. Indeed an examination of references does indicate that those who found the maximum off stoichiometry used longer anneals at higher temperatures compared to the others.

Accordingly, studies of integrated intensities from single crystals were initiated, to see if modern techniques for structural studies could shed light



on this question. We will also report briefly on preliminary studies of diffuse scattering due to the defects.

Support: NSF

#### THE NEED FOR EXPERIMENTALLY DETERMINED X-RAY ELASTIC CONSTANTS

R. H. Marion and J. B. Cohen  
[Advances in X-Ray Analysis 20, 1977,  
Plenum Publishing Corp.]

In order to convert residual strains measured by x-ray diffraction techniques into residual stresses, appropriate x-ray elastic constants have to be measured. Since these x-ray elastic constants may depend on the metallurgical state, deformation, and entire specimen history, errors in stress values may result if the constants are not measured for representative material states. In the present work, it is shown that in some cases these errors may be large.

The x-ray elastic constant,  $S_2/2 = (1 + \nu)/E$ , has been measured for the 211  $\text{CrK}_\alpha$  reflection from an Armco iron sample which had been previously deformed by rolling (69 pct. reduction in thickness) and for the 211  $\text{CrK}_\alpha$  and 310  $\text{CoK}_\alpha$  reflections from a 1045 steel specimen which had been previously elongated in tension. The measured elastic constant for the Armco iron specimen was 40 pct. lower than the value calculated from the average of the Reuss and Voigt values.

Support: ONR and ERDA

#### UNRESTRICTED DIRAC-FOCK THEORY: RELATIVISTIC DETERMINATION OF CORE POLARIZATION HYPERFINE INTERACTIONS

J. P. Desclaux, A. J. Freeman and J. V. Mallow  
[Submitted for publication]

The unrestricted Dirac-Fock (UDF) method is developed for determining relativistic contributions to the hyperfine interaction, notably that due to core polarization. Radial core-polarization of the one-electron (jj-coupled) spin orbitals is obtained by relaxing the restraint in restricted Dirac-Fock (RDF) theory that the radial part be independent of the magnetic quantum number, the projection  $m_j$  of  $j$ . Relativistic effects on the core polarization

are obtained by comparison with results obtained from the non-relativistic spin polarized Hartree-Fock ( $m_s$  unrestricted) and spin plus orbital polarized Hartree-Fock ( $m_s$  plus  $m_l$  unrestricted) calculations. For the 5d transition series ions, the relativistic core polarization enhancement factor,  $S_g(z)$ , is determined to be about a factor of two and so is much smaller than the isomer shift charge density enhancement factor ( $\sim 6$ ) found earlier for these same ions. Comparison is made with the limited experimental data available to date; for the case of atomic Re, excellent agreement is obtained with experiment.

Support: NSF and ERDA

#### ELECTRONIC BAND STRUCTURE, DENSITY OF STATES AND FERMI SURFACE OF $\alpha$ -U

T.-J. Watson-Yang, D. D. Koelling and A. J. Freeman  
[American Physical Society Meeting, March, 1977]

$\alpha$ -U exhibits a number of unusual properties (including superconductivity) which arise from the peculiar character of its 5f electrons. Its complex crystal structure (orthorhombic A20 with 4 atoms/unit cell) results in low symmetry which make relativistic calculations difficult and costly. Stimulated by recent dHvA measurements at hydrostatic pressure which suppress the low T transitions, the band structure, density of states, and FS of  $\alpha$ -U were determined using a relativistic APW method which includes orbital energy derivatives. The procedure requires only a single diagonalization of the secular equation manipulated first into a non-relativistic-like form whose solutions are used to perform the full relativistic calculation.

Support: ERDA and NSF

#### COMPARISON OF LMTO AND APW ENERGY BAND SOLUTIONS

G. Arbman, T. Asada, A. J. Freeman and T. J. Watson-Yang  
[American Physical Society Meeting, March, 1977]

We describe linear-muffin-tin-orbital (LMTO) band calculations for metals and compounds in which the tail contributions to the overlap and Hamiltonian matrices are treated exactly. The accuracy of the resulting eigenvalues and eigenfunctions are ascertained by direct comparison of results obtained with standard APW solutions using the same (muffin-tin) potential. For a metal like Cu, for example, the eigenvalues agree to within 1 mRy.

Detailed direct wave function comparisons are presented. Complications for compounds are discussed and detailed solutions are described.

Support: NSF and AFOSR

#### RELATIVISTIC SELF-CONSISTENT FIELD STUDIES OF MUONIC ATOMS

J. P. Desclaux, A. J. Freeman and J. V. Mallow  
[American Physical Society Meeting, February, 1977]

We have previously reported the development of the restricted and unrestricted Dirac-Fock methods for muonic atoms in which both electron and muon orbitals are included in the determinantal wave function. The resultant coupled Dirac-Fock (and, in the nonrelativistic case, the Hartree-Fock) integro-differential equations, including the muon-electron interaction, are then solved self-consistently. We report here results of calculations using realistic nuclear charge distributions and include core polarization effects in the presence of an excited state muon. Comparisons with single muon model calculations show measureable effects of electron screening on muon transition energies, particularly for the lighter atoms studied.

Support: NSF and ERDA

#### ELECTRONIC STRUCTURE AND PROPERTIES OF THE ACTINIDES

A. J. Freeman and D. D. Koelling  
[Physica 86-88, 1977]

We review the present state of understanding of the electronic structure and physical properties of actinide metals and intermetallic compounds as derived from relativistic APW energy band studies of some of the light (Th, U, Np and Pu) and heavy (Am, Bk and Cm) metals, the intermetallics  $URh_3$  and  $UIr_3$  and (NaCl structure compounds such as ) UC. Emphasis is placed on the importance of Coulomb correlation and the role of actinide-actinide separation in determining the itinerancy (as in the light metals) or localization (as in the heavy metals) of the 5f electrons and in turn their resulting magnetic and other properties. The  $UX_3$  systems considered are significant because the uranium sites are sufficiently separated to fall in the local moment f orbital range of the Hill superconductivity/magnetism plot but show no magnetic ordering. Comparisons to recent optical, de Haas-van Alphen and other data are given when available. The contrasting cases of the transition and rare-earth systems

make it clear that the 5f electrons are a unique species which offer exciting challenges to both experimentalists and theorists.

Support: NSF, AFOSR and ERDA

#### RELATIVISTIC MAGNETIC FORM FACTORS OF TRIPOSITIVE RARE-EARTH IONS

C. Stassis, H. W. Deckman, B. N. Harmon,  
J. P. Desclaux and A. J. Freeman  
[Phys. Rev. B, 15, 1977]

Magnetic form factors have been obtained from Dirac-Fock calculations for all the rare-earth tripositive ions. In addition to using relativistic 4f wave functions, the coupling of the neutron magnetic moment to the current density has been treated consistently using a relativistic formulation for the scattering amplitude. For each rare-earth ion we evaluated the odd magnetic multipoles, of order less or equal to seven, which are needed for the evaluation of the magnetic scattering amplitude in most cases of experimental interest. We find that in all cases the magnetic form factor decreases faster with increasing scattering angle than predicted by nonrelativistic calculations. This is because (i) the relativistic 4f-electron wave functions are more expanded in space as a result of the relativistic core contraction than the Hartree-Fock wave functions and (ii) the net effect of the spin orbit and mass correction term on the scattering of neutrons, implicitly included in our relativistic formulation of the scattering amplitude, is such that the neutron senses a current density more expanded in space than predicted by nonrelativistic calculations.

Support: ERDA and NSF

#### FIBERGLASS INSERT TO LIQUID HELIUM DEWAR

S. Y. Shen, W. P. Halperin and J. B. Ketterson

We present the design of a simple fiberglass insert to the liquid helium space of a conventional metal Dewar that minimizes the volume of liquid helium required when it is adapted for experiments not employing the full volume available at low temperatures. It was found that in using this insert the liquid helium evaporation rate was considerably reduced.

Support: Research Corp. and NSF



# REFRIGERATION BY ADIABATIC DEMAGNETIZATION OF NUCLEAR SPINS

S. Y. Shen, J. B. Ketterson and W. P. Halperin

A model is presented for a nuclear demagnetization cooling system in which the metallic refrigerant is distributed over a region where the magnetic field varies by a large amount. A method employing "quasi-steady state" approximations is used to solve the problem in the framework of finite difference procedures. The predictions from the model are used to establish a number of design parameters in cryostats for studies of superfluid  $^3\text{He}$  and ultra-low temperature metals physics.

Support: NSF

# MOBILITY OF POSITIVE AND NEGATIVE IONS IN SUPERFLUID $^3\text{He}$

Paul D. Roach, J. B. Ketterson and Pat R. Roach  
[Submitted for publication]

The mobility of positive and negative ions has been studied as a function of temperature, electric drift field, and (in the A phase) magnetic field direction in superfluid  $^3\text{He}$ ; the A phase mobility is observed to be anisotropic with  $\mu_{\perp} > \mu_{\parallel}$  for both positive and negative ions.

Support: ERDA and NSF

# ANISOTROPIC ULTRASOUND PROPAGATION IN A CHOLESTERIC LIQUID CRYSTAL

S. Bhattacharya, I. Muscutariu and J. B. Ketterson  
[Submitted for publication]

We report here a detailed study of the propagation of longitudinal ultrasound through a magnetically aligned cholesteric liquid crystal (a mixture of cholesteryl chloride and cholesteryl myristate 1.75:1 by weight). The observed velocity anisotropy is tentatively attributed to dispersion and an attenuation anisotropy was observed for the first time. The temperature dependence of several elastic constants and combinations of viscosity coefficients was determined. A new expression for the attenuation was derived from the hydrodynamic equations, and from a twisted nematic model. A more detailed report of the acoustic Brillouin zone effect is also presented.

Support: NSF, NSF-MRL and ERDA

ANISOTROPIC ULTRASOUND PROPAGATION IN A SMECTIC-C LIQUID CRYSTAL

S. Bhattacharya, C. J. Umrigar and J. B. Ketterson  
[Proc. of 6th Int. Conf. on Liquid Crystals, August, 1976]

We report here the results of longitudinal ultrasound propagation in a magnetically aligned smectic-C liquid crystal (p-p' Heptyloxyazoxy benzene). In the smectic-C phase the plane normals can lie anywhere on a cone with the axis along the magnetic field direction in which the sample was cooled. The effects of the layer normal direction and the molecular orientation within the planes on the velocity anisotropy were separated by cooling the sample into the smectic-C phase at particular orientations of the magnetic field and subsequently rotating the magnetic field. The results were analyzed on the basis of a multidomain model where the azimuthal angle of the plane normal around the field direction was averaged over.

Support: NSF, NSF-MRL and ERDA

TRANSVERSE ZERO SOUND IN NORMAL  $^3\text{He}$

Pat R. Roach and J. B. Ketterson  
[Proc. of the Sanibel Symposium on Quantum Fluids & Solids,  
January, 1977]

We have measured the complex acoustic shear impedance of liquid  $^3\text{He}$  by observing the decay of a transiently excited AC cut quartz transducer. Comparison with recent theories suggests that our results at low temperatures can only be due to the excitation of transverse zero sound. We have also observed the direct transmission of transverse excitations between two closely spaced transducers in the vicinity of 3 mK. These results are analyzed in terms of the propagation of transverse zero sound although theory suggests that a single-particle contribution must also be present.

Support: ERDA and NSF

MEASUREMENTS OF THE ACOUSTIC SHEAR IMPEDANCE OF SUPERFLUID  $^3\text{He}$

Pat R. Roach and J. B. Ketterson  
[Low Temp. Phys. 25, 1976]

Measurements of the complex acoustic shear impedance of  $^3\text{HeB}$  at 19 bar and 36 and 60 MHz, and  $\text{HeA}$  at 23 bar and 12, 36 and 60 MHz have been made by observing the time constant and the frequency shift of the decay of a transiently excited AC cut quartz transducer.

Support: ERDA and NSF

BLUE COPPER PROTEINS: SYNTHESIS, SPECTRA AND STRUCTURES  
OF  $\text{Cu}^{\text{I}}\text{N}_3(\text{SR})$  AND  $\text{Cu}^{\text{II}}\text{N}_3(\text{SR})$  ACTIVE SITE ANALOGUES

J. S. Thompson, T. J. Marks and J. A. Ibers  
[Submitted for publication]

The reaction of  $\text{Cu}(\text{SR})$  or  $[\text{Cu}(\text{SR})][\text{ClO}_4]$  derivatives,  $\text{SR} =$  p-nitrobenzenethiolate or O-ethylcysteinate, with potassium hydrotris-(3, 5-dimethyl-1-pyrazolyl)borate produces redox pairs of the stoichiometry  $\text{Cu}^{\text{I}}\text{N}_3(\text{SR})$  and  $\text{Cu}^{\text{II}}\text{N}_3(\text{SR})$ . These complexes are the first well-defined synthetic approximations to the proposed  $\text{N}_3\text{S}$  binding sites of blue (type 1) copper electron transfer proteins. The new compounds were investigated by a variety of chemical and spectral (optical, resonance Raman, electron paramagnetic resonance) techniques; the complex  $\text{K}[\text{Cu}(\text{HB}(3,5\text{Me}_2\text{pz})_3) - (\text{p-NO}_2\text{C}_6\text{H}_4\text{S})] \cdot 2$  acetone was also studied by single crystal X-ray diffraction methods. The spectrochemical characteristics of the  $\text{Cu}^{\text{II}}\text{N}_3(\text{SR})$  species are in large part similar to the native system and thus provide some perspective regarding the origin of the unique type 1 spectral parameters and electron transfer properties.

Support: NSF, NIH and Dreyfus

CHEMISTRY AND SPECTROSCOPY OF f ELEMENT ORGANOMETALLICS  
PART I: THE LANTHANIDES

Tobin J. Marks  
[Submitted for publication]

The past eight years have witnessed a period of vigorous activity in the fields of lanthanide and actinide organometallic chemistry. This activity reflects, among other factors, the growing realization that these elements may



possess a unique, interesting, and useful organometallic chemistry which, during the explosive growth of organotransition metal chemistry, has been largely and unjustifiably ignored. In particular, lanthanide and actinide ions display expansive and unusual coordination geometries, unknown or rare for d transition ions; they also possess f valence orbitals which may, in optimum cases, have the appropriate energy and spatial extensions to be of chemical significance. These features provide reason to anticipate that lanthanide and actinide organometallics may display interesting properties as reagents or catalysts, and properties which are distinctly different from those of transition metal organometallics.

The goal of this article is to survey and to analyze progress in the field of lanthanide organometallic chemistry. After an initial introduction to the general chemical and physicochemical characteristics of the lanthanide elements, recent developments in organolanthanide chemistry are presented in the light of new results in bonding theory, spectroscopy, molecular structure and structural dynamics.

Support: NSF and Dreyfus

LARGE METAL ION-CENTERED TEMPLATE REACTIONS. CHEMICAL AND SPECTRAL STUDIES  
OF THE "SUPERPHthalOCYANINE" DIOXOCYClopENTAKIS (2-IMINOISOINDOLINATO)  
URANIUM (VI) AND ITS DERIVATIVES

Tobin J. Marks and Djordje R. Stojakovic  
[Submitted for publication]

This investigation reports on chemical and spectral studies of the macrocyclic uranyl complexes dioxocyclopentakis(2-iminoisoindolinato) uranium(VI),  $\text{SPcUO}_2$ , and dioxocyclopentakis(2-imino-4-methylisoindolinato) uranium (VI),  $\text{Me}_5\text{SPcUO}_2$ . These expanded, five-subunit analogues of phthalocyanines were synthesized in template reactions from uranyl salts and the corresponding phthalonitriles. The conditions for a high yield synthesis are critical and include a basic solvent (e.g., dimethylformamide), high temperatures, and strict exclusion of water. Phthalocyanine,  $\text{PcH}_2$ , is a side-product of the reaction with the source of protons being the solvent. Attempts to displace the uranyl ion from  $\text{SPcUO}_2$  with acids of other metal ions ( $\text{M}^{+n}$ ) invariably results in macrocycle contraction to produce  $\text{PcH}_2$  or  $\text{PcM}^{n-2}$  and phthalonitrile. Proton nmr studies reveal the five-subunit macrocycle to be stereochemically dynamic. The analysis of ring current induced proton nmr shifts indicates considerably reduced  $\pi$  electron delocalization in  $\text{SPcUO}_2$  compared to  $\text{PcM}$



derivatives. The electronic spectrum of  $\text{SPcUO}_2$  exhibits strong absorption maxima at 4240 and 9140 Å. With the aid of Pariser-Parr-Pople SCF  $\pi$  electron molecular orbital calculations the electronic structure of the macrocycle and the origin of the spectral transitions can be shown to be closely analogous to phthalocyanine systems. Many of the chemical and spectral properties of  $\text{SPcUO}_2$  and  $\text{Me}_6\text{SPcUO}_2$  reflect the severe buckling and strain within the macrocyclic ligand.

Support: NSF

STEREOCHEMICAL NONRIGIDITY IN SOLID ZIRCONIUM AND HAFNIUM TETRAKISTETRA-  
HYDROBORATES. EVIDENCE FOR TWO DYNAMIC INTRAMOLECULAR REARRANGEMENT  
PROCESSES IN COVALENT TETRAHYDROBORATES

I-Ssuer Chuang, Tobin J. Marks, William J. Kennelly  
and John R. Kolb  
[Submitted for publication]

Proton nuclear magnetic resonance studies of stereochemical dynamics in  $\text{Zr}(\text{BH}_4)_4$  and  $\text{Hf}(\text{BH}_4)_4$  have been carried out in the solid state. Variable temperature investigations were conducted in both continuous wave and pulsed modes. Two intramolecular motional processes were identified for each material and the nature of these processes was interpreted on the basis of effective second moment calculations in both diffusive and positional jump regimes. The higher temperature process is assigned to rapid intramolecular bridge-terminal hydrogen exchange,  $E_a(\text{Zr}) = 5.2 \pm 0.3$  ( $\Delta G^\ddagger = 8.1$  at 214°K) kcal/mol;  $E_a(\text{Hf}) = 8.4 \pm 0.3$  ( $\Delta G^\ddagger = 7.3$  at 200°K) kcal/mol. The lower temperature motion is suggested to involve rapid three-fold rotation about the ligand M-B-H(terminal) axis with  $E_a(\text{Zr}) = 5.4 \pm 0.2$  ( $\Delta G^\ddagger = 4.3$  at 124°K) kcal/mol;  $E_a(\text{Hf}) = 4.6 \pm 0.2$  ( $\Delta G^\ddagger = 4.4$  at 133°K) kcal/mol.

Support: NSF

SYNTHESIS AND SPECTROSCOPIC INVESTIGATIONS OF SOME GERMANIUM-  
AND TIN-TRANSITION METAL COMPOUNDS AND BIS(CYCLOPENTADIENYL)  
LANTHANIDE TETRAHYDROBORATES

Gregory W. Grynkwich  
[Ph.D. Thesis]

$^{119}\text{Sn}$  Mössbauer,  $^{119}\text{Sn}$ - $^1\text{H}$  three bond nmr coupling constants, and Sn 3d5/2 ESCA electron binding energy data for the compounds  $(\text{t-C}_4\text{H}_9)_2\text{SnM}(\text{CO})_x \cdot \text{B}$ ,

where  $M = \text{Fe}$ ,  $x = 4$  and  $B = \text{DMSO}$  and pyridine, and for  $M = \text{Cr}$ ,  $x = 5$  and  $B = \text{THF}$ ,  $\text{DMSO}$ , and pyridine, favor a tin(IV) formulation. The Mössbauer QS values for the  $M = \text{Cr}$  compounds (3.4 to 4.1 mm/sec) are the largest thus far recorded for four-coordinated organotin compounds. Explanations based upon ylide structures are proposed.

The compound  $[\mu-(\text{C}_6\text{H}_5)(\text{CH}_3)\text{Sn}]_2\text{Fe}_2(\text{CO})_7$  was synthesized to differentiate bridge deformation from iron-tin bond cleavage in R group interchange processes of stereochemically nonrigid  $[\mu-\text{R}_2\text{Sn}]_2\text{Fe}_2(\text{CO})_7$  complexes. It is found from proton nmr studies that both processes can occur, the former with  $\Delta G^\ddagger = 11.8 \pm 0.6$  kcal/mole (298°K) and the latter with  $\Delta G^\ddagger = 19.2 \pm 0.9$  kcal/mole (298°K). The bridge deformation in the related, more soluble molecule  $[(n\text{-C}_4\text{H}_9)_2\text{Sn}]_2\text{Fe}_2(\text{CO})_7$  occurs with simultaneous, stereospecific interchange of bridge and terminal carbonyl ligands, as monitored by  $^{13}\text{C}$  nmr spectra. The complex  $[(\text{C}_6\text{H}_5)(\text{CH}_3)\text{SnFe}(\text{CO})_4]_2$  exists in two isomeric forms which interconvert in solution with  $\Delta G^\ddagger = 25.5 \pm 0.7$  kcal/mole (298°K). The iron-tin bond cleavages are proposed to yield  $\text{R}_2\text{Sn} \rightarrow \text{Fe}$  stannylene intermediates.

This work reports the synthesis and spectral (infrared, Raman) characterization of the series of compounds  $(\eta^5\text{-C}_5\text{H}_5)_2\text{-LnBH}_4 \cdot \text{THF}$ , where  $\text{Ln} = \text{Sm}$ ,  $\text{Er}$ ,  $\text{Yb}$ . Vibrational spectra indicate that the mode of  $\text{BH}_4^-$  coordination is sensitive to the metal ionic radius. The  $\text{Ln} = \text{Sm}$  compound is proposed to have tridentate  $\text{BH}_4^-$  ligation, whereas the  $\text{Ln} = \text{Yb}$  compound is proposed to have bidentate ligation. The tetrahydrofuran can be removed for  $\text{Ln} = \text{Yb}$ ,  $\text{Er}$  to yield complexes of the composition  $(\eta^5\text{-C}_5\text{H}_5)_2\text{LnBH}_4$ . Vibrational spectra are similar to those of  $\text{Be}(\text{BH}_4)_2$  and  $\text{CH}_3\text{Zn}(\text{BH}_4)$ , suggesting a polymeric structure with bridging  $\text{BH}_4^-$  groups. All data suggest appreciable ionic character in the bonding of the tetrahydroborate to the trivalent lanthanides.

Support: NSF - Advisor: T. Marks

PHOTOCHEMICAL SYNTHESIS OF LOW-VALENT ORGANOTHORIUM COMPLEXES.  
EVIDENCE FOR PHOTOINDUCED  $\beta$ -HYDRIDE ELIMINATION

D. C. Kalina, T. J. Marks and W. A. Wachter  
[J. Amer. Chem. Soc. 99, 1977]

Photolysis of  $(\text{C}_5\text{H}_4\text{R})_3\text{Th}$  (isopropyl),  $\text{R} = \text{H}$ ,  $\text{CH}_3$ , produces the corresponding  $(\text{C}_5\text{H}_4\text{R})_3\text{Th}$  compounds in high yield as well as comparable quantities of propane and propene. The new organometallics were characterized by chemical and spectral methods and are formulated as Th(III) organometallics. The

propane and propene are shown to arise via a photoinduced  $\beta$ -hydride on another molecule of thorium alkyl. This work represents the first unambiguous example where  $\beta$ -hydride elimination can be induced photochemically in a system that resists it thermally. It suggests new synthetic routes to hydridic and low-valent transition metal and actinide organometallics.

Support: NSF, Sloan and Dreyfus

COVALENT TRANSITION METAL, LANTHANIDE AND ACTINIDE  
TETRAHYDROBORATE COMPLEXES

Tobin J. Marks and John R. Kolb  
[Chemical Reviews 77, 1977]

The tetrahydroborate ion,  $\text{BH}_4^-$ , is the simplest known anionic boron hydride. Among its diverse chemical properties is the tendency to form unusual covalent complexes with transition metals, lanthanides and actinides. The coordination is invariably through boron-hydrogen-metal bridges.

The chemical and physical nature of such compounds has been of current interest to inorganic and organometallic chemists both within the general context of studying how metals activate small, electron-rich ligands, and also because the unique configuration of the ligand-metal bond may be related to important species in catalytic transformations. How the chemical and electronic properties of the hydride bridging system respond to variation of metal and accompanying ligands may provide some insight into metal-to-substrate and reductant-to-metal hydride transfer processes. Since  $\text{BH}_4^-$  and  $\text{CH}_4$  are iso-electronic, prototype structures for saturated hydrocarbon activation are also presented. In a more technical vein, several metal tetrahydroborates have been shown to be hydrogenation and polymerization catalysts.

It is the purpose of this work to review and to analyze recent developments in the field of covalent transition metal, lanthanide and actinide  $\text{BH}_4^-$  complexes. The approach is both chemical and physicochemical, so that recent developments in the chemistry can be presented in the light of new results in spectroscopy, molecular dynamics, and bonding theory.

Support: NSF and Dreyfus



CHEMISTRY, STRUCTURE AND MOLECULAR DYNAMICS OF THE  
TETRAHYDROBORATOTETRACARBONYLMOLYBDATE(1-) ANION,  $\text{Mo}(\text{CO})_4\text{BH}_4^-$

Stephen W. Kirtley, Mark A. Andrews, Robert Bau, Gregory W. Grynkewich,  
Tobin J. Marks, Donald L. Tipton and Bruce R. Whittlesey  
[Submitted for publication]

The compound  $[(\text{Ph}_3\text{P})_2\text{N}][\text{Mo}(\text{CO})_4\text{BH}_4]$  can be prepared in 25% yield by the reaction of  $[(\text{Ph}_3\text{P})_2\text{N}][\text{Mo}(\text{CO})_5\text{I}]$  and  $[(\text{Ph}_3\text{P})_2\text{N}][\text{BH}_4]$  in anhydrous tetrahydrofuran. Mechanistic studies show that iodide ion acts as a catalyst in the synthesis. X-ray diffraction studies reveal that this material crystallizes in the space group  $\text{P}\bar{1}$  ( $a = 17.828(8) \text{ \AA}$ ,  $b = 9.714(4) \text{ \AA}$ ,  $c = 12.371(5) \text{ \AA}$ ,  $\alpha = 101.77(1)^\circ$ ,  $\beta = 115.36(1)^\circ$ ,  $\gamma = 94.40(1)^\circ$ ,  $V = 1886.9 \text{ \AA}^3$ ,  $\rho_{\text{obs}} = 1.33 \text{ g cm}^{-3}$ ,  $\rho_{\text{calc}} = 1.34 \text{ g cm}^{-3}$  for  $Z = 2$ ). Data were collected with Zr-filtered  $\text{MoK}\alpha$  radiation to a  $2\theta$  limit of  $45^\circ$ . Standard Patterson, Fourier, and least-squares techniques resulted in final agreement factors:  $R = 8.3\%$ ,  $R_w = 8.1\%$  for 3208 reflections with  $I > 3\sigma$ . The tetrahydroborate ligand is attached to the metal via two Mo-H-B bridge bonds with  $\text{Mo-H}_b = 2.02(8) \text{ \AA}$ . The coordination about the central molybdenum atom is approximately octahedral, but two notable distortions occur in the equatorial plane:  $\text{C}(\text{eq})-\text{Mo}-\text{C}(\text{eq}) = 84.5(5)^\circ$  and  $\text{H}_b-\text{Mo}-\text{H}_b = 59(4)^\circ$ . The geometry about the boron is virtually tetrahedral, with  $\text{Mo-B} = 2.41(2) \text{ \AA}$ . The ligational analogy between  $\eta^3$ -allyl and  $\text{BH}_4^-$  is further strengthened by the results of this study. Boron-decoupled proton nmr spectra reveal that bridge-terminal hydrogen interchange occurs within the tetrahydroborate ligand with  $\Delta G^\ddagger_c = 10.0 \pm 0.2 \text{ kcal/mole}$ . As revealed by  $^{13}\text{C}$  nmr studies, this rearrangement process is not coupled to axial-equatorial CO exchange about the molybdenum coordination polyhedron;  $\Delta G^\ddagger \geq 18.6 \text{ kcal/mole}$  for this process. This result places significant restrictions on operational  $\text{GH}_4^-$  rearrangement mechanisms. These are discussed in the light of a permutational analysis of differentiable rearrangement modes in covalent metal tetrahydroborates.

Support: NSF, PRF and Research Corp.

COORDINATIVE SATURATION AND THE CHEMISTRY OF TRISCYCLOPENTADIENYL  
THORIUM(IV) ALKYL AND ALKANYLS

William A. Wachter  
[Ph.D. Thesis]

The syntheses of a variety of  $(\eta^5\text{-C}_5\text{H}_5)_3\text{ThR}$  organometallic compounds are reported. They are characterized by elemental analysis, cryoscopy in benzene, and by infrared, Raman and proton nmr spectroscopy.



$(\eta^5\text{-C}_6\text{H}_6)_3\text{Th}(\text{allyl})$  is a fluxional monohaptoallyl with a barrier to sigma-tropic rearrangement comparable to that for the analogous uranium compound. The Th-C bond reacts more readily and more specifically with protonic solvents than the U-C bond.

The thermolysis of  $(\text{C}_6\text{H}_6)_3\text{ThR}$  in aromatic solvents at 167°C yields the corresponding alkane, RH, or, in the case of an alkenyl compound, the corresponding alkene with retention of configuration. The kinetics are first order in  $(\text{C}_6\text{H}_6)_3\text{ThR}$ . The source of incorporated hydrogen is shown to be the cyclopentadienyl ligand. The thorium-containing decomposition product has been characterized by an x-ray structure to be  $[(\text{C}_6\text{H}_6)_2\text{Th}(\text{C}_5\text{H}_4)]_2$ . These results indicate that steric constraints in this system exclude  $\beta$ -elimination as a decomposition pathway and lead to high thermal stability for the thorium as well as uranium-carbon  $\sigma$ -bond.

Support: NSF - Advisor: T. J. Marks

#### SURFACE FILM SOFTENING OF IRON SINGLE CRYSTALS ORIENTED FOR SINGLE SLIP

K. Kojima and M. Meshii  
[physica status solidi (a) 39, 1977]

The surface film softening phenomena were investigated in nickel-plated iron single crystals oriented for single slip at 77°K. The surface film reduced the yield stress and the initial part of the stress-strain curve became serrated. The softening effect was greater in those specimens having a greater surface area on which the primary slip vector had a large normal component. The lowest yield stress was achieved by a combination of prestraining at 300°K and surface coating. Studies of the surface of deformed specimens indicate that cracks in the surface film promote dislocation generation and that it is the edge component of these generated dislocations which produces the observed plastic deformation.

Support: ERDA

#### SURFACE OBSERVATION OF NICKEL-PLATED IRON SINGLE CRYSTALS DEFORMED AT 77°K

S. Kobayashi and M. Meshii  
[Submitted for publication]

The surface morphology of nickel-plated iron single crystals deformed at 77°K has been investigated to identify the mechanism of surface film

softening. Two types of striation were found to form on the specimen surfaces, i.e., cracks approximately perpendicular to the tensile axis on the edge-faces and slip-like lines on the screw-faces. The direction of these lines deviated from the traces of the primary slip planes. Specimens which were electroplated on only one of the edge-faces exhibited a clear correspondence between the cracks on the plated face and the slip steps on the unplated face. Both the cracks and the slip steps were irregularly jogged. The lines connecting the corresponding points on the two faces were parallel to the primary slip direction. The observations indicate that dislocation loops are generated near the cracks below the stress level for screw dislocation motion. As the edge component of these loops can move substantially at the low stress level, the generation of a large number of dislocation loops results in macroscopic deformation. The observed angle of deviation between the direction of the slip-like lines and the trace of the primary slip plane on the screw-face is consistent with this model.

Support: ERDA

INVESTIGATION OF DISLOCATION MOTION BY ETCH PIT AND YIELD STRESS  
IN ELECTRON IRRADIATED COPPER

M. Meshii and M. Wada

[Proc. 4th Int. Conf. on Strength of Metals and Alloys 2  
Nancy, France, 1976]

The dislocation motion determined by the etch pit technique and the macroscopic stress-strain relation are examined in electron irradiated copper single crystals in the temperature range from 4.2° to 100°K. A good correlation is found between these two observations and the dislocation kinetics near the yield point has been determined.

Support: ERDA

SURFACE FILM EFFECTS ON DEFORMATION BEHAVIOR OF IRON SINGLE CRYSTALS  
AT CRYOGENIC TEMPERATURES

S. Kobayashi and M. Meshii

[Proc. 1977 Int. Cryogenics Materials Conf.,  
Boulder, Colorado, 1977]

The low temperature yield stress of an iron single crystal can be reduced significantly by coating its surface with a thin Ni film. This surface

film softening phenomenon has been investigated mechanically by varying the specimen conditions (prestrain and orientation) over the temperature range from 4.2° to 300°K. The rate controlling mechanism of the deformation of b.c.c. metals at cryogenic temperatures is discussed in conjunction with the observed results and the fundamental principles are presented for reducing the yield stress and increasing the ductility of b.c.c. metals at cryogenic temperatures.

Support: ERDA

A LASER INDUCED FLUORESCENCE STUDY OF VIBRATIONAL  
ENERGY TRANSFER PROCESSES IN CYCLOPROPANE

Gordon T. Fujimoto and Eric Weitz  
[Submitted for publication]

Cyclopropane was studied in the gas phase via an infrared laser induced fluorescence technique. Molecules were excited from the ground state to the  $\nu_{10}$  level of cyclopropane using a Q-switched  $\text{CO}_2$  laser operating on either P(14) or P(20) of the 9.6  $\mu$  laser transition. Fluorescence was observed from the  $\nu_6$ ,  $\nu_8$ ,  $\nu_{10} + \nu_{11}$  and  $\nu_6 + \nu_{10}$  levels of cyclopropane. The self-deactivation of vibrationally excited cyclopropane through  $V \rightarrow T/R$  processes was found to have a rate of 8.0 msec<sup>-1</sup> torr<sup>-1</sup>. Deactivation by rare gas collisions was also studied with comparisons being made to simple  $V \rightarrow T$  and  $V \rightarrow R$  theories.  $V \rightarrow V$  equilibration processes are discussed involving the  $\nu_6$ ,  $\nu_8$ ,  $\nu_{10}$ ,  $\nu_{11}$  and  $\nu_{10} + \nu_{11}$  levels.

Support: NSF, Research Corp and NATO

BASIC RESEARCH ON CERAMIC MATERIALS FOR ENERGY STORAGE AND CONVERSION SYSTEMS

James Ni, W. Jakubowski and D. H. Whitmore

The present research program involves utilizing appropriate probes for movement of ionic and electronic charge carriers in ceramic materials suitable for solid electrolyte and electrode applications in high-performance, secondary battery and fuel cell systems. Special emphasis is placed on developing: (1) a better understanding of the effects of structure, impurities and composition on transport mechanisms; and (2) detailed knowledge of the kinetics and mechanisms of reactions occurring (on a microscopic scale) at the electrode-electrolyte interfaces of energy storage and conversion systems.

Support: ERDA



SELF-FOCUSING OF LIGHT FROM TRANSIENT TO QUASI-STEADY-STATE LIMIT  
IN AN ISOTROPIC NEMATIC SUBSTANCE

E. G. Hanson, Y. R. Shen and George K. Wong  
[Optics Communications 20, 1977]

We have made quantitative measurements on the characteristics of self-focusing varying from transient to quasi-steady-state. The results agree well with a simple unified physical description of self-focusing and with known theoretical predictions. Stimulated Brillouin scattering is identified as the mechanism responsible for the limiting diameter of the self-focused beam in our experiment.

Support: ERDA

THEORY OF SMECTIC A: A MOLECULAR MODEL CONTAINING STERIC EFFECTS

Legesse Senbetu and Chia-Wei Woo  
[Submitted for publication]

Starting with a pairwise, spatially and orientationally dependent inter-molecular potential constructed to include steric effects, we carry out a systematic solution of the mean field equation for liquid crystals. A model parameter which is connected to the molecular structure measures the strength of the steric forces. Its inclusion makes possible a semiquantitative comparison of our results to the experimentally obtained phase diagrams of several homologous series. The model predicts phase diagrams similar to that found by Lee et al. Improvements over the latter include: (1) the characteristic feature of the smectic A phase, that the director prefers to be perpendicular to the smectic layers, arises naturally from our model; (2) the connection of one of our model parameters with the structure of molecules can now be used to explain the differences in phase transition properties between homologous series whose molecules are of similar structure but differ in the length of the rigid section.

Support: NSF

SYSTEMATIC SOLUTION OF THE MEAN FIELD EQUATION FOR LIQUID CRYSTALS

L. Shen, Hock Kee Sim, Yu Ming Shih and Chia-Wei Woo  
[Submitted for publication]

Starting with a pairwise, spatially and orientationally dependent inter-molecular potential of the Kobayashi-McMillan form, we carry out a systematic



solution of the mean field equation for liquid crystals. The mean field equation, presented as first of a hierarchy of BBCKY equations, is first reduced to a set of coupled integrodifferential equations by means of expanding the distribution function  $f(\vec{r},\theta)$  and  $\ln f(\vec{r},\theta)$  in Legendre polynomials and the reciprocal lattice space. In the first level of approximation, the expansion retains only the lowest-order coefficients, permitting a complete decoupling of the equations. In the second level of approximation, the leading coefficient which couples spatial order to orientational order is included. In the third level of approximation two more higher order coefficients are included. At each level, the free energy functional is evaluated to determine the equilibrium phase at given temperatures and chain-lengths of a homologous series. It is shown that the expansion converges very rapidly, the second level of approximation being entirely sufficient. This lends support to our earlier variational calculation which contained only three variational parameters.

Support: NSF

#### MOLECULAR THEORY OF CHOLESTERIC LIQUID CRYSTALS AND CHOLESTERIC MIXTURES

Y. R. Lin-Liu, Yu Ming Shih and Chia-Wei Woo  
[Phys. Rev. A 15, 1977]

A molecular theory of cholesteric liquid crystals is presented. By means of symmetry considerations we obtain a general form of the intermolecular potential containing chiral contributions, which are then shown to be responsible for forming the cholesteric phase. The temperature dependence of the cholesteric pitch is calculated. It is found that the pitch depends on temperature through a ratio of orientational order parameters in the form  $[\sigma_4(T)/\sigma_2(T)]^2$ . A general mean-field theory for binary cholesteric mixtures is also presented, along with a formula showing how the pitch depends on temperature and concentration. Under certain conditions, the formula reduces at fixed  $T - T_c$  to a simple quadratic rational fraction in the concentration. This is consistent with experimental observation.

Support: NSF

# THEORETICAL ANALYSIS OF ISOTROPIC-NEMATIC TRANSITION PROPERTIES

Yu Ming Shih, Y. R. Lin-Liu and Chia-Wei Woo  
[Phys. Rev. A 14, 1976]

With the aid of a modified mean-field model, one in which the spatial correlations are handled by means of a conventional classical liquid theory and the orientational ordering alone is subjected to the mean-field approximation, we find it possible to correlate thermodynamic data near the isotropic nematic transition region. In contrast with the Maier-Saupe theory, we deduce accurately the volume change, latent heat, and maximum supercooling temperature. The theoretical analysis when applied to PAA and MBBA leads to results in quantitative agreement with experiment. We propose that measured data on other nematic and cholesteric liquid crystals be subjected to tests under the same scheme.

Support: NSF

# OPTIMIZATION OF THE JASTROW FUNCTION BY PAIRED-PHONON ANALYSIS

L. Shen, Hock-Kee Sim and Chia-Wei Woo  
[Phys. Rev. B 14, 1976]

We demonstrate numerically for (i) a  $^4\text{He}$  monolayer at areal density  $0.035 \text{ \AA}^{-2}$ , and (ii) neutron star matter at density  $1 \text{ fm}^{-3}$ , that optimizing the Jastrow function by means of paired-phonon analysis is both accurate and efficient.

Support: NSF

# SOLIDIFICATION OF $^4\text{He}$ MONOLAYER

Michael A. Lee, D. N. Lowy and Chia-Wei Woo  
[Phys. Rev. B 14, 1976]

We apply a variational method to calculate ground-state properties of a  $^4\text{He}$  monolayer on a neutral substrate. A stable solid phase occurs at densities above  $0.091 \text{ \AA}^{-2}$ . The melting density is about  $0.095 \text{ \AA}^{-2}$  and the freezing density is about  $0.085 \text{ \AA}^{-2}$ , which is about 5% higher than the observed freezing density. We also describe an improved method for solving the Percus-Yevick equation.

Support: NSF

MATERIALS RESEARCH CENTER  
CENTRAL FACILITIES

1. Ceramics Facility - Director: D. L. Johnson
2. Crystal Growth and Materials Preparation Facility - Director: D. H. Whitmore
3. Electron Magnetic Resonance and Magnetic Properties Facility - Director: A. L. Allred
4. Transmission Electron Microscopy Facility - Director: M. Meshii
5. Magnetics Facility - Director: J. B. Ketterson
6. Mechanical Properties Facility - Director: J. O. Brittain
7. Metallographic, Petrographic and Photographic Facility - Director: J. E. Hilliard
8. Mössbauer Facility - Director: L. H. Schwartz
9. NMR Facility - Director: W. Halperin
10. Optical Measurements Facility - Directors: C. R. Kannewurf and D. F. Shriver
11. Polymer Characterization Facility - Director: W. W. Graessley
12. Radiotracer Facility - Director: D. H. Whitmore
13. Shop Facility - Director: L. H. Schwartz
14. Long-Term X-Ray Facility - Director: J. B. Cohen
15. Short-Term X-Ray Facility - Director: S. H. Carr

INDEX

	Pages
J. O. Brittain	58-60, 75-76
S. H. Carr	73-75
J. B. Cohen	87-90
B. Crist, Jr.	73, 78
D. E. Ellis	27-30, 60
M. E. Fine	48-51, 53-54
A. J. Freeman	21-27, 31, 61-64, 90-93
W. W. Graessley	71-72, 79
W. Halperin	66, 93-94
J. E. Hilliard	64-66
B. M. Hoffman	4, 11
J. A. Ibers	8-10, 96
C. R. Kannewurf	19-20
J. B. Ketterson	67-68, 93-96
T. J. Marks	4-10, 96-101
M. Meshii	36-38, 102-103
T. Mura	47, 51-53
M. Ratner	11-15
L. H. Schwartz	38-39
D. F. Shriver	16-17
K. S. Singwi	81-82
R. P. Van Duyne	85
J. Weertman	40-46
J. R. Weertman	44
E. Weitz	84, 104
D. H. Whitmore	15, 17, 104
G. K. Wong	82-83, 105
C.-W. Woo	84, 105-107